

EXPERIMENTAL AND COMPUTATIONAL EVALUATION OF TRANSIENT  
BEHAVIOR OF A TYPICAL SATELLITE MONOPROPELLANT PROPULSION  
SYSTEM

A THESIS SUBMITTED TO  
THE GRADUATE SCHOOL OF NATURAL AND APPLIED SCIENCES  
OF  
MIDDLE EAST TECHNICAL UNIVERSITY

BY

AYŞEGÜL ÇİLLİ TARÇIN

IN PARTIAL FULFILLMENT OF THE REQUIREMENTS  
FOR  
THE DEGREE OF MASTER OF SCIENCE  
IN  
MECHANICAL ENGINEERING

SEPTEMBER 2014



Approval of the thesis:

**EXPERIMENTAL AND COMPUTATIONAL EVALUATION OF  
TRANSIENT BEHAVIOR OF A TYPICAL SATELLITE  
MONOPROPELLANT PROPULSION SYSTEM**

submitted by **AYŞEGÜL ÇİLLİ TARÇIN** in partial fulfillment of the requirements  
for the degree of **Master of Science in Mechanical Engineering Department,**  
**Middle East Technical University** by,

Prof. Dr. Canan Özgen  
Dean, Graduate School of **Natural and Applied Sciences** \_\_\_\_\_

Prof. Dr. Tuna Balkan  
Head of Department, **Mechanical Engineering** \_\_\_\_\_

Prof. Dr. Mehmet Haluk Aksel  
Supervisor, **Mechanical Engineering Dept., METU** \_\_\_\_\_

Dr. Mehmet Ali Ak  
Co-Supervisor, **ROKETSAN** \_\_\_\_\_

**Examining Committee Members:**

Prof. Dr. Kahraman Albayrak  
Mechanical Engineering Dept., METU \_\_\_\_\_

Prof. Dr. Mehmet Haluk Aksel  
Mechanical Engineering Dept., METU \_\_\_\_\_

Dr. Mehmet Ali Ak  
Senior Manager, ROKETSAN Missile Industries \_\_\_\_\_

Assoc. Prof. Dr. Mehmet Metin Yavuz  
Mechanical Engineering Dept., METU \_\_\_\_\_

Assoc. Prof. Dr. Sinan Eyi  
Aerospace Engineering Dept., METU \_\_\_\_\_

Date: 11.09.2014  
\_\_\_\_\_

**I hereby declare that all information in this document has been obtained and presented in accordance with academic rules and ethical conduct. I also declare that, as required by these rules and conduct, I have fully cited and referenced all material and results that are not original to this work.**

Name, Last name: Ayşegül Çilli Tarçın

Signature:

## ABSTRACT

### EXPERIMENTAL AND COMPUTATIONAL EVALUATION OF TRANSIENT BEHAVIOR OF A TYPICAL SATELLITE MONOPROPELLANT PROPULSION SYSTEM

Cilli Tarcin, Aysegul

M.Sc., Department of Mechanical Engineering

Supervisor : Prof. Dr. M. Haluk Aksel

Co-Supervisor : Dr. Mehmet Ali Ak

September 2014, 153 pages

In this study, a typical satellite monopropellant propulsion system is numerically modeled by using a commercial software and analyses are conducted regarding the priming operation of satellite propulsion system. Analyses are performed for different tank pressures, downstream line pressures, distance between the tank and orifice, distance between the orifice and latch valve, distance between the latch valve and exit valve, orifice diameter and pipe diameters. Moreover, a test setup is constructed and tests are performed in order to create a database on water hammer phenomena under the same conditions with the ones faced in satellite propulsion system during priming. In the tests, different tank pressures, downstream line pressures, downstream line lengths and orifice diameters are used. Maximum pressure, frequency of flow and transient flow duration are the parameters compared.

**Keywords:** Satellite, Propulsion System, Priming, Water Hammer, Transient Analysis, Experiments

## ÖZ

### TİPİK BİR TEK YAKITLI UYDU İTKİ SİSTEMİNİN GEÇİCİ DAVRANIŞININ DENEYSSEL VE HESAPLAMALI OLARAK İNCELENMESİ

Çilli Tarçın, Ayşegül  
Yüksek Lisans, Makine Mühendisliği Bölümü  
Tez yöneticisi : Prof. Dr. M. Haluk Aksel  
Ortak tez yöneticisi : Dr. Mehmet Ali Ak

Eylül 2014, 153 sayfa

Bu çalışmada, tipik bir tek yakıtlı uydu itki sistemi ticari bir yazılım ile numerik olarak modellenmiş ve analizler, uydu itki sisteminin başlatma operasyonu göz önünde bulundurularak gerçekleştirilmiştir. Analizler, farklı tank basınçları, akış aşağı yönündeki boru basınçları, tank ile orifis arası uzunluklar, orifis ile açma-kapama vanası arası uzunluklar, açma-kapama vanası ile çıkış vanası arası uzunluklar, orifis çapları ve boru çapları kullanılarak gerçekleştirilmiştir. Bunun yanı sıra bir test düzeneği kurulmuş ve başlatma operasyonu sırasında bir uydu itki sisteminde karşılaşılan koşullar ile aynı koşullarda ortaya çıkacak su darbesi fenomeni hakkında veritabanı oluşturmak amacıyla testler gerçekleştirilmiştir. Testlerde, farklı tank basınçları, akış aşağı yönündeki boru basınçları, akış aşağı yönündeki boru uzunlukları ve orifis çapları kullanılmıştır. Elde edilen maksimum basınç, akış frekansı ve geçici akış süreleri karşılaştırılan parametrelerdir.

**Anahtar Kelimeler:** Uydu, İtki Sistemi, Başlatma, Su Darbesi, Geçici Analiz, Deneyler

*To my lovely family and husband*

## ACKNOWLEDGEMENTS

First of all I would like to thank to my dear supervisor Prof. Dr. Mehmet Haluk Aksel and co-supervisor Dr. Mehmet Ali Ak and my manager Atılğan Toker for their invaluable guidance, advices and criticism that enabled me to complete this study.

Then I would like to thank a lot to my dear colleague Başar Esirgen for his precious help during my analyses and my dear colleagues Murat Bayramođlu, Utku Olgun and Ümit Poyraz for their precious help in all of the steps of the test setup and tests.

I would like to express my thanks a lot to my lovely husband, my love, Serkan Tarçın for his patience and support during all my studies.

Moreover, I would like to thank a lot to my family and especially to my precious, my mother Aynur Çilli, for her all support during this thesis and all my studies and my sister Zeynep Çilli for her patience and infinite love.

## TABLE OF CONTENTS

ABSTRACT.....	V
ÖZ .....	VI
ACKNOWLEDGEMENTS.....	VIII
TABLE OF CONTENTS.....	IX
LIST OF FIGURES.....	XII
LIST OF TABLES.....	XVI
LIST OF SYMBOLS.....	XVII
ABBREVIATIONS.....	XVIII
CHAPTERS	
1. INTRODUCTION.....	1
1.1 Literature Survey.....	2
1.2 The Purpose and Scope of the Study.....	26
2. PIPELINE HYDRAULICS.....	29
3. FLOWNEX SIMULATION TOOL.....	33
3.1 Conservation of Mass.....	34
3.2 Conservation of Momentum.....	35
3.3 Conservation of Energy.....	35
3.4 Convergence Criteria.....	36
4. TRANSIENT NUMERICAL ANALYSES.....	37
4.1 Analyses Results Post-Processing.....	46
4.2 Analyses Results.....	48
4.2.1 CASE 1: Different Tank Pressures versus Constant Downstream Line Pressure.....	49
4.2.2 CASE 2: Constant Tank Pressure versus Different Downstream Line Pressures.....	53
4.2.3 CASE 3: Constant L1 and L2 Lengths versus Different L3 Lengths.....	56

4.2.4	CASE 4: Constant L1 and L3 Lengths versus Different L2 Lengths.....	59
4.2.5	CASE 5: Constant L2 and L3 Lengths versus Different L1 Lengths.....	62
4.2.6	CASE 6: Constant Total Length (L1+L2+L3) versus Different L1, L2 and L3 Length.....	65
4.2.7	CASE 7: Constant Pressures and Lengths versus Different Orifice Diameters.....	70
4.2.8	CASE 8: Constant Pressures and Lengths versus Different Pipe Inner Diameters.....	74
5.	EXPERIMENTAL STUDY.....	79
5.1	Test Conditions and Results.....	85
5.1.1	Case A: Test With L3=2 m, Downstream Line Condition= Ambient Pressure.....	93
5.1.2	Case B: Test With L3=2 m, Downstream Line Condition= Vacuum.....	94
5.1.3	Case C: Test With L3=1 m, Downstream Line Condition= Ambient Pressure.....	95
5.1.4	Case D: Test With L3=1 m, Downstream Line Condition= Vacuum.....	96
5.1.5	Case E: Test With L3=1 m, Downstream Line Condition= Ambient Pressure, 1.5 mm Orifice.....	97
5.1.6	Case F: Test With L3=1 m, Downstream Line Condition= Vacuum, 1.5 mm Orifice .....	99
6.	RESULTS AND DISCUSSION.....	101
6.1	Case A: Test and Analysis with L3=2 m, Downstream Line Condition= Ambient Pressure.....	101
6.2	Case B: Test and Analysis with L3=2 m, Downstream Line Condition= Vacuum .....	106
6.3	Case C: Test and Analysis with L3=1 m, Downstream Line Condition= Ambient Pressure.....	110
6.4	Case D: Test and Analysis with L3=1 m, Downstream Line Condition= Vacuum .....	114
6.5	Case E: Test and Analysis with L3=1 m, Downstream Line Condition= Ambient Pressure, 1.5 mm Orifice.....	118

6.6	Case F: Test and Analysis with $L_3=1$ m, Downstream Line Condition= Vacuum, 1.5 mm Orifice.....	122
7.	CONCLUSION.....	127
	REFERENCES.....	131
APPENDICES		
A.	PIPELINE HYDRAULICS.....	137
A.1.	Euler Equation.....	137
A.2.	Pressure Head Change.....	139
A.3.	Mass Accumulation.....	142
A.4.	Change in Pipe Volume due to Elasticity.....	143
A.5.	Wave Speed for Case (b) Restraint.....	146
A.6.	Conservation of Mass.....	149
B.	FFT Calculation in MATLAB.....	153

## LIST OF FIGURES

Figure 1-1 Propulsion systems classification [3] .....	2
Figure 1-2. Satellite propulsion systems schematics [4], [5] .....	3
Figure 1-3. Typical satellite monopropellant propulsion system schematic [6] .....	4
Figure 1-4. Initialization phases of a satellite monopropellant propulsion system.....	5
Figure 1-5. Detonation factors calculated in study [50] for the test cases in the literature .....	7
Figure 1-6. Simplified propellant feed system used in Ref. [7] .....	9
Figure 1-7. Test setup used in Ref [9].....	10
Figure 1-8. Water hammer test setup used for water, MMH and NTO tests .....	11
Figure 1-9. Water hammer test setup used for hydrazine tests .....	12
Figure 1-10. Experimental setup used in Ref. [13] .....	13
Figure 1-11. ROCSAT satellite propulsion system schematic.....	15
Figure 1-12. Test case used in the calculations of Ref. [16] .....	16
Figure 1-13. System model used in the analyses of Ref. [17].....	17
Figure 1-14. Test setup used in Ref [18].....	18
Figure 1-15. Test setup used in Ref. [19].....	20
Figure 1-16. Test setup used in Ref. [20].....	21
Figure 1-17. Test setup used in Ref. [21].....	23
Figure 3-1. Flow control volume used in Flownex calculations .....	34
Figure 4-1. Transient analysis test setup model in Flownex .....	45
Figure 4-2. Damped sine wave.....	46
Figure 4-3. Exponential decay .....	48
Figure 4-4. Pressure versus time graph for analysis No 0.....	49
Figure 4-5. Maximum pressure versus tank pressure graph for Case 1 .....	50
Figure 4-6. Pressure amplitude versus tank pressure graph for Case 1.....	51
Figure 4-7. Frequency versus tank pressure graph for Case 1 .....	52
Figure 4-8. Transient flow duration versus tank pressure graph for Case 1 .....	53
Figure 4-9. Maximum pressure versus downstream line pressure graph for Case 2..	54
Figure 4-10. Frequency versus downstream line pressure graph for Case 2.....	55
Figure 4-11. Transient flow duration versus downstream line pressure graph for Case 2.....	56
Figure 4-12. Maximum pressure versus L3 length graph for Case 3.....	57
Figure 4-13. Frequency versus L3 length graph for Case 3 .....	58
Figure 4-14. Transient flow duration versus L3 length graph for Case 3 .....	59
Figure 4-15. Maximum pressure versus L2 length graph for Case 4.....	60
Figure 4-16. Frequency versus L2 length graph for Case 4.....	61

Figure 4-17. Transient flow duration versus L2 length graph for Case 4.....	62
Figure 4-18. Maximum pressure versus L1 length graph for Case 5.....	63
Figure 4-19. Frequency versus L1 length graph for Case 5.....	64
Figure 4-20. Transient flow duration versus L1 length graph for Case 5.....	65
Figure 4-21. Maximum pressure versus long pipe code graph for Case 6.....	67
Figure 4-22. Frequency versus long pipe code graph for Case 6.....	68
Figure 4-23. Transient flow duration versus long pipe code graph for Case 6.....	69
Figure 4-24. Pressure versus time graph for analysis with 0.5 mm orifice.....	70
Figure 4-25. Pressure versus time graph for analysis with 0.5 mm orifice – zoomed view .....	71
Figure 4-26. Maximum pressure versus orifice diameter graph for Case 7.....	72
Figure 4-27. Frequency versus orifice diameter graph for Case 7.....	73
Figure 4-28. Flow through orifice.....	73
Figure 4-29. Transient flow duration versus orifice diameter graph for Case 7.....	74
Figure 4-30. Maximum pressure versus pipe inner diameter graph for Case 8.....	75
Figure 4-31. Frequency versus pipe inner diameter graph for Case 8.....	76
Figure 4-32. Transient flow duration versus pipe inner diameter graph for Case 8 ..	77
Figure 5-1. Test setup schematic.....	79
Figure 5-2. Test setup picture.....	80
Figure 5-3. Test results: maximum pressure versus tank pressure graph .....	90
Figure 5-4. Test results: frequency versus tank pressure graph.....	91
Figure 5-5. Test results: transient flow duration versus tank pressure graph.....	92
Figure 5-6. Pressure versus time graph for test No 1 .....	93
Figure 5-7. Pressure versus time graph for test No 18.....	94
Figure 5-8. Pressure versus time graph for test No 29.....	96
Figure 5-9. Pressure versus time graph for test No 30.....	97
Figure 5-10. Pressure versus time graph for test No 33.....	98
Figure 5-11. Pressure versus time graph for test No 37.....	100
Figure 6-1. Maximum pressure versus tank pressure graph for L3=2 m and ambient pressure downstream line condition.....	102
Figure 6-2. Frequency versus tank pressure graph for L3=2 m and ambient pressure downstream line condition .....	103
Figure 6-3. Transient flow duration versus tank pressure graph for L3=2 m and ambient pressure downstream line condition .....	104
Figure 6-4. Comparison of Analysis 50 and Test 1 .....	105
Figure 6-5. Maximum pressure versus tank pressure graph for L3=2 m and vacuum downstream line condition .....	106
Figure 6-6. Frequency versus tank pressure graph for L3=2 m and vacuum downstream line condition .....	107

Figure 6-7. Transient flow duration versus tank pressure graph for L3=2 m and vacuum downstream line condition.....	108
Figure 6-8. Comparison of Analysis 46 and Test 18.....	109
Figure 6-9. Maximum pressure versus tank pressure graph for L3=1 m and ambient pressure downstream line condition.....	110
Figure 6-10. Frequency versus tank pressure graph for L3=1 m and ambient pressure downstream line condition .....	111
Figure 6-11. Transient flow duration versus tank pressure graph for L3=1 m and ambient pressure downstream line condition .....	112
Figure 6-12. Comparison of Analysis 53 and Test 29.....	113
Figure 6-13. Maximum pressure versus tank pressure graph for L3=1 m and vacuum downstream line condition .....	114
Figure 6-14. Frequency versus tank pressure graph for L3=1 m and vacuum downstream line condition .....	115
Figure 6-15. Transient flow duration versus tank pressure graph for L3=1 m and vacuum downstream line condition.....	116
Figure 6-16. Comparison of Analysis 56 and Test 30.....	117
Figure 6-17. Maximum pressure versus tank pressure graph for L3=1 m and ambient pressure downstream line condition and 1.5 mm orifice .....	118
Figure 6-18. Frequency versus tank pressure graph for L3=1 m and ambient pressure downstream line condition and 1.5 mm orifice.....	119
Figure 6-19. Transient flow duration versus tank pressure graph for L3=1 m and ambient pressure downstream line condition and 1.5 mm orifice.....	120
Figure 6-20. Comparison of Analysis 58 and Test 33.....	121
Figure 6-21. Maximum pressure versus tank pressure graph for L3=1 m and vacuum downstream line condition and 1.5 mm orifice.....	122
Figure 6-22. Frequency versus tank pressure graph for L3=1 m and vacuum downstream line condition and 1.5 mm orifice.....	123
Figure 6-23. Transient flow duration versus tank pressure graph for L3=1 m and vacuum downstream line condition and 1.5 mm orifice .....	124
Figure 6-24. Comparison of Analysis 59 and Test 37.....	125
Figure A. 1 Fluid control volume at the pipe centerline .....	137
Figure A. 2. Unsteady Flow .....	139
Figure A. 3. Steady Flow .....	140
Figure A. 4. Steady Flow Control Volume for Momentum Analysis .....	141
Figure A. 5. Flow Control Volume when the wave has just arrived to the Control Volume .....	142
Figure A. 6. Flow Control Volume when the wave has just passed the Control Volume.....	143

Figure A. 7. Control Volume used for Applying Mass Conservation ..... 149

## LIST OF TABLES

Table 4-1. Analyses inputs and results .....	42
Table 4-2. Analysis codes used in comparisons.....	66
Table 5-1. Pressure transducer and data acquisition system properties .....	82
Table 5-2. Test conditions and results.....	87
Table 6-1. Comparison of Analysis 50 and Test 1 inputs and results .....	105
Table 6-2. Comparison of Analysis 46 and Test 18 inputs and results .....	109
Table 6-3. Comparison of Analysis 53 and Test 29 inputs and results.....	113
Table 6-4. Comparison of Analysis 56 and Test 30 inputs and results.....	117
Table 6-5. Comparison of Analysis 58 and Test 33 inputs and results.....	121
Table 6-6. Comparison of Analysis 59 and Test 37 inputs and results.....	125

## LIST OF SYMBOLS

$\beta$	Compressibility
$\forall$	Volume
$p, P$	Pressure
$K$	Bulk modulus of elasticity
$D, d$	Diameter
$\varepsilon$	Strain
$a$	Speed of sound
$\rho$	Density
$E$	Modulus of elasticity
$e$	Pipe wall thickness
$\mu$	Poisson's ratio
$t$	Time
$V$	Velocity
$f$	Frequency, Friction factor
$x, s$	Distance
$A$	Area
$m$	Mass
$\dot{m}$	Mass flow rate
$T$	Temperature, Period
$g$	Gravitational acceleration
$z$	Height
$c_p$	Specific heat at constant pressure
$\dot{q}_H$	Heat rate per unit mass
$\dot{Q}_H$	Heat rate
$\dot{w}$	Work rate per unit mass
$\dot{W}$	Work rate
$\delta$	Logarithmic decrement
$\xi$	Damping ratio
$\omega_d$	Damped angular frequency
$\omega_0$	Undamped natural frequency
$\alpha$	Exponential decay rate
$\tau$	Time constant, Shear stress
$\theta$	Angle
$\gamma$	Density times gravitational acceleration
$L$	Length
$Q$	Volumetric flow rate
$H$	Head
$\sigma$	Stress

## ABBREVIATIONS

AFT	Applied Flow Technologies
AIAA	American Institute of Aeronautics and Astronautics
CFD	Computational Fluid Dynamics
CNES	Centre National d'Etudes Spatiales
DFT	Discrete Fourier Transform
ECSS	European Cooperation for Space Standardization
ESPSS	European Space Propulsion System Simulation
FFT	Fast Fourier Transform
FSI	Fluid Structure Interaction
HVAC-R	Heating Ventilating Air Conditioning and Refrigeration
IPCM	Implicit Pressure Correction Method
MMH	Monomethylhydrazine
MON	Mixed Oxides of Nitrogen
NTO	Nitrogen tetroxide
RACS	Roll and Attitude Control System

## CHAPTER 1

### INTRODUCTION

Satellites are backbone of nowadays' world communication system. More than a hundred of satellites are launched in a year for military, commercial or scientific reasons [1]. Propulsion systems are used in the satellites for orbit insertion and the orbit and attitude control of the satellite. Those satellite propulsion systems are mainly monopropellant or bipropellant liquid systems. Many safety precautions should be taken in accordance to the space safety standards. According to ECSS-Q-40B : Space Product Assurance – Safety standard, three independent inhibits shall be used if it induces catastrophic consequences which are loss of life, loss of launch site or loss of the system [2]. Since in case of some of propellants' leakage, life of the personnel or the satellite can be lost, three inhibits shall be used in the propulsion systems for preventing the propellant leakage. This precaution causes the propulsion system to include pipelines without propellant but with only pressurant gas during launch of the satellite. For this reason, the pipelines without propellant shall be filled with propellant before the activation of the satellite propulsion system. At this point, water hammer problem is faced in the systems as it is explained in detail in Chapter 1.1. In order to avoid problems due to water hammer effect, transient pressure analysis should be performed during the detailed design of the propulsion system.

Developing its own satellites is one of the objectives of Turkish Government at the moment. In this frame, gaining the capability of developing the propulsion system by using only Turkish resources is also seen as a “must” for possessing the capability of developing our own satellites. Hence, possessing the capability of performing the transient pressure analysis of the designed propulsion system is also as a “must”.

In this study, transient analyses of a simplified satellite monopropellant propulsion system using the commercial software named as Flownex are performed. For evaluating the performed analyses, a test setup is constructed and tests are performed

using water instead of toxic hydrazine propellant. The analysis results are compared with the test results.

### 1.1 Literature Survey

Propulsion system is the subsystem in charge of providing thrust to the satellite generally for insertion to the orbit, attitude and orbit control of the satellite and deorbiting. There are different types of propulsion systems used in satellite propulsion such as chemical propulsion, including cold gas propulsion, monopropellant propulsion, bipropellant propulsion; electrical propulsion and rarely, solid propulsion. There are also propulsion types as nuclear propulsion or solar sailing that stay as theoretical for the moment. The classification of propulsion systems is shown in Figure 1-1.

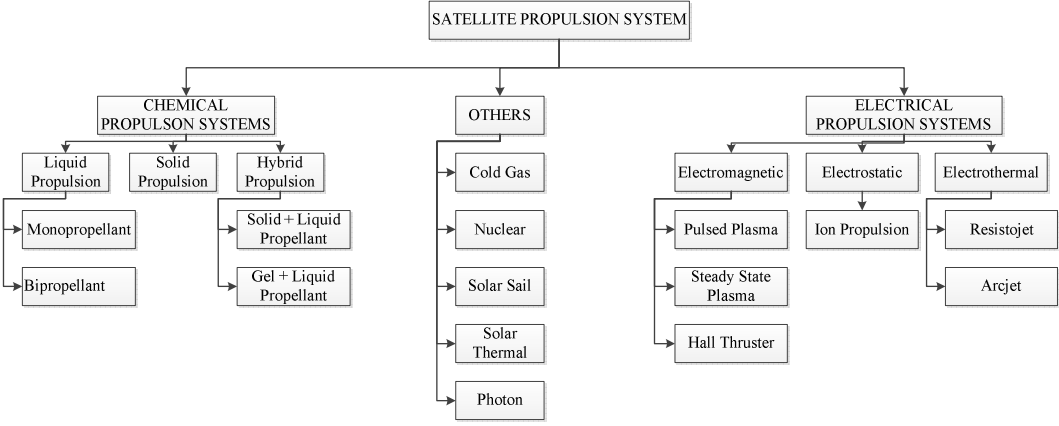
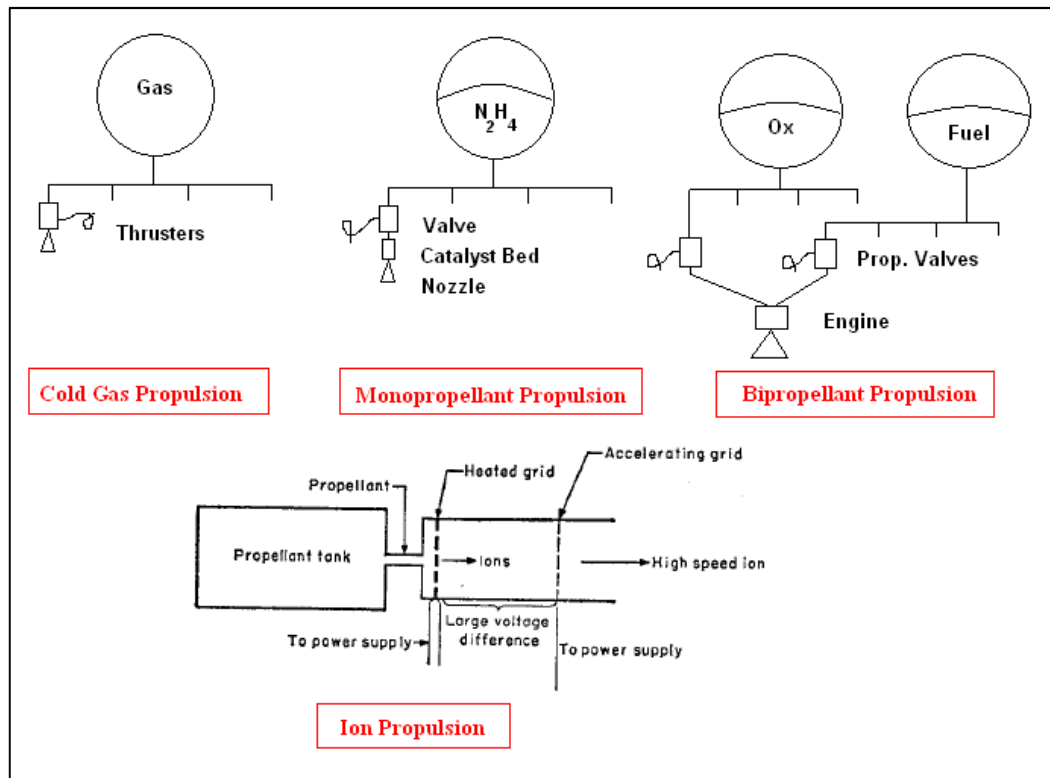


Figure 1-1 Propulsion systems classification [3]

The simple schematic of main satellite propulsion systems are presented in Figure 1-2.



**Figure 1-2.** Satellite propulsion systems schematics [4], [5]

A satellite monopropellant propulsion system includes components as tank, thrusters, latch valves, fill and drain valves, pressure transducer and filter. A satellite bipropellant propulsion system includes pressure regulator, pyrovalves and check valves in addition to monopropellant system components. A typical monopropellant propulsion system is shown in Figure 1-3.

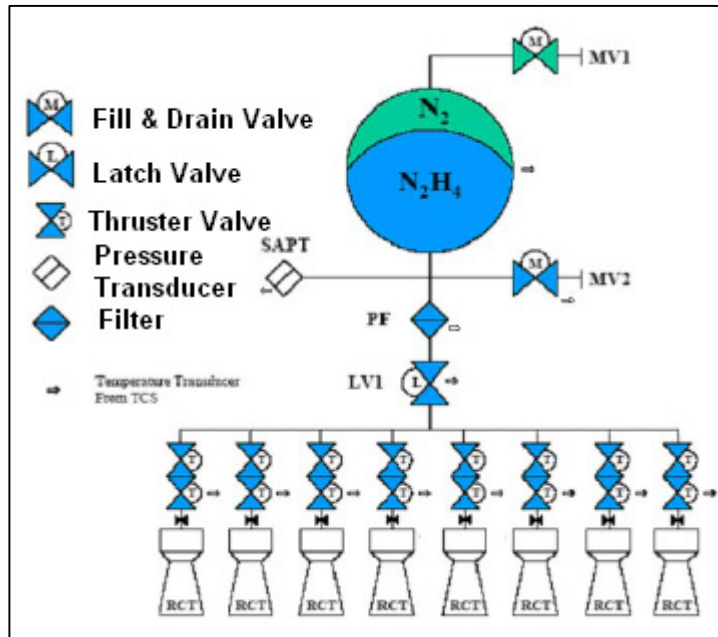


**Figure 1-3.** Typical satellite monopropellant propulsion system schematic [6]

A satellite propulsion system needs to be initialized before operating in space. This initialization process generally includes 3 phases (Figure 1-4). In the first phase, that is same as the phase of launch of the satellite and named as beginning of life phase, latch valve and thruster valves are in closed position. From tank till latch valve, there is propellant in the lines and from latch valve till thruster valves, there is helium in the lines. Phase two is optional and called as venting phase. In this phase, thruster valves are opened and the helium in the lines is purged to space. Then the thruster valves are closed again. In this way, the tubing between the latch valves and thruster valves fills with vacuum. In the third phase, latch valves are opened while the thruster valves are in closed position. In this way, the tubing between the latch valve and thruster valves fill with propellant. This phase is named as priming phase.

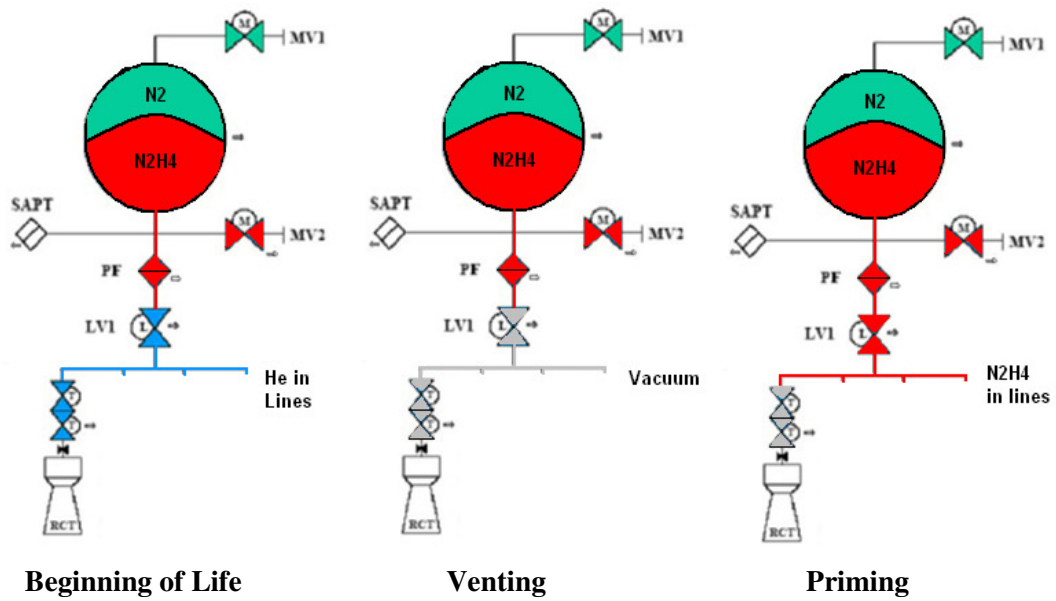


**Figure 1-4.** Initialization phases of a satellite monopropellant propulsion system

Phase 2 that is the venting phase is called as optional because the pressure downstream of the latch valve before priming phase is a design decision. The pressure downstream of the latch valve before priming phase can be any pressure less than the tank pressure, theoretically. However if gas exists in the downstream of the latch valve, adiabatic compression occurs and due to the temperature increase, hydrazine can decompose and detonation can occur. In the study [50], hydrazine detonability studies were surveyed and assessment is presented. A parameter called as the Detonation Factor is defined and calculated. The Detonation Factor,  $D_f$ , is calculated as follows:

$$D_f = C_M \cdot C_D \cdot C_G \cdot C_{CG} \cdot C_{PG} \cdot D_{f_{reference}}$$

In this formula, the correction factors are:

- $C_M$ : Catalytic effects of the material
- $C_D$ : Pipe diameter
- $C_G$ : Hydrazine propellant grade

- $C_{CG}$ : Cavity gas
- $C_{PG}$ : Push gas

Above correction factors and the reference detonation factor,  $Df_{reference}$ , need to be calculated when a new case is to be evaluated. Otherwise each correction factor equals to unity. The reference detonation factor is calculated as follows:

$$Df_{reference} = \frac{m_{gas} \cdot c_{p_{gas}} \cdot T_0 \cdot \left(\frac{P_{peak}}{P_0}\right)^{\frac{\gamma-1}{\gamma}}}{\pi \cdot D \cdot \frac{m_{gas} \cdot \left(\frac{1000 \cdot R}{MW_{gas}}\right) \cdot T_0 \cdot \left(\frac{P_{peak}}{P_0}\right)^{\frac{\gamma-1}{\gamma}}}{P_{peak} \cdot \left(\frac{\pi D^2}{4}\right)} + \frac{\pi D^2}{4}}$$

As the downstream line is vacuumed,  $P_0$  decreases and  $P_{peak}$  increases. So, the ratio of  $\frac{P_{peak}}{P_0}$  increases. At the same time, as the line is vacuumed,  $m_{gas}$  decreases dramatically. Even though, according to the above formula, the increase of detonability factor would be expected as  $\frac{P_{peak}}{P_0}$  increases; due to the dramatic decrease in  $m_{gas}$ , the detonation factor converges to zero, as the line is vacuumed. In the study, the detonability regions are determined depending on the detonability factor as shown in Figure 1-5. When the detonability factor is less than 120000J/m<sup>2</sup>, it is determined that no detonation occurs. One of the tests in this region is the first test that is done with vacuum (N<sub>2</sub> at 0.005kPa) in the downstream of latch valve. As seen from this figure, there is no detonation for this test case (in the green area). The other tests in this region are the tests from 39 to 46 that include hydrazine in the downstream line of latch valve (although this design violates the safety regulations). The other detonability regions are the partial hydrazine decomposition region and the exact hydrazine detonation region. The partial hydrazine decomposition region is defined for the detonation factors between 120000 and 250000 J/m<sup>2</sup> and shown with yellow in this figure. The exact hydrazine detonation region starts from 250000 J/m<sup>2</sup> and shown with red in this figure. The tests from 2 to 38 are performed with pressurized downstream line (downstream pressures changing from 7 bar to 141 bar).

These tests are located either in the partial hydrazine decomposition range (yellow area) or in the exact hydrazine detonation range (red area). By analyzing these results, it is evaluated that in order to avoid hydrazine decomposition due to adiabatic compression in the lines, it is better to evacuate the pipelines before the priming phase on orbit.

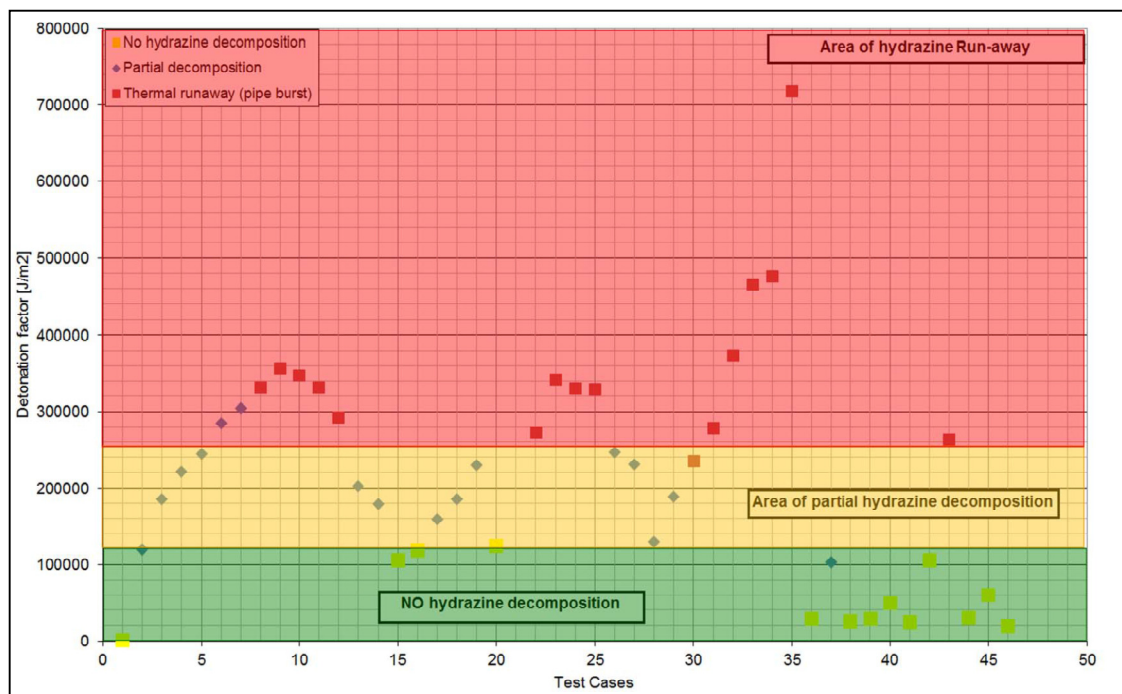


**Figure 1-5.** Detonation factors calculated in study [50] for the test cases in the literature

During this initialization process some phenomena, in addition to the adiabatic compression, may occur. First of all, water hammer effect occurs due to impact of liquid propellant to the closed thruster valve. Moreover, cavitation occurs due to opening of liquid propellant to vacuum environment in the tubing (in case of evacuating the lines before priming). Pressure and temperature increase in the lines and propellant waves move with high wave speed. Because of these effects, hydrazine might decompose in the lines. This is totally undesired effect since, in case of hydrazine decomposition in the propellant lines, catastrophic failure occurs and satellite is lost. Hence, first of all, the water hammer effect should be well analyzed during the design phase of the propulsion system. If necessary, orifice should be used in the propulsion line and dangerous pressure and temperature values should be avoided in addition to the high pressure increase speeds.

Hence, the water hammer phenomenon is one of the most important issues regarding the satellite propulsion system design. Because of that, constant research has been performed on this issue including performing analyses and tests. In addition to that, water hammer phenomenon is investigated for many pipeline systems especially for petrol, natural gas and water distribution system applications.

Water hammer effects that occur during the priming phase in a spacecraft bipropellant propulsion system are investigated in Ref [7]. A setup (shown in Figure 1-6) representing a basic propellant feed system and a setup with complex network including many branches are used for the tests. Water is used as the working fluid during the tests. Fluid properties of water, Monomethylhydrazine (MMH) and Nitrogen tetroxide (NTO) are compared and it is evaluated from the simulations that peak pressure is greater for MMH than NTO while it is slightly higher for water than MMH.

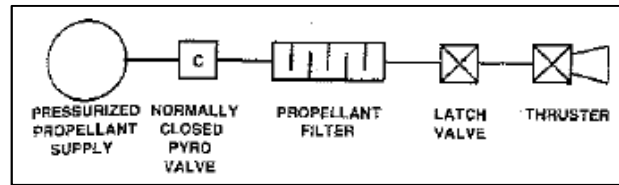


**Figure 1-6.** Simplified propellant feed system used in Ref. [7]

In another study [8], experimental results and simulation results obtained using ANABEL software conducted for a simplified propulsion system (similar to the system given in Figure 1-6) are compared. In this study, water is also used as the working fluid. In addition, simulations utilizing MMH and MON have been performed. The tubing line in the downstream of the valve is filled with air before priming the network. Liquid cavitation is not taken into account in the simulations. It is evaluated that the simulation and test results are in consistency.

A test setup (Figure 1-7) representing a monopropellant satellite system is constructed in another study [9]. The test results are compared with the simulation results obtained using CEDRIC software. In this study, the effects of flow control valve closing / opening time, mass flow rate and tubing design (material used, dimensions, etc.) on the water hammer are investigated. It is stated that the valve closing impact depends on the closing time. There are two types of perturbations: The first type of perturbation is the savage perturbation, when the wave propagation time in the tubing ( $=2L/a$ ) is higher than the valve closing time. In this case, there is not sufficient time for the waves created due to valve closing to reach to the tank, and so the valve closing does not have effects on the tank boundary condition. The second perturbation type is the slow perturbation, when the wave propagation time in the tubing is less than the valve closing time. In this case, the valve closing has a significant effect on the tank boundary condition, such that the tank is used as an expansion vessel (shock absorber). In the test setup, an accelerometer is used on the

tubing in order to measure the vibrations. Also FFT (Fast Fourier Transform) of pressure measurement and accelerometer measurement are taken. It is concluded that first hydraulic frequency can be predicted by CEDRIC; but the pressure damping cannot be predicted correct. It is evaluated that this difference can be due to the viscosity used in the simulations.

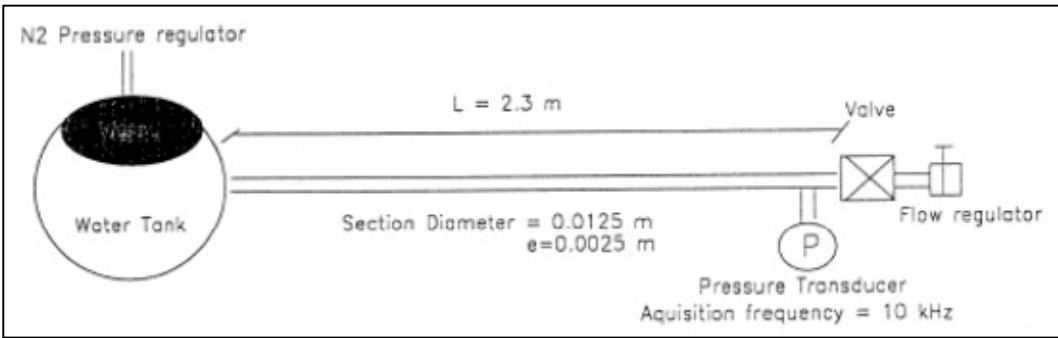


**Figure 1-7.** Test setup used in Ref [9]

A test study for analyzing the water hammer effects has been performed by ONERA under a CNES contract. In this study (Ref. [10]), real propellants have been used for the test in addition to water. The test setup used for water, MMH and NTO is shown in Figure 1-8 while the test setup used for hydrazine tests is presented in Figure 1-9. Vacuum is obtained downstream of the fast opening valve for the tests with water, MMH and NTO. On the other hand, at least atmospheric pressure was used at the downstream line of the fast opening valve for hydrazine tests. Straight pipe, bent pipe, elbow pipe and tee pipe were used as the test element. It has been concluded that the test results were in line with the predictions. In addition, the test results regarding pressure for straight pipe were reproducible while the results for other pipes were not

reproducible for water, MMH and NTO. It is evaluated that this result might be because of other phenomenon such as friction, cavitation, deformation etc. that are not taken into account in the study. The highest pressure peak is obtained for the highest downstream line pressure in the tests with hydrazine. The obtained pressure peak was about 125 bar while the tank pressure was 22 bar and the downstream line pressure was 5 bar. However, the obtained peak pressure was about 35 bar for the test when the tank pressure was 22 bar and the downstream line pressure was 1 bar. It is declared that the results obtained for the test with downstream line pressure of 5 bar are not understood and complementary test should be performed.

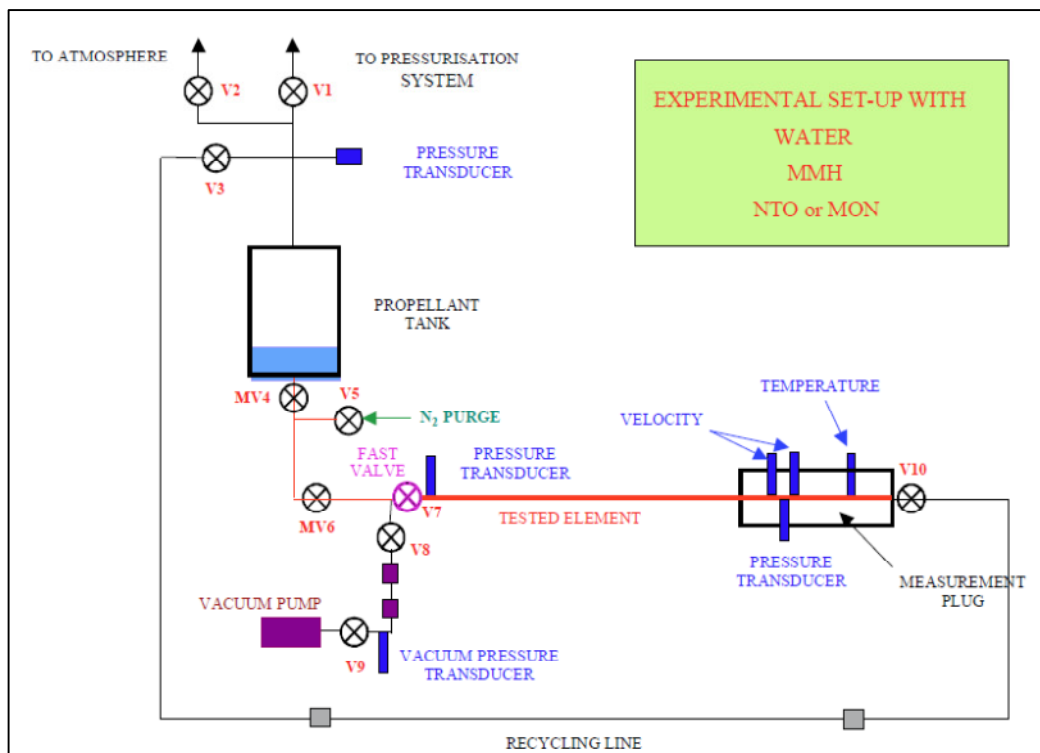


**Figure 1-8.** Water hammer test setup used for water, MMH and NTO tests

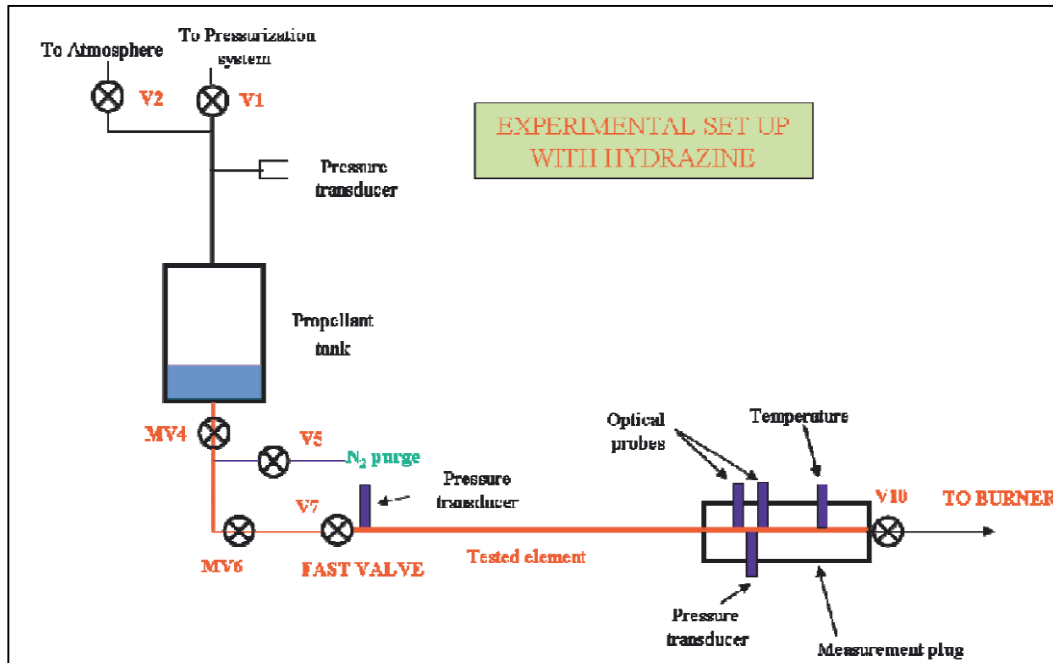
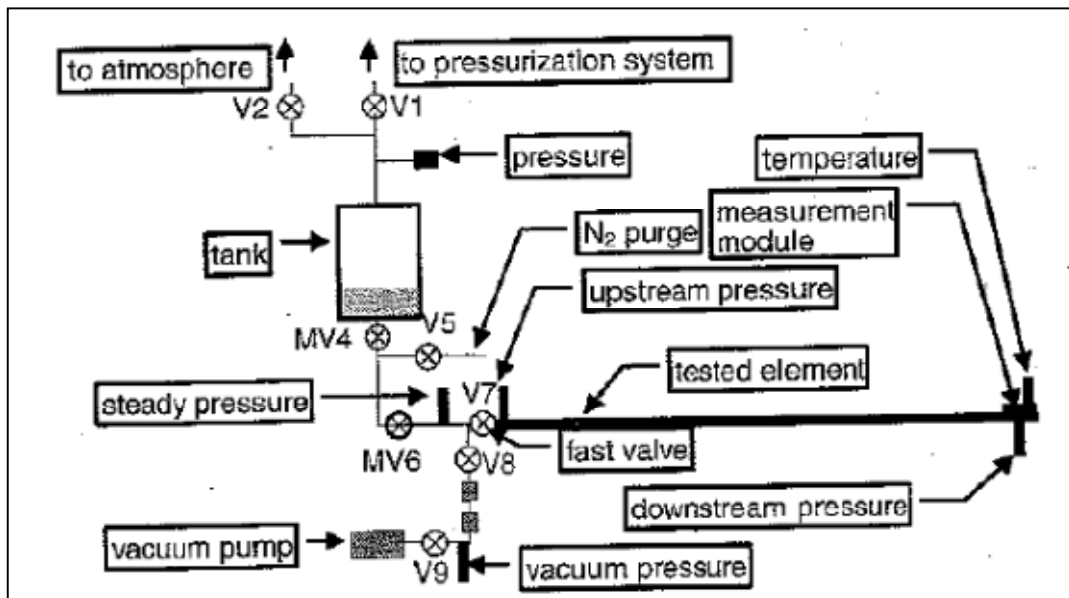


Figure 1-9. Water hammer test setup used for hydrazine tests

EcosimPro software is one of the most common softwares used in the satellite propulsion system analysis with its ESPSS (European Space Propulsion System Simulation) library. In the references [11] and [12] the libraries of ESPSS are introduced in addition to the test and simulation comparison program performed for validating the software. It is expressed that in the 1-D Fluid Flow Library that is a part of ESPSS library, 1D pipe flow is simulated using the central differencing scheme and optionally upwind differencing scheme. Also bubble formation due to cavitation or existence of a noncondensable gas in a liquid in pipelines or components are taken into consideration in calculations. Simulation results for water, MMH, NTO and Hydrazine were in consistency with the test results obtained in Ref [10] without the need of using a fudge factor.

In the reference [13], experiments performed utilizing the inert fluids ethanol and acetaldehyde in place of MMH and NTO, respectively, are explained. The test setup utilized in this study is almost the same as the one utilized in the study Ref. [10]. The test setup used in this study is presented in Figure 1-10. According to the performed tests, it is assessed that ethanol can be used instead of MMH for the water hammer amplitude estimation. It is explained in this paper that in case of working with a compound fluid comprising two components such as liquid propellant and pressurizing gas, the sound velocity will change, depending on the volume fraction of the compounds, with respect to the case that those components are used alone. Consequently, the amplitude, frequency and damping characteristics of the water hammer will be different. Also it is mentioned that in case of existence of areas with pressures lower than the vapor pressure of the fluid, during the transient phase, unsteady cavitation pockets may occur.



**Figure 1-10.** Experimental setup used in Ref. [13]

In another study performed for investigating the satellite propulsion system water hammer effect, ROCSAT Satellite (Figure 1-11) is taken as the model (Ref. [14], [15]). For the steady state analysis, flow channel network numerical scheme is utilized while Method of Characteristics is utilized for the transient flow analysis in this study. Different sizes of tank and thrust values are used in the investigation of water hammer effects. It is stated in this study that using the conventional steady state Darcy friction formula may cause significant error in simulating the water hammer effects and the studies performed for improving the Darcy friction equation are referred. Experiments are conducted in order to verify the steady state flow analysis while the results of already performed tests are used in order to validate the transient analysis simulations. Results of analyses with different sized tanks showed that for a certain amount of propellant, the pressure of the tank remains always higher for a larger tank with respect to a smaller tank. Also, it is seen that higher thrust values cause higher pressure rise in the flow. One of the most important outcomes of this study is that the pressure rise created due to the closure of thruster valves will be lower than the pressure rise created by the closure of latch valve in a system. This is due to the fact that the pipe length until the thruster valves is longer than the pipe length until the latch valve. Moreover, the modes of the fluid flow are found by transforming the pressure fluctuations from time domain to frequency domain in order to prevent the structure of the system enter into resonance due to the pressure fluctuations.

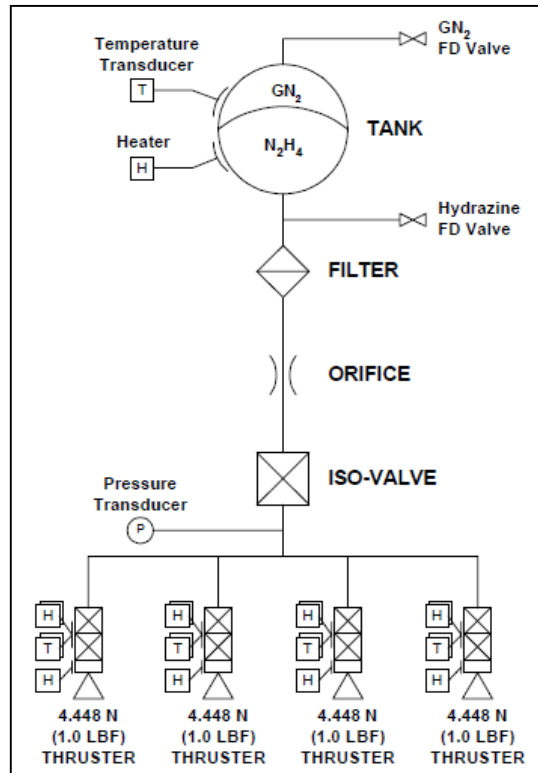


**Figure 1-11.** ROCSAT satellite propulsion system schematic

In the study of Ref [16], water hammer is solved using the eigenfunction method in addition to numerical solution of obtained differential-integral pressure wave equation. Moreover the results of analytical solution are compared with the results obtained from a computer code named COMMIX and results of previously performed tests. The studied tests case is shown in Figure 1-12. It is stated that all results are in good consistency.

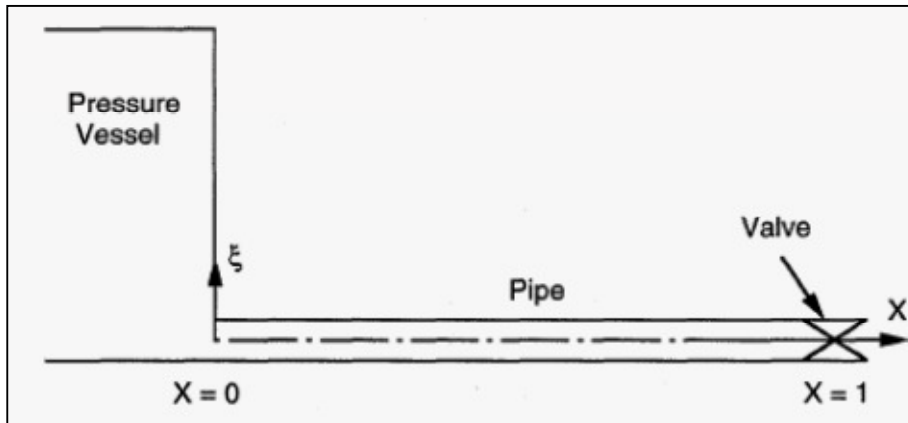


**Figure 1-12.** Test case used in the calculations of Ref. [16]

Propellant flow into evacuated and pressurized lines is investigated in Ref. [17]. In this study, the system model shown in Figure 1-13 is analyzed regarding the different initial line pressures, pipe lengths upstream and downstream of the isolation valve, propellant and friction factors. In the calculations, it is assumed that the negligible amount of propellant vapor is created with respect to the amount of pressurant gas in the line. So, the gas in the line is accepted as the single species, Helium. Moreover, the propellant lines are assumed to be infinitely rigid, in the analyses. MMH and NTO are used as the propellants in the system. Before opening of the isolation valve, the propellant exists upstream of the valve while the downstream line is evacuated or initially pressurized. The differential equations obtained in calculation are solved utilizing the Adams method of integration. It is concluded that for a constant tank pressure, the obtained peak pressure increases while the upstream line length is elongated and the downstream line length is kept constant. In addition, the obtained peak pressure increases while the downstream line length gets smaller and the upstream line length is kept constant. Moreover, the obtained peak pressure will be smaller for the larger initial pressure in the downstream line. The peak pressures obtained for MMH are higher than the ones obtained for NTO for the evacuated lines

because of the lower density and higher fluid velocity of MMH with respect to NTO. However the peak pressures were higher for NTO than the pressures for MMH for pressurized lines. The effects of valve opening time seem to be slight.

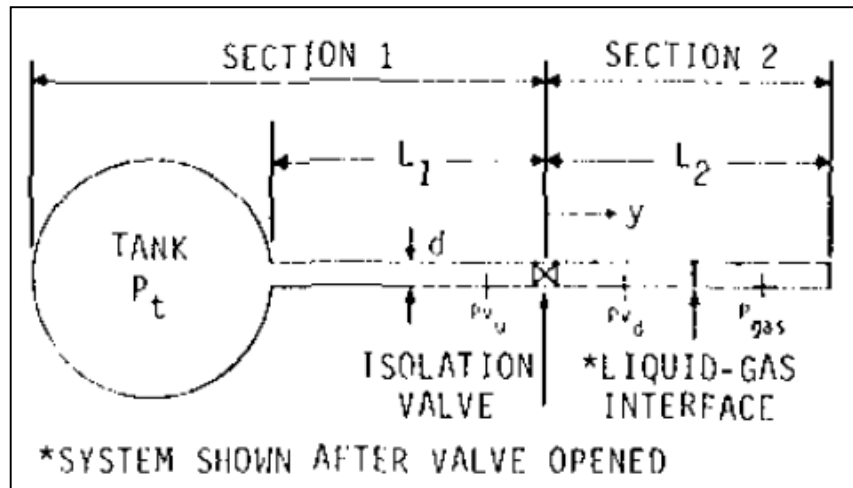


**Figure 1-13.** System model used in the analyses of Ref. [17]

In the study of Ref [18], a test setup has been designed with vertical tank, valve and tubing assembly on contrary to other studies. Moreover, in this test setup design, a liquid deaeration stand has been settled. The aim of this stand is to have the liquid free of gas bubbles. However when this paper was written, the mentioned test setup could not have been constructed. Hence the tests have been performed with a simpler test setup. This preliminary test setup is constructed in horizontal position (Figure 1-14), similar to the rest of studies and water has been utilized as the working fluid. One of the outcomes of this study is that considering the different tests at constant tank pressure, the time delay between the valve opening and the first pressure peak is slightly increasing when the initial pressure in the tubing downstream of the latch

valve is higher. Moreover according to the analyses performed, it can be assessed that as the tank pressure increases, regarding the peak pressure, the sensitivity to the pressure in the piping increases. The results of tests have been compared with the simulations performed with EcosimPro software and it is evaluated that EcosimPro overpredicts the pressure peak. Moreover a plateau has been detected in the variation. However such a pressure variation could not have been predicted by EcosimPro. It is assessed that the over prediction of EcosimPro might be because of the missing calculations about this pressure plateau. Finally, it is assessed that the overall comparison of tests with EcosimPro results are well matching.

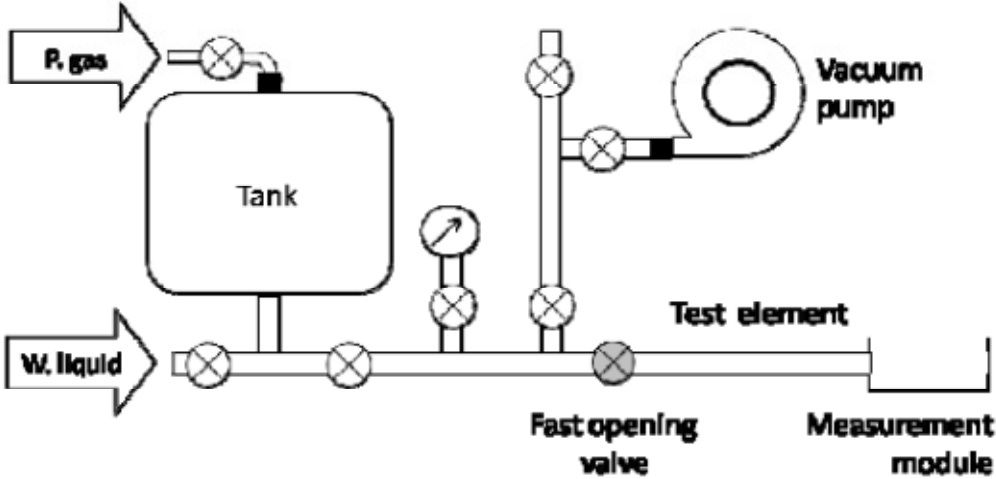


**Figure 1-14.** Test setup used in Ref [18]

In another study [19] on water hammer effects of satellite monopropellant propulsion system, the test setup shown in Figure 1-15 is constructed. Water is used as the working fluid. First, the pressure drop across the components has been found to be

functions of both pressure and flow rate. Later, steady state behavior (named as “blowdown” behavior, in Ref [19]) of the system has been observed and thirdly the water hammer effects occurring in the pulse mode operation of the system is investigated. It is evaluated that the obtained results for steady state operation are in well conformance to the theoretical calculations.

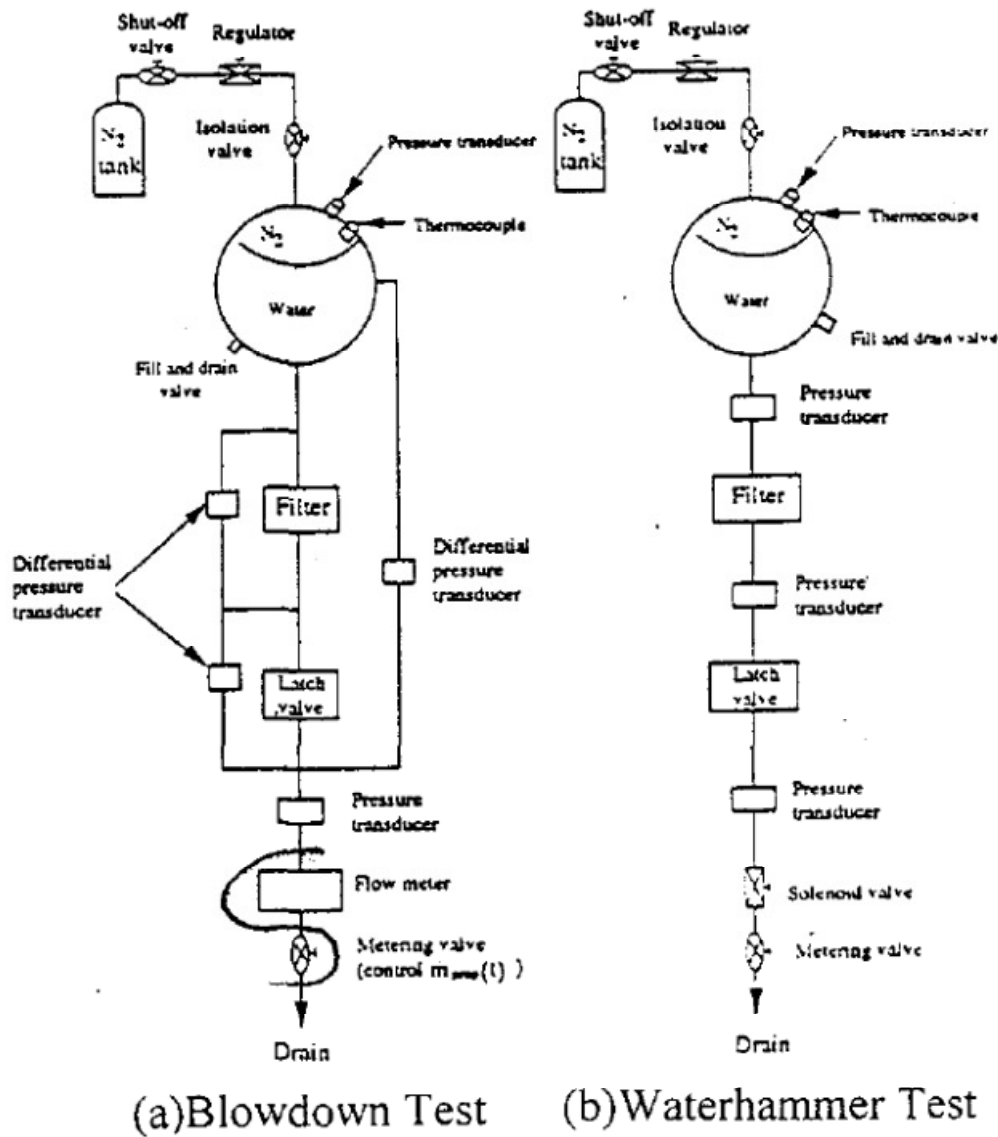
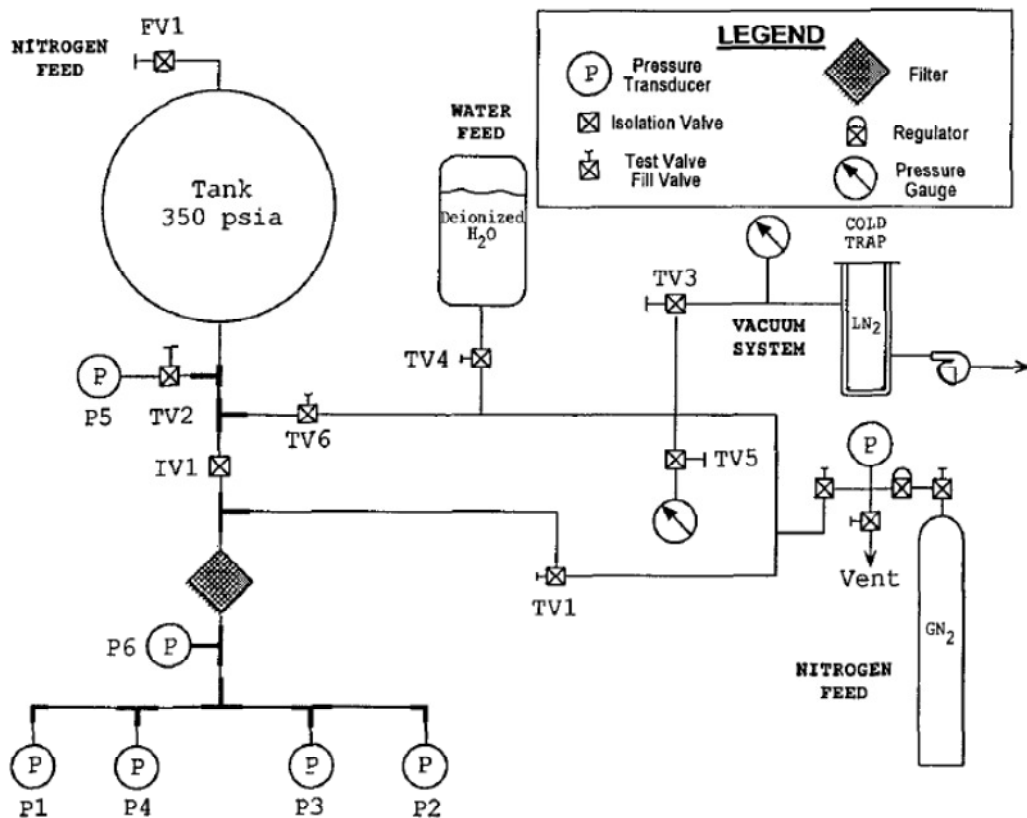


Figure 1-15. Test setup used in Ref. [19]

A test study has been conducted for Seastar Monopropellant Propulsion System, Ref [20]. In this study, the test setup seen in Figure 1-16 is constructed and water is used as the working fluid. The tank pressure is kept as 24.1 bar (350 psi). Tests with vacuum or nitrogen gas up to pressures 3.4 bar (50 psi) at the line downstream of the

IV1 valve have been conducted. Moreover, tests with water up to pressures 13.8 bar (200 psi) at the downstream line have been conducted for comparing with the results of tests with nitrogen. It is evaluated that for the downstream line pressure below 0.2 bar (3.2 psi), the pressure peak increases up to 269 bar (3900 psi). However when the downstream line pressure is kept about 1 bar, a pressure peak of 27 bar is obtained. It is decided to keep the downstream line pressure of Seastar Propulsion System at about 2 bar ( $30 \pm 5$  psi) during the launch. Inconsistent results have been obtained from the tests with water in the downstream line. It is concluded that as the downstream line pressure increases, the pressure peak decreases.



**Figure 1-16.** Test setup used in Ref. [20]

Another test campaign [21] has been conducted by the request of Ball Aerospace & Technologies Corp. The aim of this study was to verify the commercial Applied Flow Technologies (AFT) Impulse software by means of which the Ball Aerospace company models propulsion subsystem flow circuitry. The test setup used in the study is shown in Figure 1-17. Three branches with three pressure transducers and one valve in each branch are included in the setup. All the connections are constructed via Swagelok fittings so, the tubing lengths can be changed whenever desired. One large valve and two small valves produced by Moog are preferred in this study while Unistrut has been used for the supports. Labview is used for data acquisition and control. It is concluded that correlation between the simulations and test results is created and valuable information is obtained about the driving sensitivities of AFT software has been learned.

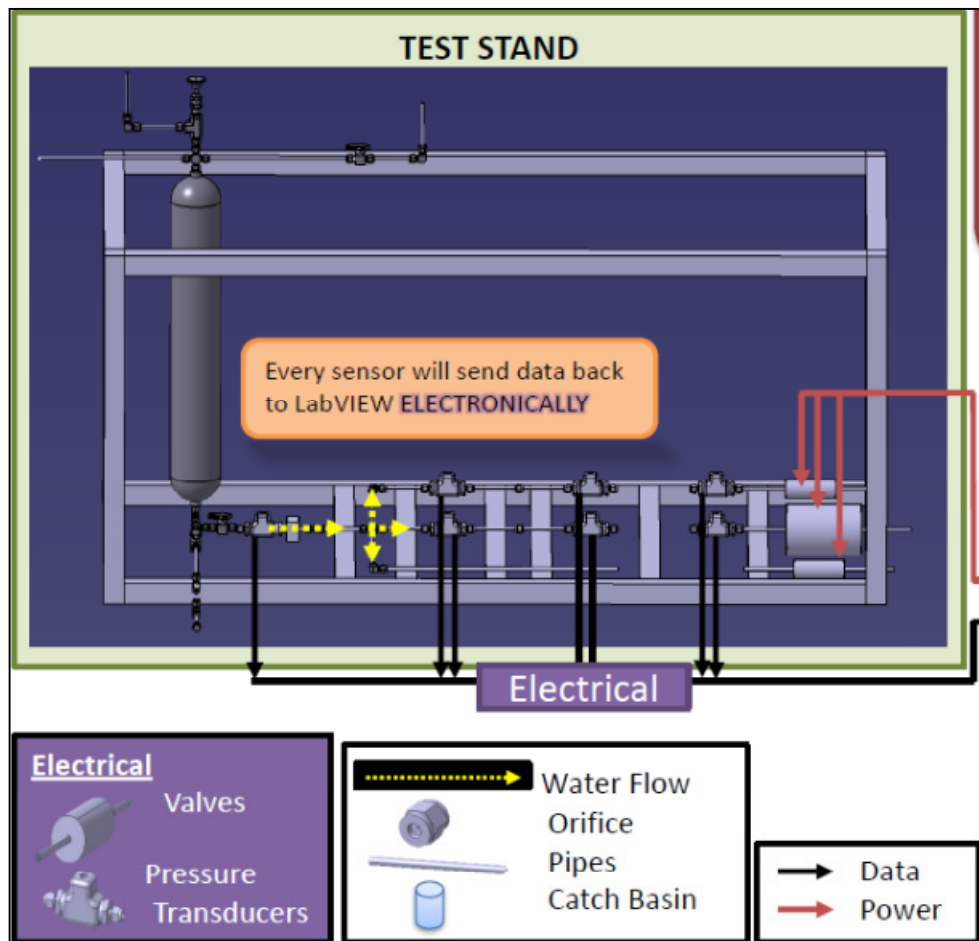


**Figure 1-17.** Test setup used in Ref. [21]

In the study of Ref [22], an analytical model has been developed. The results obtained with the developed model have been compared with the results in the literature. It is observed that the results from analytical model overpredicts the peak pressure with percentages changing from 3% to 100%. Moreover, a satellite bipropellant propulsion system has been analyzed via the developed model and it is evaluated that the results are well matching with the telemetry data of the satellite

with acceptable overprediction of the peak pressure. No tests have been conducted in the frame of this study.

Propulsion Systems similar to the ones used in satellites are used in the reaction control system of launch vehicles' upper stages. In the study of Ref. [23], water hammer has been analyzed for Ares I launch vehicle upper stage reaction control system that has a monopropellant propulsion system. In this study, the case of closing the thruster valve while a steady state flow exists is investigated. EASY5 commercial software that is developed by MSC Software is utilized in calculations. This software solves the governing equations using lumped parameter method taking also cavitation into account. Moreover, the fraction of gas in the propellant is also considered in the calculations. It is stated that the prediction of maximum pressure, flow rate and pressure drop are successful while the prediction of natural frequency is not successful.

A test campaign has been conducted for safe priming and depletion of Vega Launcher Hydrazine Roll and Attitude Control System (RACS) (Ref [24]). The test setup fully representative of flight tubing set was used while flow control valves were used instead of the pyro valves existing in the flight model. Hydrazine was used as the working fluid during tests. The hydrazine priming procedure has been verified in addition to successful depletion. Moreover, firing tests have been performed for investigating the effect of nitrogen bubbles in the hydrazine. It is assessed that the bubbles cause the thrust level to decrease when the bubbles pass through the thruster. After the bubbles pass from the thruster, no effects are observed in the thruster.

In addition to those mentioned studies, there are many studies on water hammer effects in the pipeline systems in the literature. Those studies are generally about the petroleum or water supply systems. References [25] to [30] are some examples of the studies done in Middle East Technical University on those topics.

In the study of Ref. [25], a computer code is written in Fortran IV language for the numerical solutions of developed equations. The results are compared with a previous study. Similarly, in Ref [26], a computer code is prepared in Fortran77 language for analyzing a liquid pipeline. The first Iraq-Turkey crude oil pipeline system is utilized as the case study. The results obtained via the developed software are again compared with the analysis results obtained in a previous study. In a similar way, in the study of Ref. [27], a computer code is written in Visual Basic language and graphically visualized; while in the study of Ref. [28], a computer code is written in Matlab and graphically visualized utilizing C# Graphical User Interface. Method of Characteristics is used in solution of the obtained differential equations in both studies. Iraq-Turkey oil pipeline is studied in also those theses. In the theses of [29] and [30], HAMMER commercial software is utilized for solving the governing differential equations.

There are also studies on the Fluid-Structure Interaction (FSI) of liquid filled pipeline systems. Tijsseling has published a very valuable literature survey [31] on this issue in addition to his numerous studies on this area. He introduces friction coupling, Poisson coupling and junction coupling and water hammer solutions with 2; 4; 6 or 14 equations in this paper. Moreover, Tijsseling has published the literature survey studies on water hammer with cavitation together with Bergant and Simpson (Ref. [32], [33]).

Many researches have been performed for the simulation of transient fluid flow for analyzing the water hammer effects. There are many scientists developing their own software in addition to the many commercial softwares in the market. Some of these commercial softwares are as follows:

EcosimPro / ESPSS Library	[34]
AFT Impulse	[35]
Deltares / WANDA	[36]
Flowmaster	[37]

Flownex	[38]
ANSYS CFX	[39]
HAMMER	[40]
EASY 5	[41]
COMMIX	[42]
KYPipe	[43]
Pipeline Studio	[44]
Etc.	

EcosimPro is the software developed by Empresarios Agrupados Internacional S.A. (EAI) [34]. The ESPSS (European Space Propulsion System Simulation) library of this software has been developed by the foundation of European Space Agency (ESA) for constructing a simulation platform for spacecraft and launch vehicle propulsion systems. Hence now there are many studies done with EcosimPro in the space propulsion area with the support of ESA. Unfortunately, since Turkey is not a member of ESA, establishments in Turkey cannot get access to the ESPSS library of EcosimPro software while it is the only library in the market specifically developed and verified for space propulsion. Hence, for Turkey, it is necessary to build its own space propulsion library after selecting or developing the software to make the transient flow analysis.

## **1.2 The Purpose and Scope of the Study**

The purpose of the study is to create a database on the water hammer phenomena under the same conditions with the ones faced in satellite propulsion system. In this frame, 1-D pressure transient analyses are performed. A test setup is constructed in ROKETSAN facilities and tests are performed in different conditions. As a consequence, the results of analyses and tests are compared.

In Chapter 2, pipeline hydraulics and consecutive correlations are presented. Later, in Chapter 3, Flownex Simulation tool and in Chapter 4, transient numerical analyses results are presented. In Chapter 5, detailed information about tests is given. In Chapter 6, test results and analyses results are compared, discussions about results are made. In Chapter 7, the conclusion of the thesis is done.

This page is left intentionally blank.

## CHAPTER 2

### PIPELINE HYDRAULICS

Steady flow is the flow condition where the properties of the flow do not change with time. On contrary, if the flow properties change with time, the flow is named as the transient flow. Water hammer is a type of transient flow where the elastic properties of the pipe and flow are important in the analysis of the flow.

Water hammer occurs when there is a sudden valve closure or opening or pump stopping or starting. In case of water hammer, the flow pressure increases dramatically. In order to be sure that the structural resistance will not be exceeded hence there will not be a failure in the system, a transient flow analysis should be performed.

In this chapter, the main formulas that are used in pipeline hydraulics are presented. The detailed explanation of their derivation is presented in Appendix A.

One of the important parameters is the change in liquid volume due to compressibility. As it is stated in Ref [45], during the passage of a pressure wave, the pressure increases and the velocity decreases while the density of the flow increases slightly due to the slight volume decrease in the control volume. The relation between the pressure increase and volume decrease is defined by the compressibility of fluid and bulk modulus of elasticity.

Compressibility is the measure of the relative volume change as a response to a pressure change.

$$\beta = -\frac{1}{V} \frac{\partial V}{\partial p}$$

Where,  $\beta$  is the compressibility and  $V$  is volume.

Bulk modulus of elasticity is the measure of the substance's resistance to uniform

compression. It is the inverse of compressibility and given by:

$$K = -V \frac{\partial p}{\partial V}$$

Hence,

$$\delta V = -\Delta p \frac{V}{K} \quad (2-1)$$

where,  $\delta V$  is the change in the liquid volume in the control volume due to pressure change,  $\Delta p$ .

Change in pipe volume due to elasticity is as below:

$$\delta V = \frac{\pi}{4} D^2 \delta L (\Delta \varepsilon_1 + 2\Delta \varepsilon_2) \quad (2-2)$$

Where,  $\varepsilon_1$  and  $\varepsilon_2$  are the strains in the direction along pipe axis and in circumferential direction, respectively.

Using the Euler equation, mass accumulation, change in liquid volume due to compressibility and change in pipe volume due to elasticity, the speed of sound in the liquid is calculated as in equation (2-3). Here, three cases are considered for longitudinal stress and strain:

- Case (a): Pipe anchorage only at the upstream end
- Case (b): Full pipe restraint from axial movement
- Case (c): Longitudinal expansion joints along the pipeline

$$a = \frac{\sqrt{\frac{K}{\rho}}}{\sqrt{1 + \frac{K D}{E e} (C)}} \quad (2-3)$$

Where, For Case (a) restraint:  $C = \frac{5}{4} - \mu$

For Case (b) restraint:  $C = 1 - \mu^2$

For Case © restraint:  $C = 1.0$

According to [9], in case of sudden valve closing while the fluid flows, the pressure increase due to water hammer depends on the valve closing time. As explained in section 1.1, two types of perturbation exist:

- In the savage perturbation, the valve closing time  $t$  is lower than the wave propagation time in tubing ( $t < 2L/a$ ). In this case the pressure peak is calculated with equation (2-4) such that:

$$\Delta P = \rho a V \quad (2-4)$$

- In the slow perturbation, the valve closing time is greater than the wave propagation time in tubing ( $t > 2L/a$ ). In this case the pressure peak is calculated as:

$$\Delta P = 2\rho L V / t \quad (2-5)$$

Frequency of wave speed for the case where a valve is closed suddenly while a fluid flow exists in the pipeline is as shown below according to [9] and [49]:

$$f = \frac{a}{4L} \quad (2-6)$$

Where,  $a$  is the wave speed calculated according to equation (2-3) and  $L$  is the pipe length.

According to this formula, the frequency of the wave is independent from the pressure.

Solving the conservation of mass utilizing the governed equations below differential

equation is obtained:

$$\frac{1}{\rho} \frac{dp}{dt} = a^2 \frac{\partial V}{\partial s} \quad (2-7)$$

Above equations are valid for the water hammer case that happens if a valve is closed while steady liquid flow exists. However they are not applicable in our case where, the latch valve is opened and the liquid at rest starts to flow into pipeline filled with air. The reason of that is the existence of air at the end of pipeline and its cushioning effect to the liquid flow.

## CHAPTER 3

### FLOWNEX SIMULATION TOOL

Flownex has been developed by the Flownex Simulation Environment Company starting from 1986. ISO 9001:2008 and NQA1 quality assurance system are the accreditations of Flownex. Flownex is used for power generation systems, aerospace systems, oil and gas systems, mining systems, HVAC-R systems, etc where fluid flow exists. Flownex is the only software of its kind that has a nuclear accreditation [47]

Flownex has the ability to solve the steady state and dynamic flow simulations of systems in any combination of liquid systems, gas systems, mixtures of gases, two phase systems, with phase changes, incondensable mixtures of two phase fluids with gases, etc.

Conservation of mass, momentum and the energy equations are the governing equations solved in Flownex for simulations.

Implicit Pressure Correction Method (IPCM) is used as the solution algorithm. This method has below steps as stated in Ref. [48]:

1. Guess initial node pressures
2. Calculate mass flows using  $\Delta p$ - $Q$  relationships
3. Test for continuity at all nodes
4. Adjust pressures to ensure continuity at all nodes
5. Update mass flows using new updated pressures
6. Repeat 1 to 5 until convergence
7. Solve the energy equation
8. Repeat 1 to 7 until convergence
9. Move to next time step and repeat 1 to 8 (only for transient simulations)

The equations solved for transient analysis are as shown below (Ref. [48]):

### 3.1 Conservation of Mass

The flow control volume used for the one dimensional flow analysis is shown in Figure 3-1. *i* and *e* subscripts are used for inlet and exit parameters.

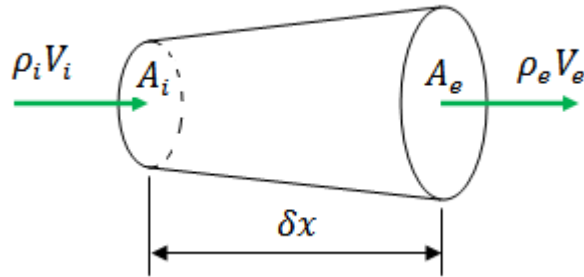


**Figure 3-1.** Flow control volume used in Flownex calculations

$$\frac{\partial \bar{\rho}}{\partial t} + \frac{\partial (\bar{\rho} V)}{\partial x} = 0 \quad (3-1)$$

Equation (3-1) is the generic continuity equation. By integrating equation (3-1) first over control volume and later over time span, equation (3-2) is obtained. The superscript “o” is used for the parameters in previous time step. The bars above the variables are used indicating the average values of the variables across the control volume.

$$\bar{\rho} - \bar{\rho}^0 = \frac{\Delta t}{V} (\alpha (\sum \dot{m}_i - \sum \dot{m}_e) + (1 - \alpha) (\sum \dot{m}_i^0 - \sum \dot{m}_e^0)) \quad (3-2)$$

$\alpha = 0$  For fully explicit

$\alpha = 0.5$  For Crank-Nicholson

$\alpha = 1$  For fully implicit

### 3.2 Conservation of Momentum

The conservation of momentum equation used for the one dimensional compressible flow is shown in equation (3-3).

$$\rho \frac{\partial V}{\partial t} + \frac{p}{p_0} \frac{\partial p_0}{\partial x} + \rho g \frac{\partial z}{\partial x} + \frac{\rho V^2}{2T_0} \frac{\partial T_0}{\partial x} + \frac{f\rho|V|V}{2D} = 0 \quad (3-3)$$

Integrating equation (3-3) first over control volume and then over time span, equation (3-4) is obtained.

$$\begin{aligned} \bar{\rho}\bar{V} - \bar{\rho}^0\bar{V}^0 = & -\frac{\Delta t}{L} \left\{ \alpha \left[ \frac{\bar{p}}{\bar{p}_0} (p_{0e} - p_{0i}) + \bar{\rho}g(z_e - z_i) \right. \right. \\ & + (T_{0e} - T_{0i}) \frac{1}{\bar{T}_0} \frac{\bar{m}^2}{2\bar{\rho}\bar{A}^2} + \left( \frac{fL}{D} + \sum K \right) \frac{|\bar{m}|\bar{m}}{2\bar{\rho}\bar{A}^2} \\ & + (1 - \alpha) \left[ \frac{\bar{p}^0}{\bar{p}_0^0} (p_{0e}^0 - p_{0i}^0) + \bar{\rho}^0g(z_e - z_i) \right. \\ & \left. \left. + (T_{0e}^0 - T_{0i}^0) \frac{1}{\bar{T}_0^0} \frac{(\bar{m}^0)^2}{2\bar{\rho}^0\bar{A}^2} + \left( \frac{f^0L}{D} + \sum K^0 \right) \frac{|\bar{m}^0|\bar{m}^0}{2\bar{\rho}^0\bar{A}^2} \right] \right\} \end{aligned} \quad (3-4)$$

### 3.3 Conservation of Energy

The conservation of energy equation used for one dimensional flow is shown in equation (3-5) in terms of stagnation temperature.

$$\frac{\partial(\rho c_p T_0 - p)}{\partial t} + \frac{\partial(\rho V c_p T_0)}{\partial x} + \rho V g \frac{\partial z}{\partial x} - \dot{q}_H + \dot{w} = 0 \quad (3-5)$$

Integrating equation (3-5) first over control volume and then over time span,

equation (3-6) is obtained.

$$\begin{aligned}
& (\bar{\rho}c_p\bar{T}_0 - \bar{p}) - (\bar{\rho}^0c_p\bar{T}_0^0 - \bar{p}^0) \\
&= -\frac{\Delta t}{V} \left\{ \alpha \left[ \sum (\dot{m}_e c_p T_{0e}) \right. \right. \\
&\quad \left. \left. - \sum (\dot{m}_i c_p T_{0i}) + \sum (\dot{m}_e g z_e) - \sum (\dot{m}_i g z_i) - \dot{Q}_H + \dot{W} \right] \right. \\
&\quad \left. + (1 - \alpha) \left[ \sum (\dot{m}_e^0 c_p T_{0e}^0) - \sum (\dot{m}_i^0 c_p T_{0i}^0) \pm \sum (\dot{m}_e^0 g z_e) \right. \right. \\
&\quad \left. \left. - \sum (\dot{m}_i^0 g z_i) - \dot{Q}_H^0 + \dot{W}^0 \right] \right\} \quad (3-6)
\end{aligned}$$

### 3.4 Convergence Criteria

The convergence criteria for steady-state and transient solutions are 1e-6. The solution is considered to have converged if all conservation equations are applied with an error value smaller than the convergence criterion.

## CHAPTER 4

### TRANSIENT NUMERICAL ANALYSES

In the satellite propulsion design, below parameters are the main design decisions. So, in order to understand the effect of change of these parameters on the water hammer transients, the transient numerical analyses were performed with different values of below input parameters:

- Tank pressure
- Downstream line pressure
- Distance between tank and orifice (L1)
- Distance between orifice and latch valve (L2)
- Distance between latch valve and exit valve (L3)
- Orifice diameter
- Pipe diameter

As described in the thesis before, the maximum pressure is one of the most critical parameters in transient analysis during priming. In addition to that, the frequency of the pressure waves is important in order to evaluate the effect of liquid waves fluctuation on the structural integrity of the system. In the literature, there are many studies on maximum pressure and the pressure wave frequency. However, there is no study explaining the change of pressure amplitude with respect to the tank pressure change and transient flow duration change with respect to the other design parameters. In order to understand their behavior and analyze the effects of above design criteria on the maximum pressure and frequency, below parameters from analyses results were compared:

- Maximum pressure
- Maximum amplitude of pressure (Difference between the maximum pressure and tank pressure)
- Frequency from the FFT of pressure data

- Transient flow duration

In total, 60 analyses were performed in this study. The analysis matrix and results are presented in Table 4-1. The design philosophy of the analysis matrix is as explained below:

- **Different Tank Pressures:** Analyses from 0 to 6 are the cases with different tank pressures but with the other parameters such as downstream line pressure (0.5 bar), L1 (1 m), L2 (1 m) and L3 (1 m) lengths, orifice diameter (5.53 mm, same as the pipe inner diameter, no orifice condition) and pipe inner diameter (5.53 mm) remaining the same. The tank pressure of a satellite propulsion system generally changes in the range of 15-25 bar. So, the analyses points were started from 10 bar and cover pressures until 30 bar. The tank pressures from 40 bar to 70 bar were used in order to have larger number of data points to see the trend of parameters' change.
- **Different Downstream Line Pressures:** Analyses from 6 to 12 are the cases with different downstream line pressures but with the other parameters such as tank pressure (70 bar), L1 (1 m), L2 (1 m) and L3 (1 m) lengths, orifice diameter (5.53 mm, same as the pipe inner diameter, no orifice condition) and pipe inner diameter (5.53 mm) remaining the same. The downstream line pressure of a satellite propulsion system generally changes in the range of vacuum-1 bar. With this aim, the downstream pressure data points were started from 0.5 bar in the analysis matrix. Moreover, in order to see the effect of downstream line pressure change easily and to have larger number of data points, the downstream line pressure was increased up to 60 bar in the analysis matrix.
- **Different Distances Between Tank and Orifice (L1):** Analyses 13 and from 22 to 25 are the cases with different distances between tank and orifice (L1) but with the other parameters such as tank pressure (10 bar), downstream line pressure (0.5 bar), L2 (0.5 m), L3 (0.5 m) lengths, orifice diameter (5.53 mm, same as the pipe inner diameter, no orifice condition) and pipe inner diameter (5.53 mm) remaining the same. The L1 length of a

satellite propulsion system generally changes in the range of 0.5 m – 1 m. Hence 0.5 m was selected as the minimum value of the L1 length data points. In addition, in order to increase the number of data points for observing the trend of change of parameters easily, the L1 length was increased up to 4 m in the analysis matrix.

- **Different Distances Between Orifice and Latch Valve (L2):** Analyses 13 and from 18 to 21 are the cases with different distances between orifice and latch valve (L2) but with the other parameters such as tank pressure (10 bar), downstream line pressure (0.5 bar), L1 (0.5 m), L3 (0.5 m) lengths, orifice diameter (5.53 mm, same as the pipe inner diameter, no orifice condition) and pipe inner diameter (5.53 mm) remaining the same. The L2 length of a satellite propulsion system generally changes in the range of 0.5 m – 1m. Hence 0.5 m was selected as the minimum value of the L2 length data points. In addition, in order to increase the number of data points for observing the trend of change of parameters easily, the L2 length was increased up to 4 m in the analysis matrix.
- **Different Distances Between Latch Valve and Exit Valve (L3):** Analyses from 13 to 17 are the cases with different distances between latch valve and exit valve (L3) but with the other parameters such as tank pressure (10 bar), downstream line pressure (0.5 bar), L1 (0.5 m), L2 (0.5 m) lengths, orifice diameter (5.53 mm, same as the pipe inner diameter, no orifice condition) and pipe inner diameter (5.53 mm) remaining the same. The L3 length of a satellite propulsion system generally changes in the range of 0.5 m – 3 m. Hence 0.5 m was selected as the minimum value of the L3 length data points. In addition, in order to increase the number of data points for observing the trend of change of parameters easily, the L3 length was increased up to 4 m in the analysis matrix.
- **Different Orifice Diameters:** Analyses 1 and from 26 to 34 are the cases with different orifice diameters but with the other parameters such as tank pressure (10 bar), downstream line pressure (0.5 bar), L1 (1 m), L2 (1 m),

L3 (1 m) lengths and pipe inner diameter (5.53 mm) remaining the same. In a typical monopropellant satellite propulsion system the pipe outer diameter is ¼” (6.35 mm). Generally the titanium is used as the pipe material and under these conditions the pipe thickness can be selected as 0.016” (0.41 mm). Hence, the pipe inner diameter equals to 5.53 mm. In order to see the effect of different orifice diameters, they were chosen starting from 0.5 mm up to 5.53 mm that means no orifice restriction case.

- **Different Pipe Diameters:** Analyses 1 and from 35 to 39 are the cases with different pipe inner diameters but with the other parameters such as tank pressure (10 bar), downstream line pressure (0.5 bar), L1 (1 m), L2 (1 m), L3 (1 m) lengths and pipe thickness (0.41 mm) remaining the same. The orifice diameters were used same as the pipe inner diameters meaning that no orifice restriction were used in these cases. As explained above, in a typical monopropellant satellite propulsion system the pipe outer diameter is ¼”. In the bipropellant propulsion systems, the outer diameter of the pipe is generally 3/8” (9.525 mm) or ½” (12.7 mm). In order to cover these diameters and to have larger number of data points, the pipe inner diameters were selected between 2 mm and 15 mm in the analysis matrix.
- **Test Conditions:** Analyses from 40 to 60 are the cases representing the test conditions that were done in the frame of this thesis. The tank pressures of the analyses were chosen on the integer limits of the test cases. As an example, if the test was done with tank pressure of 13.67 bar, the analyses were performed both with tank pressures of 13 bar and 14 bar. The downstream line pressures of the analyses were chosen the same as the test condition. It can be either 0.94 bar (atmospheric pressure in Ankara/Elmadag) or 0.15 bar (vacuum pressure). The L1 and L2 lengths are 30 cm and the same as used in the test setup constructed. L3 is either 1 m or 2 m, same as the test condition performed. Pipe outer diameter is ¼” (6.35 mm) as used generally in the monopropellant satellite propulsion systems and the thickness of the pipe is 0.035” (0.889 mm). Under these

conditions, the pipe inner diameter is 4.57 mm. The orifice diameter is either 4.57 mm (same as pipe inner diameter, meaning that no orifice restriction) or 1.5 mm, same as the test condition performed.

**Table 4-1. Analyses inputs and results**

Analysis No	Inputs							Outputs			
	Tank Pressure (bar)	Downstream Line Pressure (bar)	L1 (cm)	L2 (cm)	L3 (cm)	Orifice Diameter (mm)	Pipe Inner Diameter (mm)	Maximum Pressure (bar)	Amplitude (bar)	Frequency	Transient Flow Duration (s)
0	10	0.5	100	100	100	5.53	5.53	114.4	104.46	18.62	0.426
1	20	0.5	100	100	100	5.53	5.53	186.7	166.75	35.4	0.822
2	30	0.5	100	100	100	5.53	5.53	241.1	211.13	49.44	0.631
3	40	0.5	100	100	100	5.53	5.53	288.8	248.86	56.76	0.546
4	50	0.5	100	100	100	5.53	5.53	329.2	279.19	55.24	0.548
5	60	0.5	100	100	100	5.53	5.53	367.3	307.3	59.81	0.501
6	70	0.5	100	100	100	5.53	5.53	404.3	334.27	63.48	0.465
7	70	10	100	100	100	5.53	5.53	295.8	225.77	30.52	0.209
8	70	20	100	100	100	5.53	5.53	200.6	130.6	21.67	0.236
9	70	30	100	100	100	5.53	5.53	139.5	69.46	17.09	0.304
10	70	40	100	100	100	5.53	5.53	107.8	37.84	14.04	0.405
11	70	50	100	100	100	5.53	5.53	90.3	20.3	12.21	0.534
12	70	60	100	100	100	5.53	5.53	79.1	9.1	10.68	0.811
13	10	0.5	50	50	50	5.53	5.53	144.4	134.44	42.11	0.654
14	10	0.5	50	50	100	5.53	5.53	127.8	117.8	25.02	0.286
15	10	0.5	50	50	200	5.53	5.53	91.3	81.29	16.17	0.346
16	10	0.5	50	50	300	5.53	5.53	68.2	58.24	11.6	0.422
17	10	0.5	50	50	400	5.53	5.53	53.5	43.47	9.16	0.501
18	10	0.5	50	100	50	5.53	5.53	130.6	120.59	35.1	0.774
19	10	0.5	50	200	50	5.53	5.53	109.9	99.92	27.16	0.975
20	10	0.5	50	300	50	5.53	5.53	96.4	86.35	22.58	1.119
21	10	0.5	50	400	50	5.53	5.53	86.6	76.61	19.53	1.273
22	10	0.5	100	50	50	5.53	5.53	130.8	120.75	35.1	0.774
23	10	0.5	200	50	50	5.53	5.53	110.8	100.8	27.16	0.976
24	10	0.5	300	50	50	5.53	5.53	97.0	86.98	22.58	1.122
25	10	0.5	400	50	50	5.53	5.53	87.2	77.19	19.53	1.276
26	10	0.5	100	100	100	0.5	5.53	10.1	0.08	21.28	0.263
27	10	0.5	100	100	100	0.8	5.53	10.5	0.51	21.1	0.267

**Table 4-1. Analyses inputs and results (cont.)**

28	10	0.5	100	100	100	1	5.53	11.3	1.25	20.45	0.275
29	10	0.5	100	100	100	1.5	5.53	16.5	6.47	21.36	0.253
30	10	0.5	100	100	100	2	5.53	31.0	20.95	21.36	0.239
31	10	0.5	100	100	100	2.5	5.53	53.5	43.49	21.06	0.263
32	10	0.5	100	100	100	3	5.53	74.6	64.58	20.75	0.306
33	10	0.5	100	100	100	4	5.53	100.7	90.71	20.45	0.363
34	10	0.5	100	100	100	5	5.53	111.5	101.47	18.62	0.421
35	10	0.5	100	100	100	2	2	37.1	27.08	42.42	0.143
36	10	0.5	100	100	100	3	3	48.6	38.63	22.89	0.267
37	10	0.5	100	100	100	5	5	70.5	60.48	21.36	0.365
38	10	0.5	100	100	100	10	10	99.1	89.11	47.3	0.338
39	10	0.5	100	100	100	15	15	160.2	150.2	20.75	1.147
40	5	0.94	30	30	2	4.57	4.57	11.6	6.61	5.49	0.772
41	5	0.15	30	30	2	4.57	4.57	58.3	53.3	14.04	0.426
42	6	0.94	30	30	2	4.57	4.57	17.0	10.95	6.71	0.612
43	6	0.15	30	30	2	4.57	4.57	68.9	62.91	16.48	0.407
44	7	0.94	30	30	2	4.57	4.57	23.6	16.62	7.93	0.507
45	7	0.15	30	30	2	4.57	4.57	78.4	71.44	17.4	0.417
46	8	0.15	30	30	2	4.57	4.57	87.1	79.12	22.58	0.339
47	9	0.15	30	30	2	4.57	4.57	95.2	86.19	24.72	0.322
48	13	0.94	30	30	2	4.57	4.57	74.9	61.93	14.95	0.308
49	14	0.94	30	30	2	4.57	4.57	82.8	68.77	16.17	0.298
50	15	0.94	30	30	2	4.57	4.57	90.4	75.44	17.09	0.294
51	16	0.94	30	30	2	4.57	4.57	97.7	81.73	18.31	0.286
52	6	0.94	30	30	1	4.57	4.57	35.7	29.69	11.29	0.331
53	7	0.94	30	30	1	4.57	4.57	49.6	42.62	13.12	0.294
54	8	0.94	30	30	1	4.57	4.57	62.8	54.84	14.95	0.275
55	6	0.15	30	30	1	4.57	4.57	93.4	87.37	27.77	0.296
56	7	0.15	30	30	1	4.57	4.57	104.0	97.01	30.52	0.280
57	7	0.94	30	30	1	1.5	4.57	9.2	2.2	13.12	0.426
58	8	0.94	30	30	1	1.5	4.57	10.9	2.94	14.95	0.369

**Table 4-1.** Analyses inputs and results (cont.)

59	7	0.15	30	30	1	1.5	4.57	22.4	15.4	32.96	0.161
60	8	0.15	30	30	1	1.5	4.57	26.2	18.19	36.93	0.149

The test setup model used in the analyses is shown in **Error! Reference source not found.** Tank is modeled as a boundary condition, similar to the exit solenoid valve. Latch valve is modeled similar to orifice where it is totally closed at time  $t = 0^-$  and it is totally open at  $t = 0^+$ . The pipe between the latch valve and exit solenoid valve is modeled as an accumulator with a diaphragm separating liquid and air. At  $t = 0$  the length of the pipe filled with liquid is 0.1 mm while the rest of the pipe is filled with air (at ambient pressure or vacuum pressure). As time elapses, the length of the pipe section filled with liquid and air changes. Water is used as the working fluid in the analyses. Pipe material taken into account is titanium alloy Ti6Al4V. The pressure of the pipeline between the latch valve and exit solenoid valve where it is vacuumed normally is named as downstream line pressure.



## 4.1 Analyses Results Post-Processing

First of all, it is necessary to explain the post-processing method of the results. Fast Fourier Transform (FFT) is used for determining the frequency of the pressure waves. FFT is the fast form of Discrete Fourier Transform (DFT). DFT operates with discrete data and transforms  $N$  spatial/ temporal points to  $N$  frequency points. DFT of function  $f(x)$  and its inverse operation are as shown below:

$$F(k) = \int_{-\infty}^{\infty} f(x) e^{-2\pi i x k} dx$$

$$f(x) = \int_{-\infty}^{\infty} F(k) e^{2\pi i x k} dk$$

MATLAB is used as the calculation tool for FFT and the `fft.m` function of MATLAB has been utilized. The written function `FFT_THESIS.m` used in FFT calculation of pressure waves is presented in Appendix B.

The frequency,  $f$ , of the pressure wave is obtained from the FFT of data.

$$T = \frac{1}{f}$$

where,  $T$  is the period of the wave as shown in Figure 4-2.

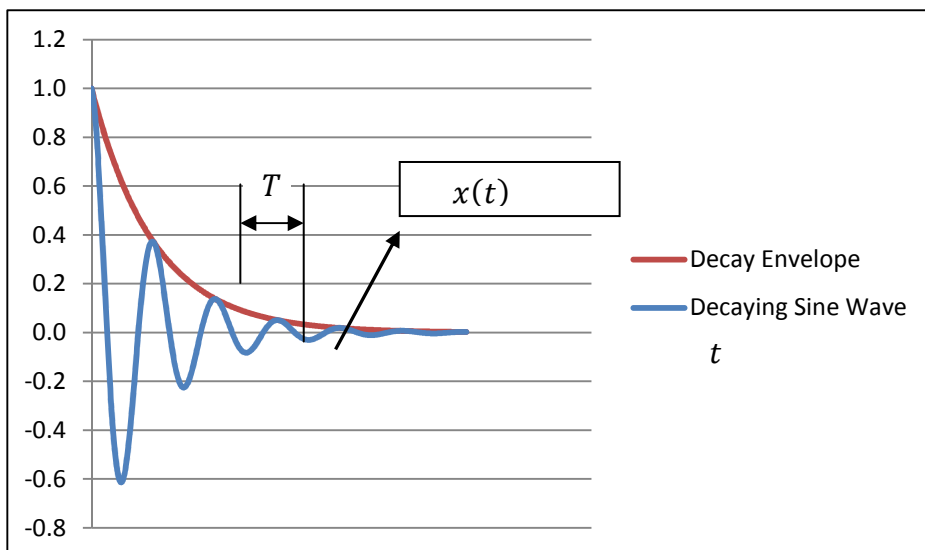


**Figure 4-2.** Damped sine wave

Exponential decay rate,  $\alpha$ , is the important parameter for evaluating the decay performance of an underdamped ( $\xi < 1$ ) wave. For the amplitude  $x(t)$  of the peak at time  $t$  and amplitude  $x(t + nT)$  of the peak at time  $t + nT$  where  $n$  is the number of peaks between those two peaks are used for the calculation of logarithmic decrement,  $\delta$ , as shown below.

$$\delta = \frac{1}{n} \ln \frac{x(t)}{x(t + nT)} \quad (4-1)$$

For two successive peaks,  $n$  equals to one and above equation becomes:

$$\delta = \ln \frac{x_1}{x_2}$$

Damping ratio,  $\xi$ , is find as:

$$\xi = \frac{\delta}{\sqrt{(2\pi)^2 + \delta^2}} \quad (4-2)$$

The damped angular frequency,  $\omega_d$ , is find as:

$$\omega_d = 2\pi f = \frac{2\pi}{T} \quad (4-3)$$

Undamped natural frequency,  $\omega_0$ , is find as:

$$\omega_0 = \frac{\omega_d}{\sqrt{1 - \xi^2}} \quad (4-4)$$

Finally, the exponential decay rate,  $\alpha$ , is find as:

$$\alpha = \xi \omega_0 \quad (4-5)$$

The wave decays faster as the exponential decay rate increases. The change of decay envelope with respect to the decay rate is shown in Figure 4-3 as an example.

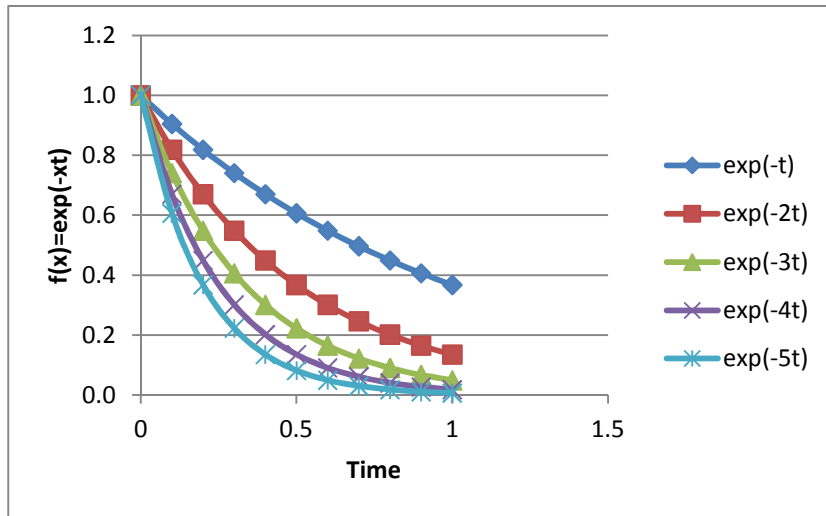


**Figure 4-3.** Exponential decay

The transient flow duration is another important parameter for a decaying sine wave. It is determined using the time constant,  $\tau$ , where;

$$\tau = \frac{1}{\alpha} \quad (4-6)$$

As a rule of thumb, it is accepted that the steady state is reached in an exponentially decaying system after  $t = 5\tau$ . Hence, the transient flow duration is calculated accordingly.

## 4.2 Analyses Results

Eight different cases are investigated in the analyses. They are such as:

1. Different tank pressures versus constant downstream line pressure
2. Constant tank pressure versus different downstream line pressures
3. Constant L1 and L2 lengths versus different L3 lengths
4. Constant L1 and L3 lengths versus different L2 lengths
5. Constant L2 and L3 lengths versus different L1 lengths
6. Constant total length (L1+L2+L3) versus different L1, L2 and L3 lengths
7. Constant pressures and lengths versus different orifice diameters
8. Constant pressures and lengths versus different pipe inner diameters

Those analysis results are explained here below in detail.

#### 4.2.1 CASE 1: Different Tank Pressures versus Constant Downstream Line Pressure

Analysis numbers 0, 1, 2, 3, 4, 5 and 6 (as presented in Table 4-1) are compared. Downstream line pressure is 0.5 bar and the dimensions are L1: 100 cm, L2: 100 cm and L3: 100 cm while the orifice diameter is 5.53 mm (same as pipeline diameter: no restriction).

The pressure versus time change of analysis number 0 is presented in Figure 4-4 as an example. The water hammer effect and the damped harmonic motion of the waves can be seen clearly from this figure. It is seen that the pressure fluctuates around the tank pressure (red line) and converges to tank pressure at the end.

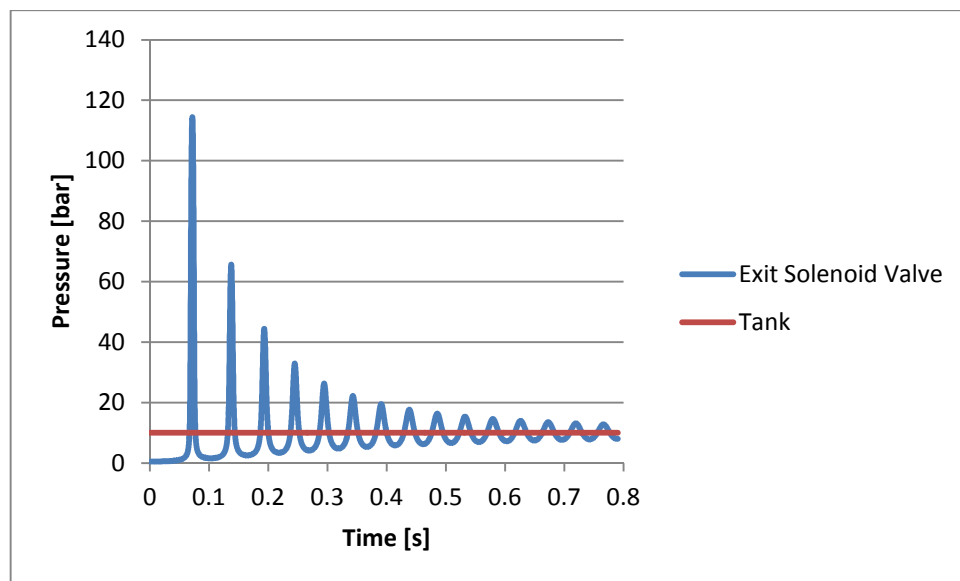
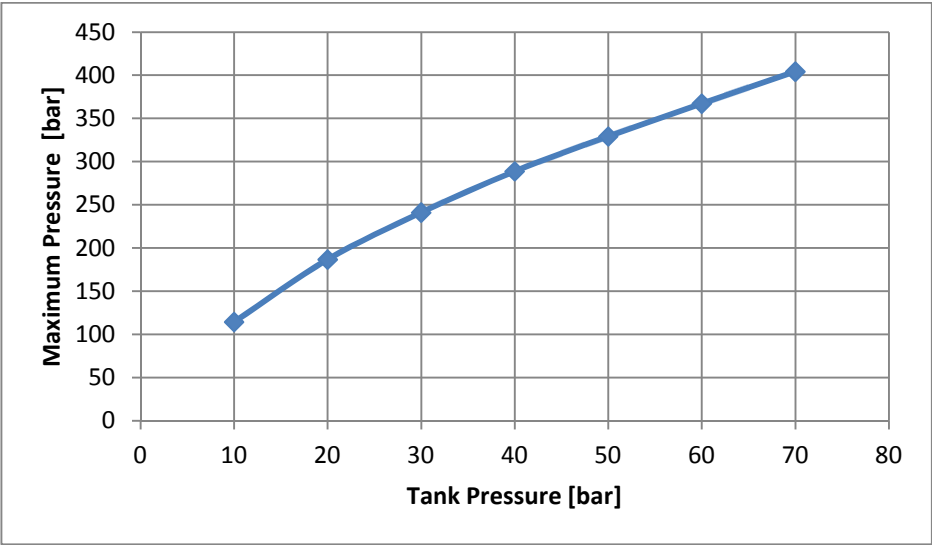
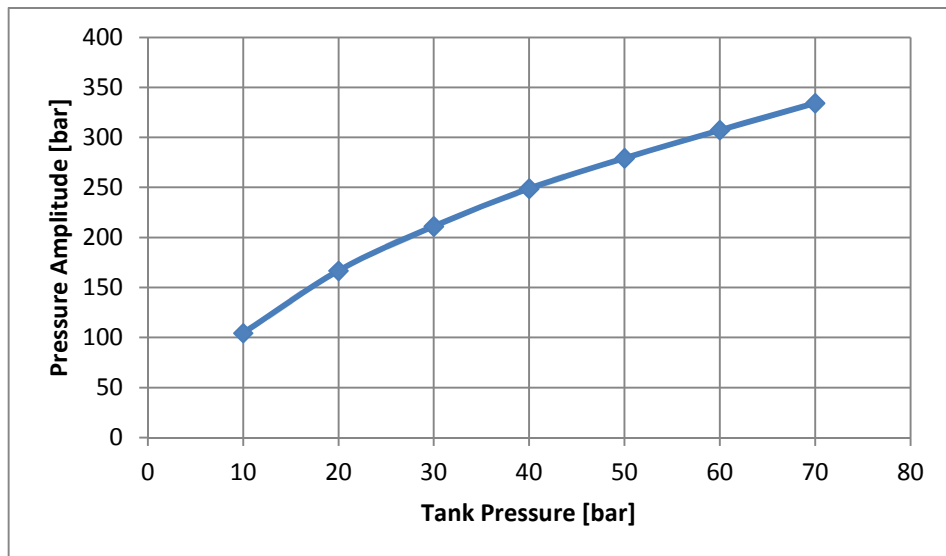


Figure 4-4. Pressure versus time graph for analysis No 0

Maximum pressures occurring in the mentioned analyses are compared in Figure 4-5. It is seen from that figure that as the tank pressure increases, the maximum pressure also increases linearly. In order to see whether the amplitudes are the same or not, the amplitudes are compared as presented in Figure 4-6. It is seen that the amount of pressure rise increases linearly as the tank pressure increases.



**Figure 4-5.** Maximum pressure versus tank pressure graph for Case 1



**Figure 4-6.** Pressure amplitude versus tank pressure graph for Case 1

Frequencies of the analyses are shown in Figure 4-7. This variation of frequency with respect to the tank pressure is different than what would be expected with the formula presented in equation (2-6). As explained at the end of Chapter 2, it is evaluated that this difference is because of the air trapped in the pipeline and equation (2-6) cannot be used for our case.

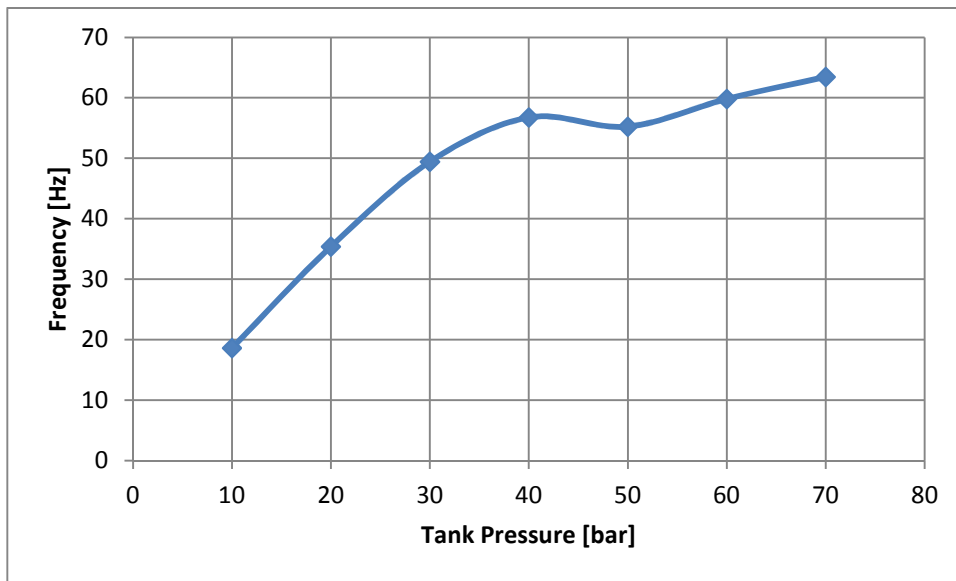


**Figure 4-7.** Frequency versus tank pressure graph for Case 1

The transient flow duration calculated as explained in section 4.1 is shown in Figure 4-8. As can be seen from this figure, the transient flow duration does not follow a certain trend. Hence, it is not possible to comment on the change of transient flow duration with respect to the tank pressure change.

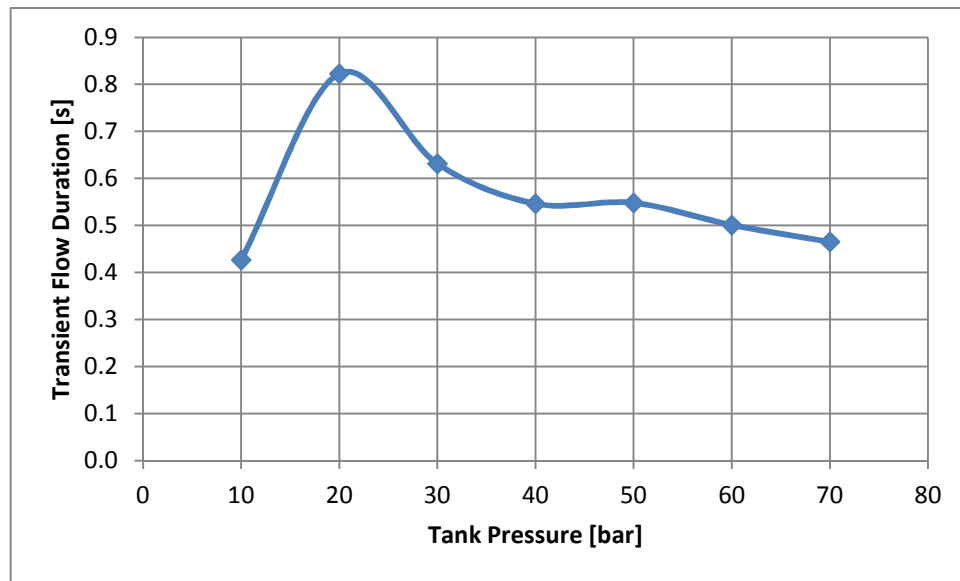


**Figure 4-8.** Transient flow duration versus tank pressure graph for Case 1

#### **4.2.2 CASE 2: Constant Tank Pressure versus Different Downstream Line Pressures**

Analysis numbers 6, 7, 8, 9, 10, 11, 12, where the tank pressure is 10 bar are compared. The dimensions are L1: 100 cm, L2: 100 cm and L3: 100 cm while the orifice diameter is 5.53 mm (same as pipeline diameter: no restriction).

First, the maximum pressures are compared as shown in Figure 4-9. The maximum pressure decreases exponentially as the downstream line pressure increases. This is an expected result because as the downstream line is vacuumed to lower pressure, the velocity of the flow increases and this higher velocity turns to higher pressure when the fluid hits to the end valve. Since the amplitude of the flow is found by subtracting the obtained pressure from the tank pressure, it is clear that the amplitude versus time graph will have the same trend as maximum pressure graph but just with the values less than the tank pressures. So, the amplitude versus time graph has not been drawn.

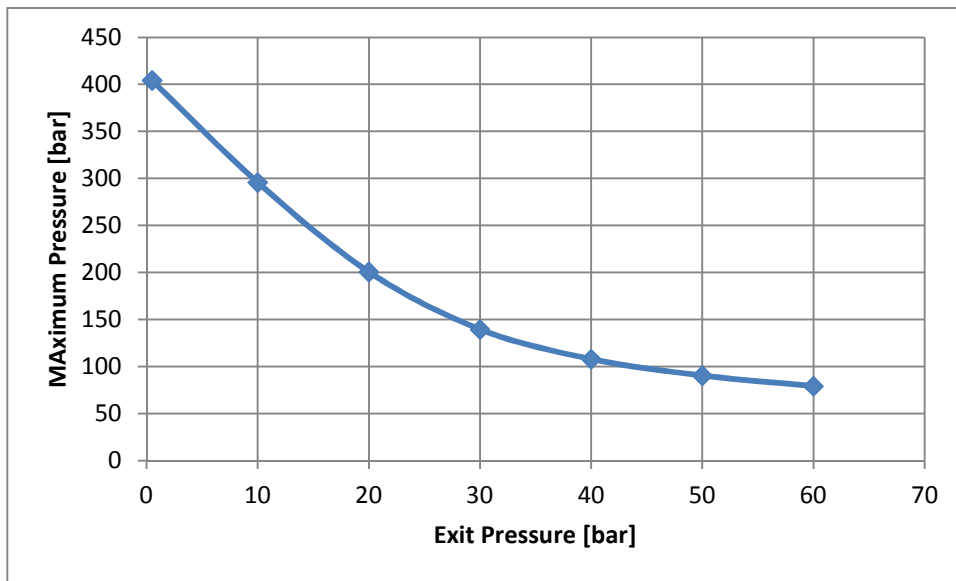


**Figure 4-9.** Maximum pressure versus downstream line pressure graph for Case 2

The change of frequency with respect to the downstream line pressure is presented in Figure 4-10. Similar to the result in Case 1, the frequency is not constant but changes exponentially. It is evaluated that the reason of this change is the trapped air in the pipeline.

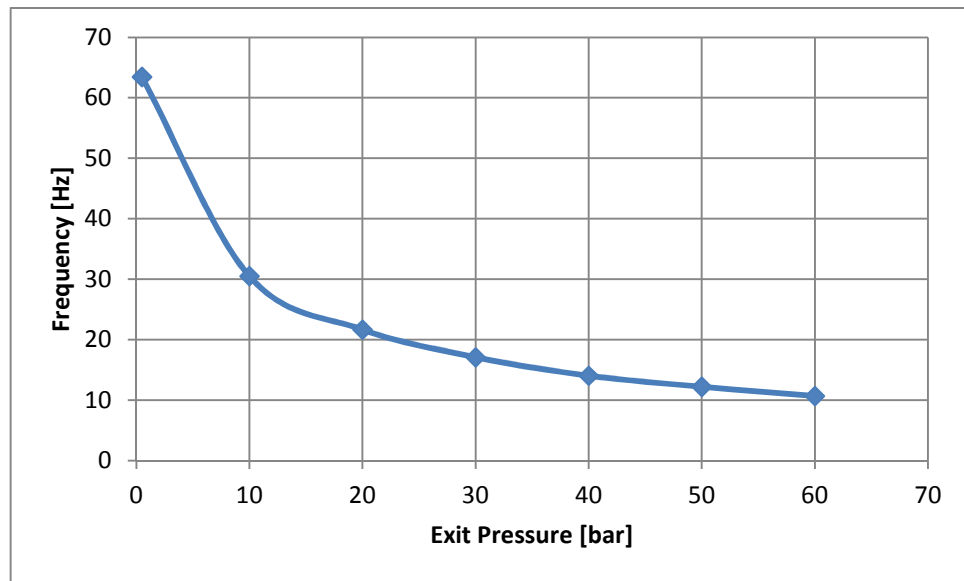


**Figure 4-10.** Frequency versus downstream line pressure graph for Case 2

The variation of the transient flow duration with respect to the downstream line pressure is shown in Figure 4-11. The transient flow duration first decreases but then starts to increase. However, it is assessed that this trend may not be kept constant but change as more downstream line pressure data points are analyzed. The reason of this assessment is that the transient flow duration does not follow a certain trend in Case 1.

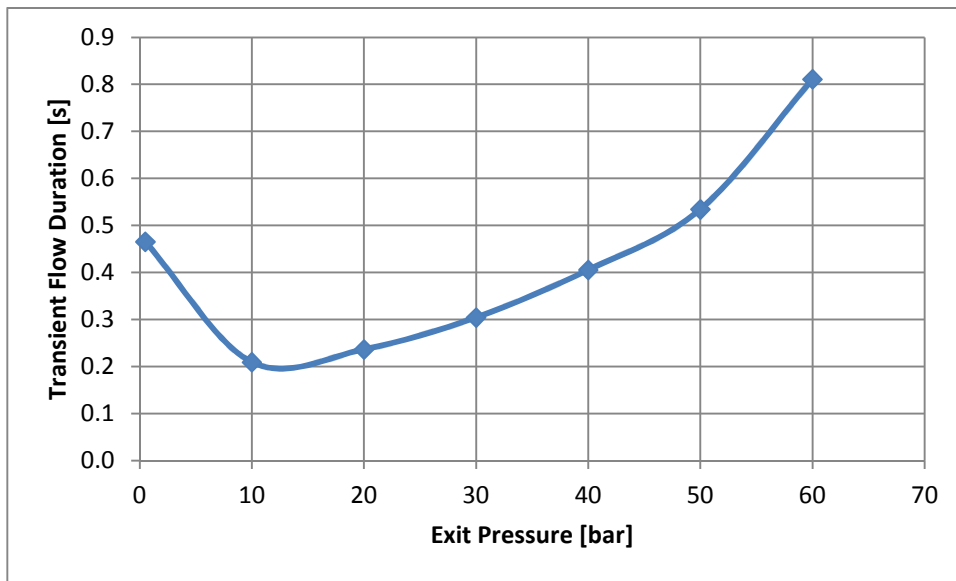


**Figure 4-11.** Transient flow duration versus downstream line pressure graph for Case 2

### 4.2.3 CASE 3: Constant L1 and L2 Lengths versus Different L3 Lengths

Analysis numbers 13, 14, 15, 16 and 17 are compared. The dimensions are L1: 50 cm and L2: 50 cm while L3 takes different values. The orifice diameter is 5.53 mm (same as pipeline diameter: no restriction). The tank pressure is 10 bar and downstream line pressure is 0.5 bar in these analyses.

Maximum pressure decreases linearly as the L3 length increases as shown in Figure 4-12 in conformance to the analysis results in [17]. From the results, it is assessed that as the L3 length increases more air is enclosed in L3 before the latch valve opening. And as more air exists in L3, the damper effect of air on water increases and the water cannot accelerate more.

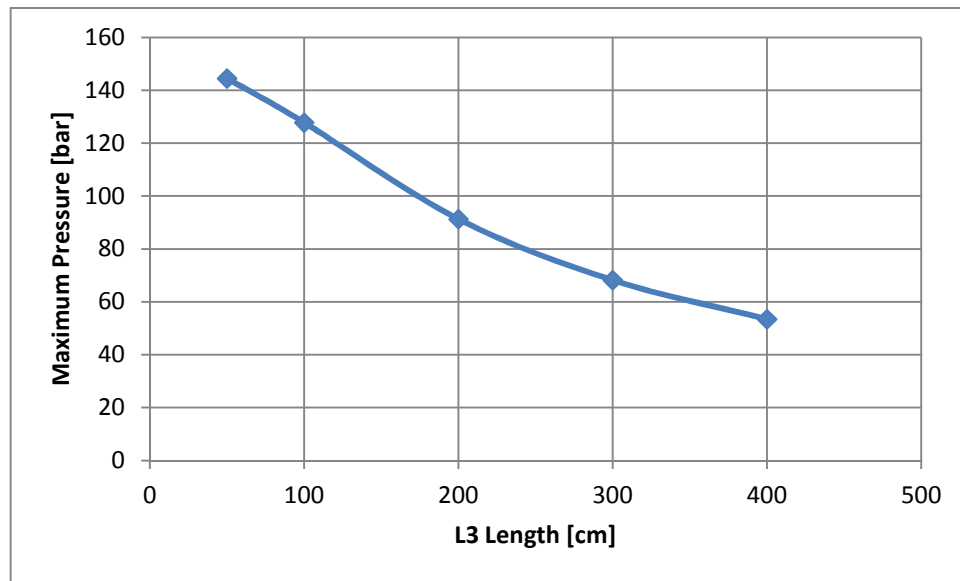


**Figure 4-12.** Maximum pressure versus L3 length graph for Case 3

Frequency of the flow decreases as the L3 length increases as shown in Figure 4-13. It is assessed that the reason of this decrease might be such that as the damper effect of air increases with the increase of L3 length, the flow goes back and forth more slowly. As a result the frequency decreases.

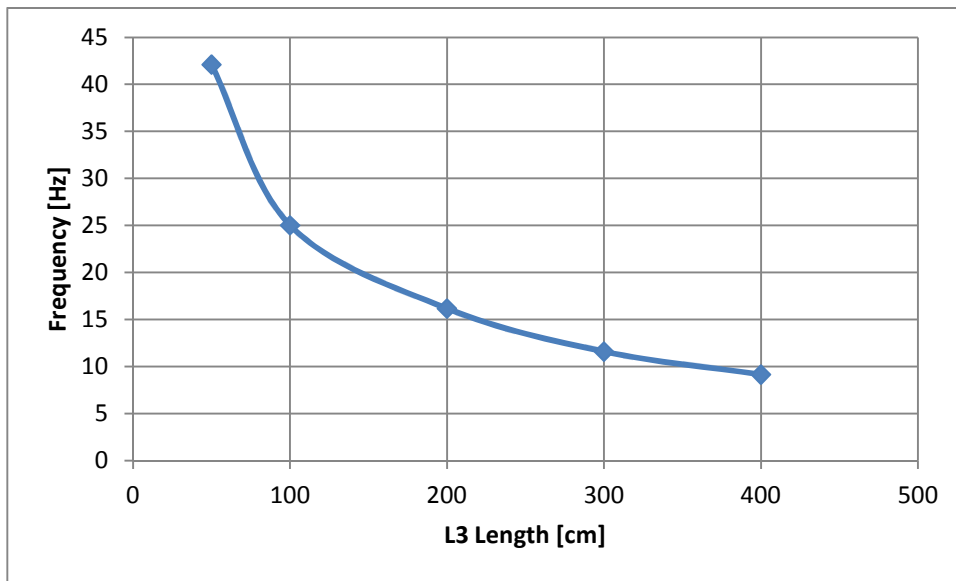


**Figure 4-13.** Frequency versus L3 length graph for Case 3

Transient flow duration change with respect to the L3 length change is shown in Figure 4-14. Similar to the Case 2, as the L3 length increases, the transient flow duration first decreases but then increases. However it is assessed that that trend might change in case of more analyses with more L3 data points.

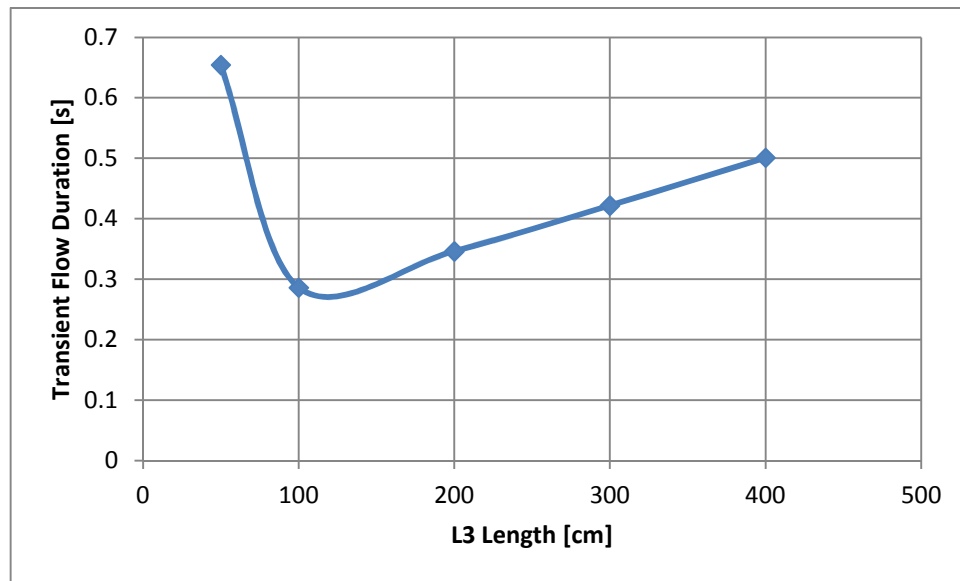


**Figure 4-14.** Transient flow duration versus L3 length graph for Case 3

#### **4.2.4 CASE 4: Constant L1 and L3 Lengths versus Different L2 Lengths**

Analysis numbers 13, 18, 19, 20 and 21 are compared. The dimensions are L1: 50 cm and L3: 50 cm while L2 takes different values. The orifice diameter is 5.53 mm (same as pipeline diameter: no restriction). The tank pressure is 10 bar and downstream line pressure is 0.5 bar in these analyses.

The variation of the maximum pressure with respect to the changes in L2 length change is shown in Figure 4-15. According to the analyses, the maximum pressure decreases as L2 length increases, on contrary to the study in [17]. It is assessed that the reason of this result might be because of the friction.

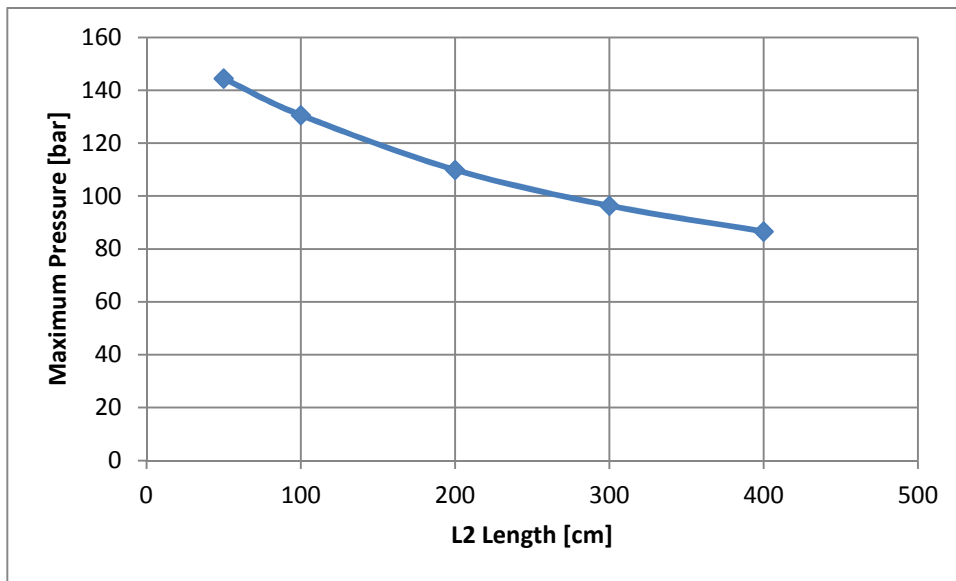


**Figure 4-15.** Maximum pressure versus L2 length graph for Case 4

Frequency change with respect to the change in L2 length is shown in Figure 4-16. It is clear that as the L2 length increases, the frequency of the flow decreases. It is assessed that as the length between the tank and exit solenoid valve increases whether via L1, L2 or L3; the frequency decreases due to the increase in time between the strikes of pressure waves to the exit solenoid valve and tank.

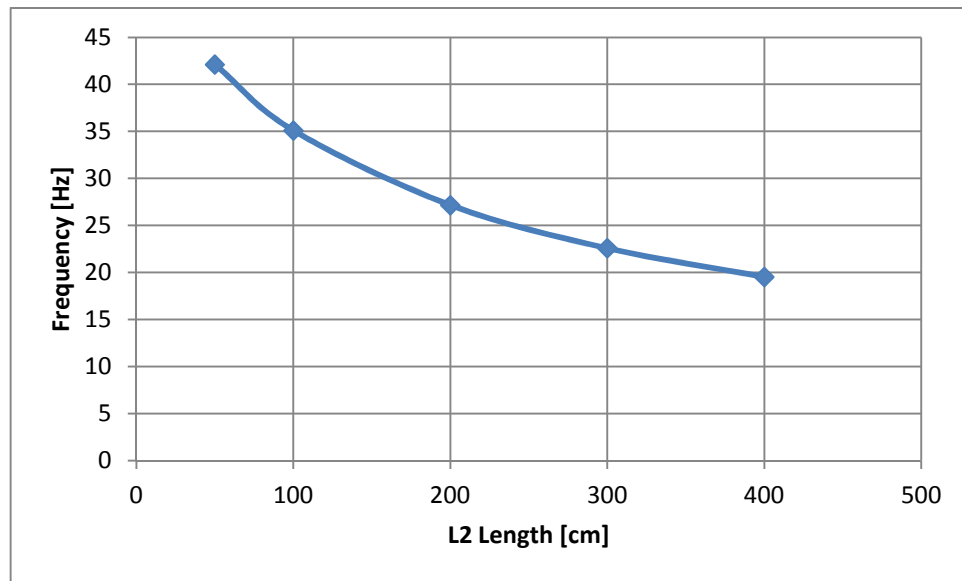


**Figure 4-16.** Frequency versus L2 length graph for Case 4

The variation of the transient flow duration with respect to the changes in L2 length is shown in Figure 4-17. Transient flow duration increases as L2 increases.

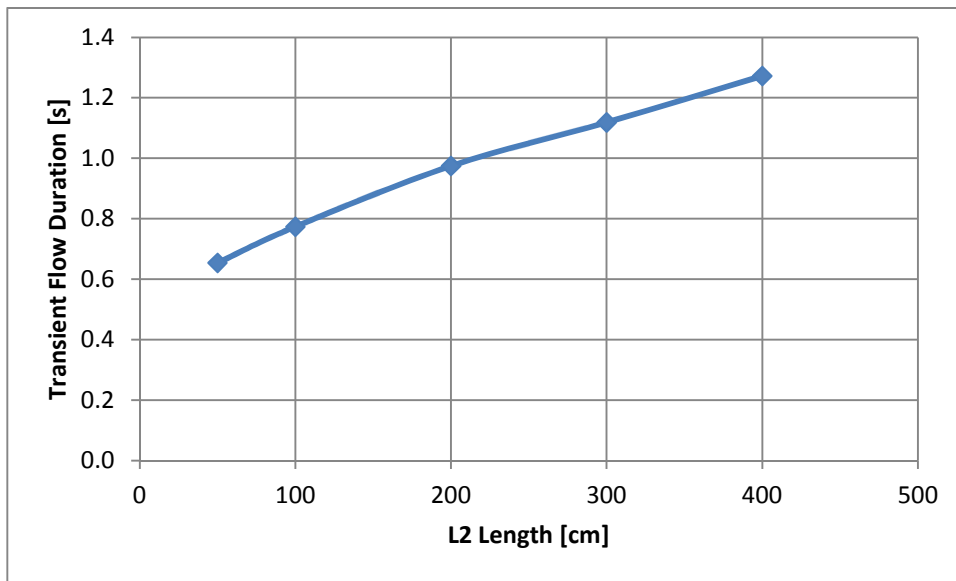


**Figure 4-17.** Transient flow duration versus L2 length graph for Case 4

#### **4.2.5 CASE 5: Constant L2 and L3 Lengths versus Different L1 Lengths**

Analysis numbers 13, 22, 23, 24 and 25 are compared. The dimensions are L2: 50 cm and L3: 50 cm while L1 takes different values. The orifice diameter is 5.53 mm (same as pipeline diameter: no restriction). The tank pressure is 10 bar and downstream line pressure is 0.5 bar in these analyses.

The variation of maximum pressure with respect to L1 length is presented in Figure 4-18. It is clear from the figure that as L1 length increases the maximum pressure decreases similar to the Case 4 on contrary to the study [17]. Similar to Case 4, it is assessed that the reason of this decrease might be friction.

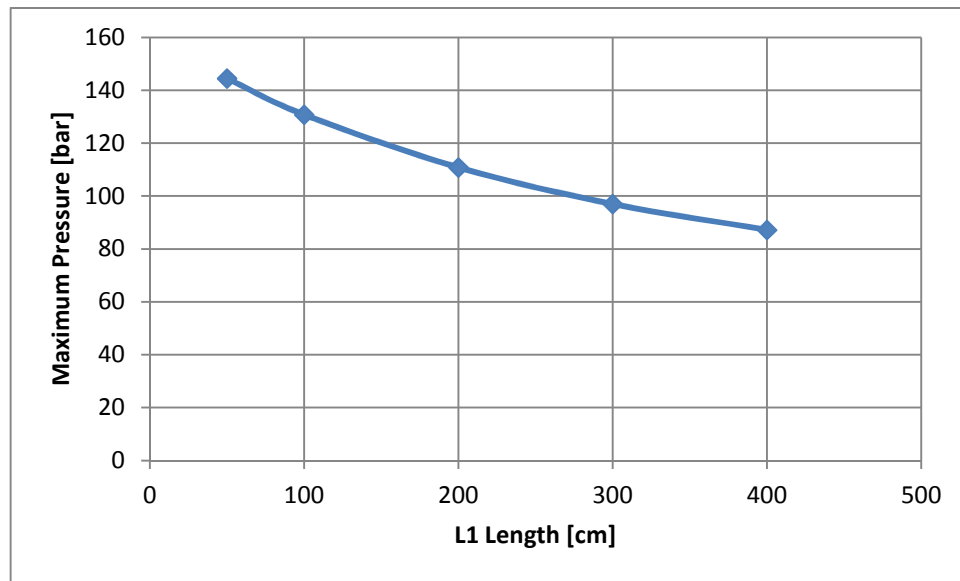


**Figure 4-18.** Maximum pressure versus L1 length graph for Case 5

The frequency change of flow with respect to the change in L1 length is presented in Figure 4-19. It seems that the frequency of flow decreases as the L1 length increases similar to Case 4.

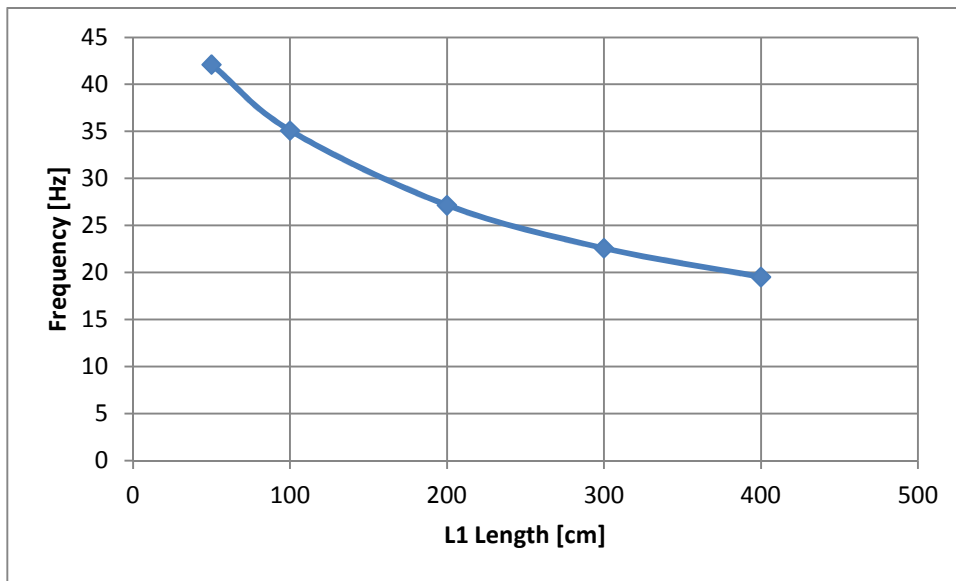


**Figure 4-19.** Frequency versus L1 length graph for Case 5

Transient flow duration versus L1 length change is presented in Figure 4-20. It seems that as L1 length increases, the transient flow duration increases.

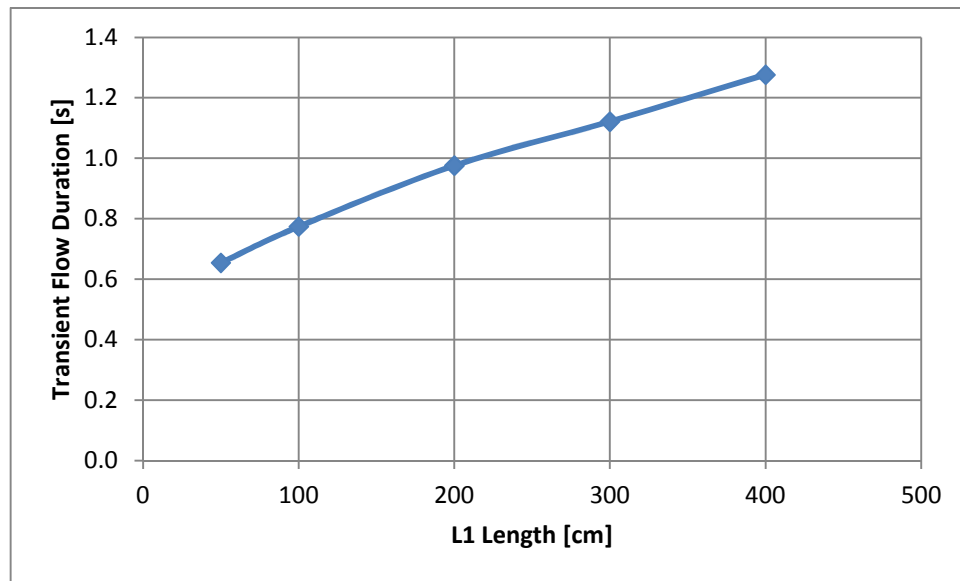


**Figure 4-20.** Transient flow duration versus L1 length graph for Case 5

#### **4.2.6 CASE 6: Constant Total Length (L1+L2+L3) versus Different L1, L2 and L3 Lengths**

Analysis numbers 14, 18 and 22 where the total length is 200 cm (Case 6.1); analysis numbers 15, 19 and 23 where the total length is 300 cm (Case 6.2); analysis numbers 16, 20 and 24 where the total length is 400 cm (Case 6.3) and analysis numbers 17, 21 and 25 where the total length is 500 cm are compared. The orifice diameter is 5.53 mm (same as pipeline diameter: no restriction). The tank pressure is 10 bar and downstream line pressure is 0.5 bar in these analyses.

In order to compare the effects of L1, L2 and L3 with respect to each other, analyses are performed by keeping the total length constant as explained above. Depending on the place or the longest pipe, the pipes are coded as shown in Table 4-2. These codes are used for the graphs in this subsection

**.Table 4-2.** Analysis codes used in comparisons

<b>Analysis No</b>	<b>L1 (cm)</b>	<b>L2 (cm)</b>	<b>L3 (cm)</b>	<b>Long Pipe Code</b>
14	50	50	100	3
18	50	100	50	2
22	100	50	50	1
15	50	50	200	3
19	50	200	50	2
23	200	50	50	1
16	50	50	300	3
20	50	300	50	2
24	300	50	50	1
17	50	50	400	3
21	50	400	50	2
25	400	50	50	1

The variation of the maximum pressure with respect to the location of longest pipe is shown in Figure 4-21. It seems from this graph that the change in L1 and L2 lengths does not affect the maximum pressure but the increase in L3 decreases the maximum pressure while the total pipeline length is kept constant. As an example, when the pipeline total length is 500 cm, whether the longest line (400 cm) is L1 or L2, the maximum pressure is 87 bar. That means as the total length of L1+L2 is kept 450 cm, whichever is longer, the maximum pressure will be 87 bar for the constant L3 length. However if the longest line (400 cm) is L3, the maximum pressure is 53 bar for L1+L2 total length of 100 cm. It is assessed that this result is obtained because as longer L3 exists, more air is trapped in the pipeline and more damping effect occurs. As a result, the maximum pressure decreases.

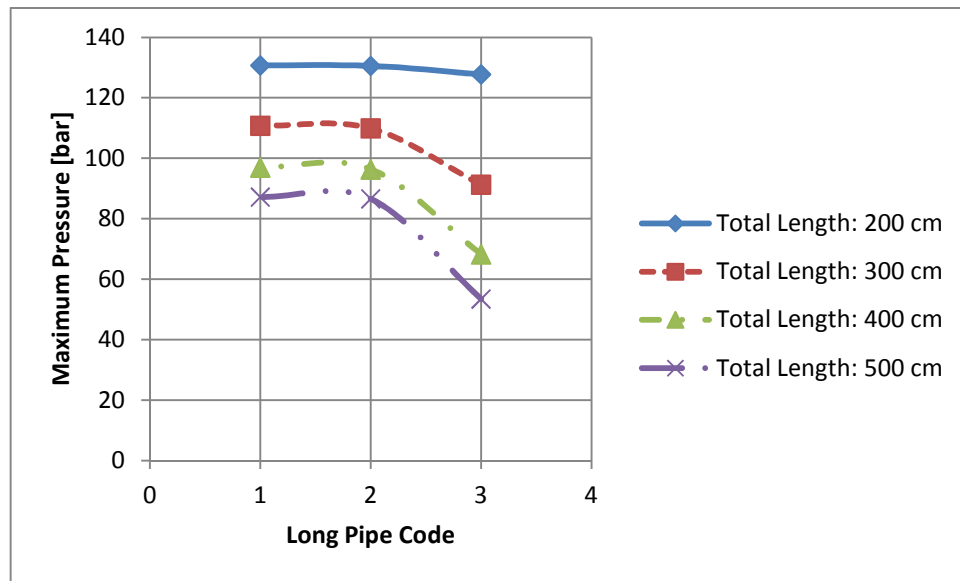


**Figure 4-21.** Maximum pressure versus long pipe code graph for Case 6

The variation of the frequency of flow with respect to the location of longest pipe is presented in Figure 4-22. Similar to the maximum pressure, it seems that increase in L1 or L2 while keeping L1+L2 constant does not affect the frequency on contrary to the increase in L3 length for a constant total pipeline length.

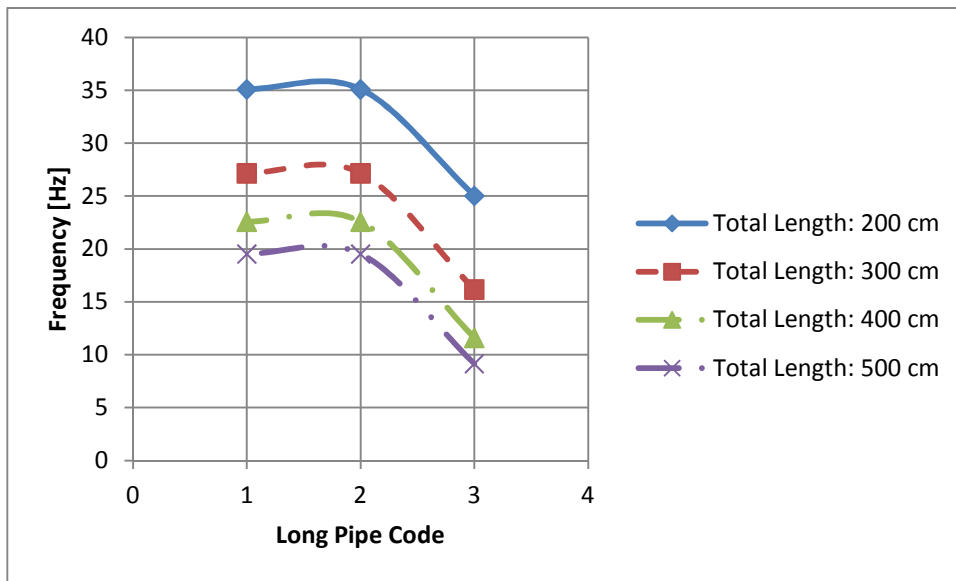


**Figure 4-22.** Frequency versus long pipe code graph for Case 6

The variation of transient flow duration with respect to the location of longest pipe is presented in Figure 4-23. Similar to maximum pressure and frequency, whether the longest pipe is L1 or L2, the transient flow duration does not change for a constant L3. But if the longest pipe is L3, the transient flow duration decreases. This situation can be explained such that as L1 or L2 is the longest pipe (meaning that L3 is short), more energy exists in the flow due to momentum as there is more water in the upstream part of the latch valve. Since more energy exists in the flow, the duration of the water hammer effect increases. However if L1 and L2 are short but L3 is long, less energy exists in the flow with respect to the case before. Also more air exists in the pipeline and this causes more damper effect and the water hammer effect damps more quickly.

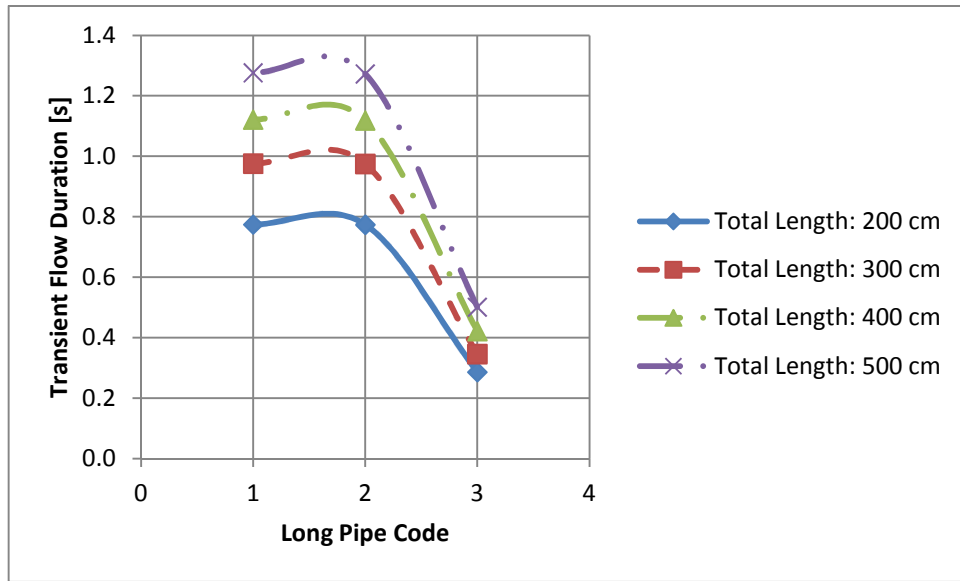


**Figure 4-23.** Transient flow duration versus long pipe code graph for Case 6

#### 4.2.7 CASE 7: Constant Pressures and Lengths versus Different Orifice Diameters

Analysis numbers 26-34 and 0 are compared. The dimensions are L1:100 cm, L2: 100 cm and L3: 100 cm. The orifice diameter changes while the pipe inner diameter is 5.53 mm. The tank pressure is 10 bar and downstream line pressure is 0.5 bar in these analyses.

The pressure change of the exit solenoid valve with respect to time is shown in Figure 4-24 for the analysis with 0.5 mm orifice. The zoomed view of the damped harmonic motion can be seen in Figure 4-25. For comparison, the pressure versus time graph without any orifice had been shown in Figure 4-4.

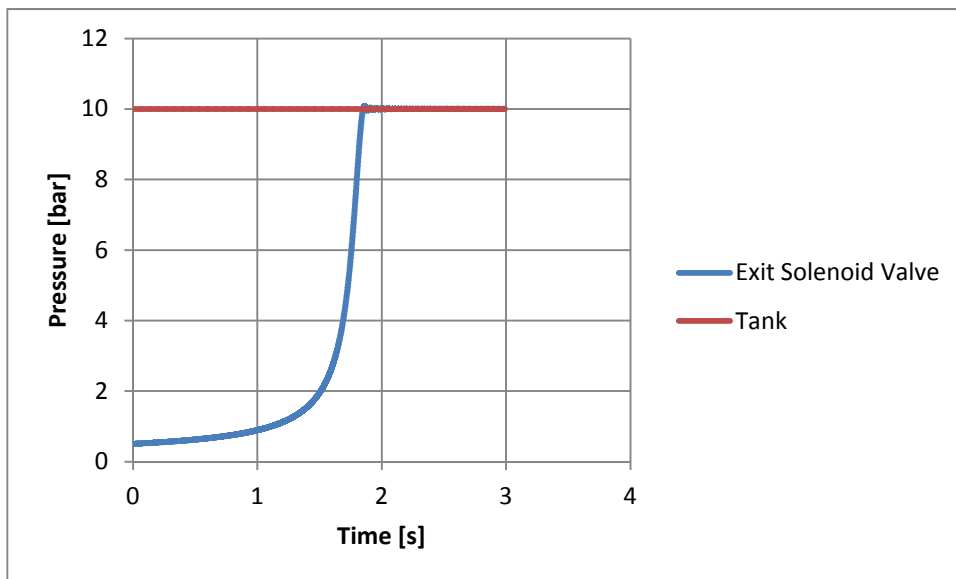


**Figure 4-24.** Pressure versus time graph for analysis with 0.5 mm orifice

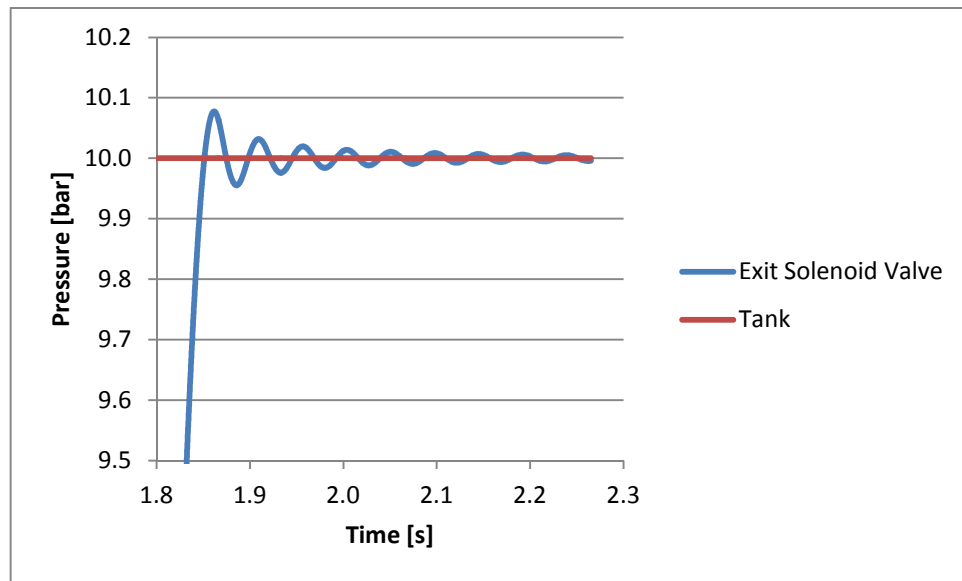


**Figure 4-25.** Pressure versus time graph for analysis with 0.5 mm orifice – zoomed view

Maximum pressure versus orifice diameter graph is presented in Figure 4-26. As it can be seen from the figure, as the orifice diameter gets smaller, the maximum pressure decreases. The reason of this result is the pressure drop effect of the orifice.

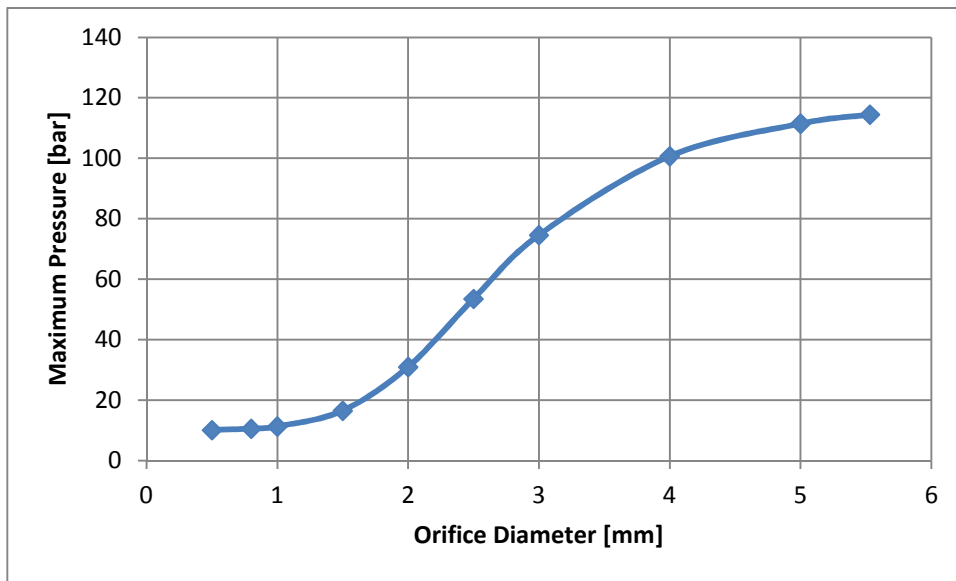


**Figure 4-26.** Maximum pressure versus orifice diameter graph for Case 7

The variation of the frequency with respect to orifice diameter is presented in Figure 4-27. As it can be seen from the figure, the frequency of the pressure waves does not follow a certain trend. It is assessed that the reason of this result is the constraining effect of the orifice such that in the downstream part of the orifice, recirculation zones exist in the sides of the continuous flow as shown in Figure 4-28. When the pressure wave turns back, these recirculation zones disturb the waves and cause the frequency of the flow to be irregular.

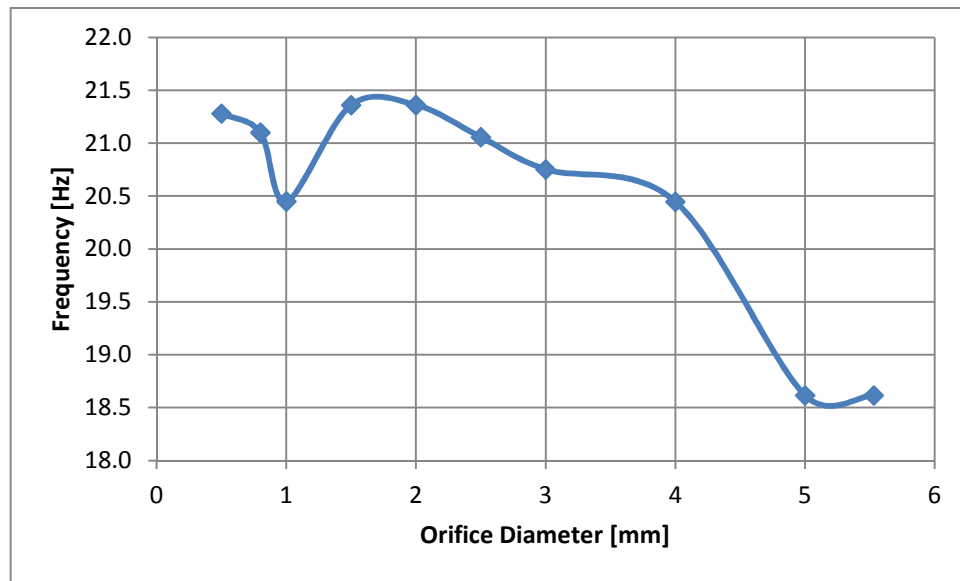


**Figure 4-27.** Frequency versus orifice diameter graph for Case 7



**Figure 4-28.** Flow through orifice

The variation of the transient flow duration with respect to orifice diameter is presented in Figure 4-29. Even though there is a section with decrease, it is assessed that the trend of transient flow duration is increasing with the increasing orifice diameter. It can be explained that as the diameter of the orifice decreases, the water

hammer effect in the flow damps more quickly, so the transient flow durations lasts shorter.

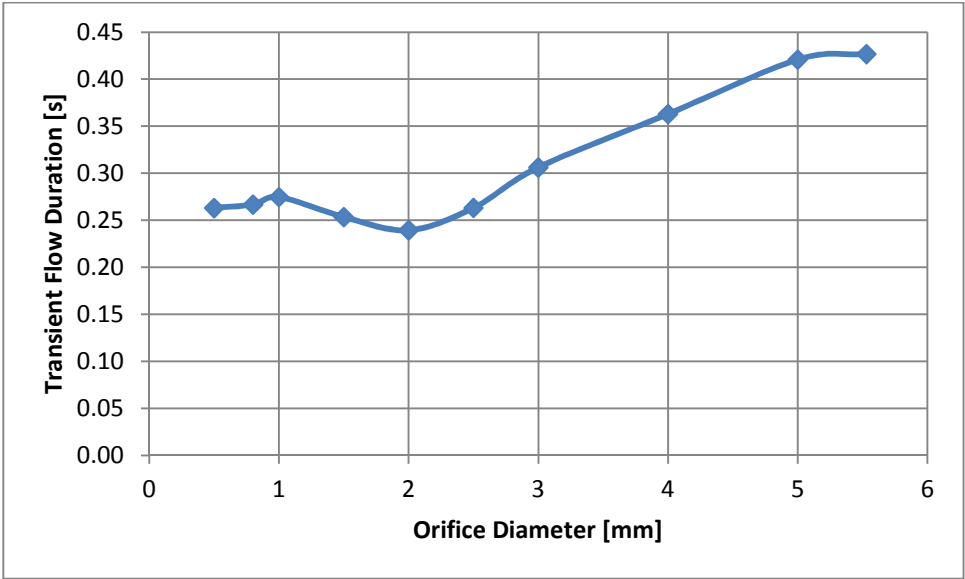


**Figure 4-29.** Transient flow duration versus orifice diameter graph for Case 7

**4.2.8 CASE 8: Constant Pressures and Lengths versus Different Pipe Inner Diameters**

Analysis numbers 35-39 are compared. The dimensions are L1:100 cm, L2: 100 cm and L3: 100 cm. The pipe inner diameter changes while the orifice diameter is equal to the pipe inner diameter in each analysis (that means no restriction exists). The tank pressure is 10 bar and downstream line pressure is 0.5 bar in these analyses. The thickness of the pipe is constant.

The variation of the maximum pressure with respect to the pipe inner diameter change is shown in Figure 4-30. As can be seen from this figure, when the pipe inner

diameter increases, the maximum pressure increases. It is assessed that the reason of this result is that as the inner diameter increases the mass flow rate increases and momentum of the flow increases. As a result, the maximum pressure due to water hammer increases.

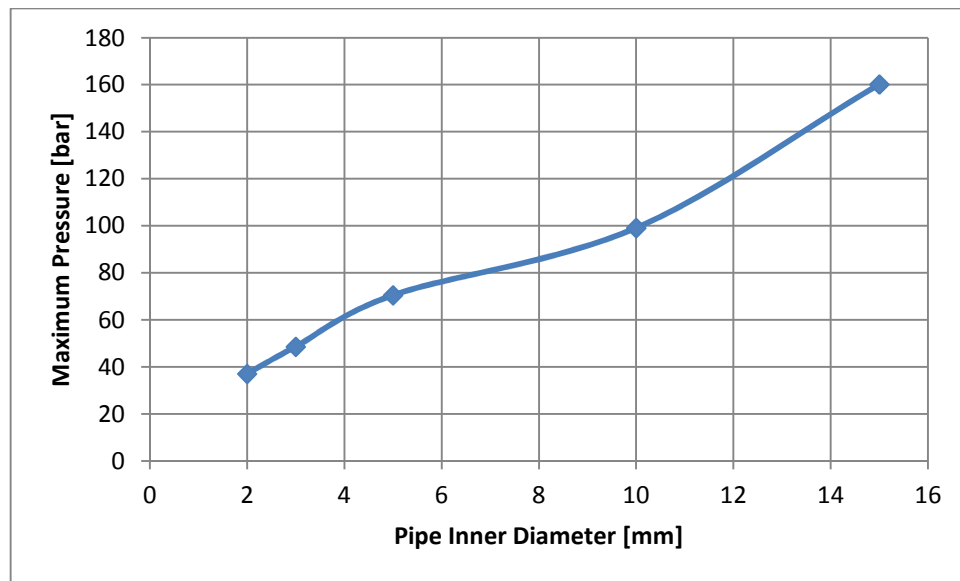


**Figure 4-30.** Maximum pressure versus pipe inner diameter graph for Case 8

The frequency change with respect to the pipe inner diameter is presented in Figure 4-31. As can be seen from this figure, the frequency changes abruptly with the pipe inner diameter increase. This behavior could not be understood.

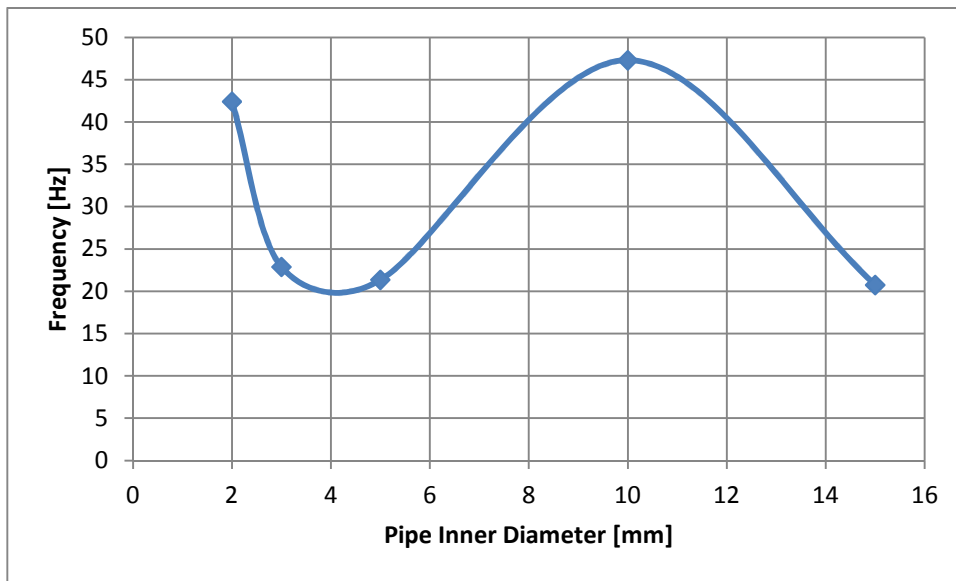


**Figure 4-31.** Frequency versus pipe inner diameter graph for Case 8

The variation of the transient flow duration with respect to the pipe inner diameter is shown in Figure 4-32. It is seen from this figure that the transient flow duration increases as the pipe diameter increases.

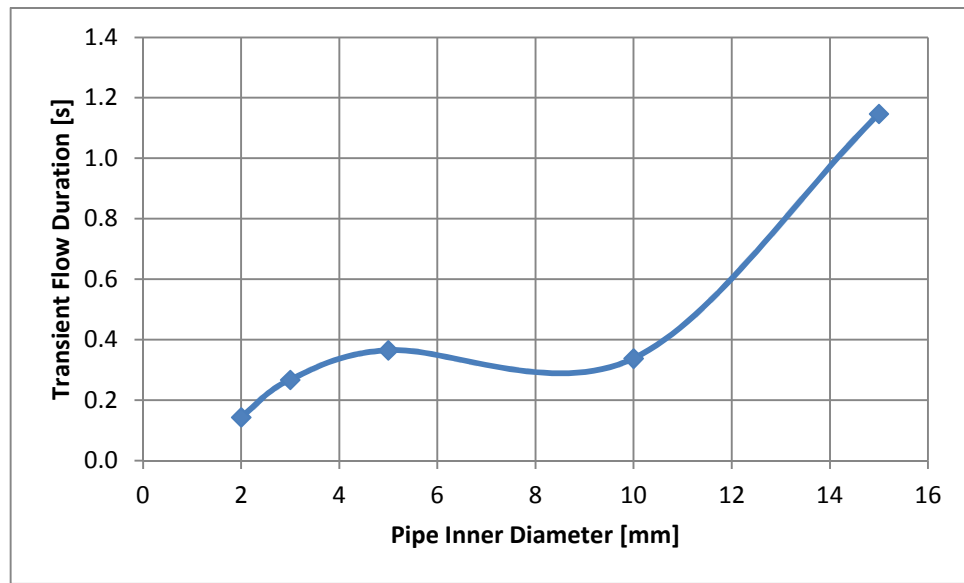


**Figure 4-32.** Transient flow duration versus pipe inner diameter graph for Case 8

This page is left intentionally blank.

## CHAPTER 5

### EXPERIMENTAL STUDY

Tests are performed in order to create a database on the water hammer phenomena under the same conditions with the ones faced in satellite propulsion system. In this frame a test setup is designed and constructed as shown in Figure 5-1. Water is used as the test fluid instead of poisonous hydrazine. The components of the test setup are chosen from stainless steel 316 in order to ensure that the test setup will not corrode due to the usage of water. Swagelok fittings are preferred to be used for easy connection of the components. The test setup has been built in ROKETSAN Missile Industries premises.

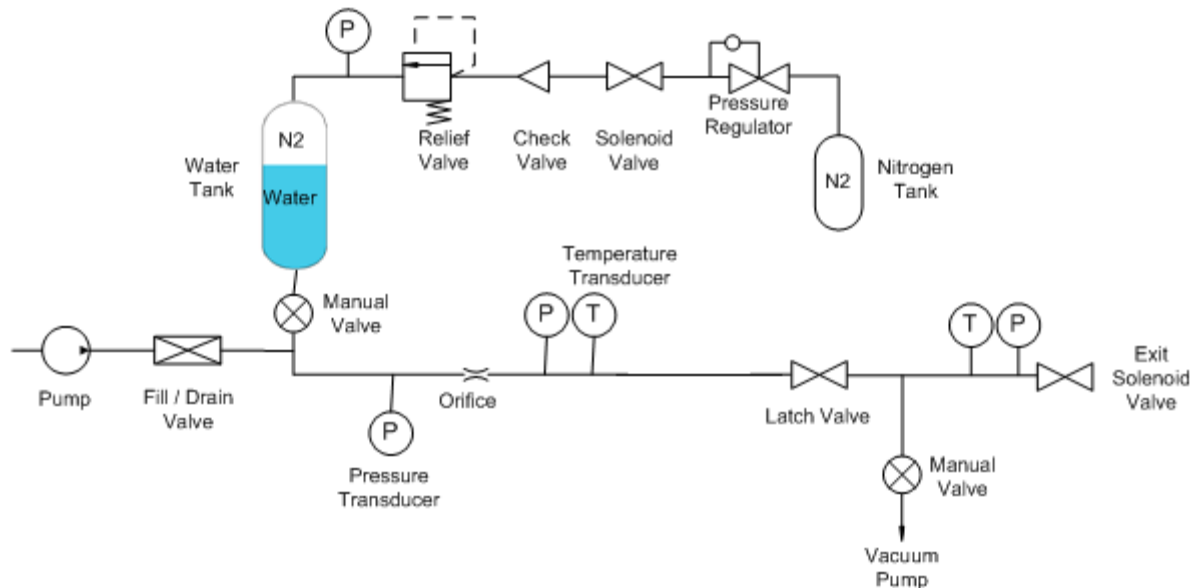


**Figure 5-1.** Test setup schematic



**Figure 5-2.** Test setup picture

The components of the test setup are as explained below:

- **Nitrogen Tank:** It is used in order to pressurize the water.
- **Pressure Regulator:** It is used in order to decrease the pressure of highly pressurized nitrogen to normal operating pressure (~10 bar).
- **Solenoid valve (Before the water tank):** It is used in order to control the nitrogen supply to the water tank.
- **Check Valve:** It is used in order to prevent the water vapor to reach to the components existing in the upstream line of check valve.

- **Relief Valve:** It is used in order to drain the pressure in the lines if any pressure above the expected value exists (e.g. if the pressure regulator breaks)
- **Pressure Transducer (Before the water tank):** It is used in order to measure the pressure of nitrogen gas that is supplied to the water tank.
- **Water Tank:** It is used in order to accommodate the water that will be used in the tests and the nitrogen gas.
- **Manual Valve (Before Latch Valve):** It is used in order to cut the connection between the tank and the components downstream of the tank.
- **Fill and Drain Valve:** It is used in order to fill and drain the water tank and to eject nitrogen gas or air to the pipeline downstream of the tank.
- **Pump:** It is used in order to fill the water tank.
- **Pressure Transducer (After the Water Tank):** It is used in order to measure the pressure of water in the place where the transducer is used.
- **Orifice:** It is used in order to decrease the effect of water hammer.
- **Temperature Transducer:** It is used in order to measure the temperature of water in the place where the transducer is used.
- **Latch Valve:** It is used in order to supply water to the vacuum environment. In order to enable the valve to be opened fast, solenoid ball valve is used.
- **Manual Valve (After the Latch Valve):** It is used in order to vacuum the pipeline downstream of the latch valve and then to isolate the vacuum pump from the testing pipeline.
- **Vacuum Pump:** It is used in order to vacuum the pipeline downstream of the latch valve.
- **Solenoid Valve (After Latch Valve):** It is used in order to drain the water from the lines. In order to enable the valve to operate in pulse mode by opening and closing successively and observe the water hammer effect under this condition, the valve is preferred to be solenoid ball valve.
- **Tubing:** Since water is used in the lines, ¼" stainless steel 316 pipeline is used.

The pressure transducer and data acquisition system properties are presented in Table 5-1

**Table 5-1.** Pressure transducer and data acquisition system properties

<b>Pressure Transducer</b>	
Brand / Model	Kulite HKM-375
Type	Piezoresistive
Pressure Sensing Principle	Fully Active Four Arm Wheatstone Bridge Dielectrically Isolated Silicon on Silicon
Pressure Range	0-70 bar (Abs)
Full Scale Output	100 mV
Combined Non-Linearity, Hysteresis and Repeatability	±0.1% FSO BFSL (Typ.), ±0.5% FSO (Max.)
Sensitivity	1.517 mV/Bar
Resolution	Infinitesimal
<b>Data Acquisition</b>	
System	National Instruments
Rate	25kHz

Test procedure is as presented below:

1. Open all valves on the path from nitrogen tank to exit valve and purge nitrogen gas through the pipeline.
2. Close exit solenoid valve.
3. Adjust the pressure to the level that you want with the pressure regulator.
4. Again open the exit solenoid valve and purge the gas in the test setup.
5. Close the solenoid valve just after the pressure regulator, hence stop pressurizing the system.
6. After all the gas in the test setup exits and the pressure of the system drops down to ambient pressure, close latch valve and exit solenoid valve.

7. Open relief valve in order to keep the pressure of the tank at ambient pressure during the filling operation for filling water to the tank.
8. Open pump and fill the tank with 2.5kg water, then close the pump.
9. Close the relief valve.
10. Open the solenoid valve just after the pressure regulator and pressurize the system.
11. Open latch valve and exit solenoid valve and let the water to flow through exit valve a little amount.
12. Close latch valve.
13. After the flow of water from the exit valve is completed, close the exit solenoid valve.
14. Open vacuum pump and take the line between latch valve and exit solenoid valve to vacuum. (Applicable only for the test cases with the vacuum downstream line condition.
15. Open latch valve. (Water hammer effect is seen after this step).
16. Open exit solenoid valve and purge all the water in the tank.
17. Close all valves.

Difficulties met during the tests:

- Initially the tests were performed without the steps of 11, 12 and 13. In these tests, the maximum pressure due to the water hammer effect was obtained about 15 bar instead of obtaining higher than 60 bar according to the analyses while the tank pressure was 12 bar. It is evaluated that this result was due to the air trapped in the upstream of the latch valve during water filling operation. In an ideal application, for avoiding this phenomenon, normally the tank should have been filled with water after vacuuming the tank and pipeline up to the latch valve. However, this result was not expected and the test setup had not been designed taking into account the vacuuming of the tank. So, such an application could not be performed. In order to get rid of this result, a solution such as opening the latch valve and exit valve and draining the water

for a while was found. In this way, the air trapped between the water column and the latch valve was expelled. When the tests were repeated with this test procedure, the maximum pressures were obtained above 60 bar as expected.

- When some amount of water is drained from the system with steps, 11, 12 and 13, some amount of water stays at the pipeline between the latch valve and the exit solenoid valve. If the tests are performed with vacuum condition in the downstream line, all the water that stayed in the downstream line is pumped out. However, in the tests with ambient pressure in the downstream line, the mentioned water stays in the line. This unknown amount of water creates uncertainty in the test results. Because the amount of air between the latch valve and exit solenoid valve changes according to the amount of water stayed in this pipeline section. In order to avoid this uncertainty, tests were performed by performing the 14<sup>th</sup> step and adding a step as opening the exit solenoid valve, filling the downstream line with air at ambient pressure and closing the exit solenoid valve for the test cases with ambient pressure at downstream line. The steps from 15 to 17 were again performed following this additional step. In this way, the downstream line could be obtained free of water molecules and filled with air at ambient pressure as needed for the test. However, under this condition, the maximum pressure of 8 bar was obtained when the tank pressure was 6 bar on contrary to what was expected. These results show that when the latch valve is opened, the air existing in the downstream line is squeezed and the air creates a cushioning effect so much that the pressure cannot increase. However, it is not understood why the cushioning is affecting so much in this case, on contrary to what was expected with the analyses. As a result, it is preferred not to apply the 14<sup>th</sup> step and the mentioned additional step in the tests with ambient pressure. In all the tests that presented in Table 5-2, there exist water droplets in the downstream line before the 15<sup>th</sup> step is applied.

## 5.1 Test Conditions and Results

A total of 38 tests were performed in the frame of this study. The tests matrix and results are presented in Table 5-2. Each test condition was repeated three times in order to be sure about the repeatability of the results. However, depending on the sensitivity of pressure regulator, the tank pressures of each repetitive test changes with  $\pm 7\%$  maximum.

The design philosophy of the tests matrix is as explained below:

- **Tank Pressures:** As presented in Table 5-1, the maximum design pressure of the pressure transducer is 70 bar. Above this design pressure, the pressure transducers can still operate but with less sensitivity. Hence, in the tank pressure selection of tests, attention is paid not to exceed 70 bar. With this aim, the tests are performed mainly in the region of 6-8 bar tank pressure. However, it is desired to see the effect of higher tank pressures on the transients. So, although the maximum pressure is obtained higher than 70 bar, some tests are performed also in the 13-16 bar tank pressure range. In a typical monopropellant satellite propulsion system, the tank pressure is about 24 bar which is much higher than the ones in our test cases. In order not to damage the pressure sensors and the structural integrity of the test setup, tests are not performed at about 24 bar or higher than 16 bar tank pressure.
- **Downstream Line Pressure:** The downstream line pressures are either 0.94 bar (atmospheric pressure at Elmadağ/ Ankara/ TURKEY) or 0.15 bar that is the vacuuming capacity of our vacuum pump.
- **Conditions:** Conditions are constructed regarding three different parameters such as:
  - Different downstream line pressures: Either atmospheric pressure or vacuum pressure
  - Different L3 lengths: Either 2m or 1m
  - Different orifice diameters: Either 4.57 mm (no orifice condition) or 1.5 mm

Tests for below conditions have been performed:

- Case A:  $L_3 = 2$  m, Downstream Line Condition = Ambient Pressure, No Orifice
- Case B:  $L_3 = 2$  m, Downstream Line Condition = Vacuum, No Orifice
- Case C:  $L_3 = 1$  m, Downstream Line Condition = Ambient Pressure, No Orifice
- Case D:  $L_3 = 1$  m, Downstream Line Condition = Vacuum, No Orifice
- Case E:  $L_3 = 1$  m, Downstream Line Condition = Ambient Pressure, 1.5 mm Diameter Orifice
- Case F:  $L_3 = 1$  m, Downstream Line Condition = Vacuum, 1.5 mm Diameter Orifice

**Table 5-2.** Test conditions and results

Test No	Inputs						Outputs			
	Tank Pressure [bar]	Downstream Line Pressure [bar]	Conditions				Max Pressure [bar]	Frequency	Time Constant	Transient Flow Duration (s)
			Vacuum	L3=2m	L3=1m	1.5mm Orifice				
1	15.19	0.92		X			83.92	32.04	0.01785	0.089
2	13.55	0.94		X			68.2	28.99	0.03047	0.152
3	13.87	0.95		X			76.39	30.52	0.02036	0.102
4	13.67	0.96		X			60.13	27.47	0.03587	0.179
5	13.67	0.95		X			79.53	30.52	0.03404	0.170
6	14.86	0.94		X			89.06	37.38	0.02058	0.103
7	16.05	0.94		X			96.23	41.96	0.0184	0.092
8	16.04	0.94		X			90.69	38.14	0.021	0.105
9	16.01	0.94		X			95.98	36.62	0.0175	0.088
10	16	0.94		X			97.55	38.15	0.01923	0.096
11	6.27	0.94		X			24.57	14.5	0.04218	0.211
12	6.32	0.94		X			28.91	16.78	0.02937	0.147
13	6.33	0.94		X			30.53	17.55	0.0303	0.151
14	5.99	0.16	X	X			43.13	22.13	0.02853	0.143
15	5.57	0.13	X	X			31.87	19.07	0.02903	0.145
16	5.91	0.16	X	X			41.07	21.36	0.02851	0.143
17	5.73	0.13	X	X			42.62	22.13	0.02973	0.149
18	8.12	0.23	X	X			50.24	22.89	0.03068	0.153
19	6.13	0.17	X	X			46.39	22.89	0.02895	0.145
20	5.93	0.94		X			37.02	18.31	0.02777	0.139
21	7.84	0.94			X		33.19	25.94	0.02325	0.116
22	7.03	0.94			X		29.09	22.88	0.02792	0.140
23	7.39	0.94			X		31.99	24.41	0.02682	0.134
24	7.32	0.94			X		32.21	23.65	0.02582	0.129
25	6.74	0.17	X		X		35.75	25.94	0.02524	0.126
26	6.73	0.16	X		X		45.8	33.57	0.02318	0.116
27	6.58	0.94			X		26.77	25.94	0.03185	0.159
28	6.8	0.94			X		30.59	25.94	0.03239	0.162
29	6.99	0.94			X		30.23	26.7	0.02785	0.139
30	4.13	0.23	X		X		38.23	29.75	0.03144	0.157
31	6.84	0.25	X		X		39.67	29.75	0.02419	0.121
32	6.99	0.24	X		X		42.65	32.04	0.02117	0.106
33	7.89	0.94			X	X	12.57	22.13	0.04859	0.243

**Table 5-2.** Test conditions and results (cont.)

34	7.7	0.94			X	X	12.34	24.41	0.04176	0.209
35	7.76	0.94			X	X	12.94	27.47	0.03916	0.196
36	7.44	0.24	X		X	X	14.84	32.81	0.0338	0.169
37	7.51	0.24	X		X	X	15.61	34.33	0.04703	0.235
38	7.57	0.25	X		X	X	15.66	35.1	0.03898	0.195

Test results are presented and discussed below:

Maximum pressure change with respect to the tank pressure is presented in Figure 5-3 covering all tests. From that figure below outcomes are determined:

- In some tests it is detected that even though less tank pressure is used in the test, higher maximum pressures could be obtained for the same test condition. It is assessed that the reason of this result may be the unknown amounts of parameters such as the staying water droplets in L3 and water amount in the tank.
- In the tests with vacuum downstream line condition, higher maximum pressures are obtained with respect to the tests with ambient pressure in L3.
- Orifice usage decreases the maximum pressure significantly.
- No significant effect of the L3 pipe length change could be observed in the tests. It is assessed that the reason of this situation is not being able to perform the test in ambient pressure and vacuum pressure for the downstream line condition with the same tank pressure. There is pressure difference between the tank pressures of tests with ambient pressure and vacuum pressure downstream line conditions.

Frequency change with respect to the tank pressure change is shown in Figure 5-4 covering all tests. From that figure below outcomes are determined:

- Frequency of pressure waves changes with the tank pressure, downstream line pressure and length of L3.

- Usage of orifice does not affect the frequency of pressure waves significantly.
- It is observed that different frequencies could be obtained from the tests with the same tank pressures. The frequency difference between these test results can reach to 22.7%. It is assessed that the reason of this result can be the difference in amount of water droplets stayed in L3.

Transient flow duration change with respect to the tank pressure change is presented in Figure 5-5 covering all tests. From that figure below outcomes are determined:

- With the increasing tank pressure, the transient flow duration can both increase and decrease (Ex. L3=2m, Ambient Pressure).
- Transient flow duration does not change significantly with the downstream line condition, e.g. ambient pressure or vacuum.
- Orifice usage increases the transient flow duration significantly.

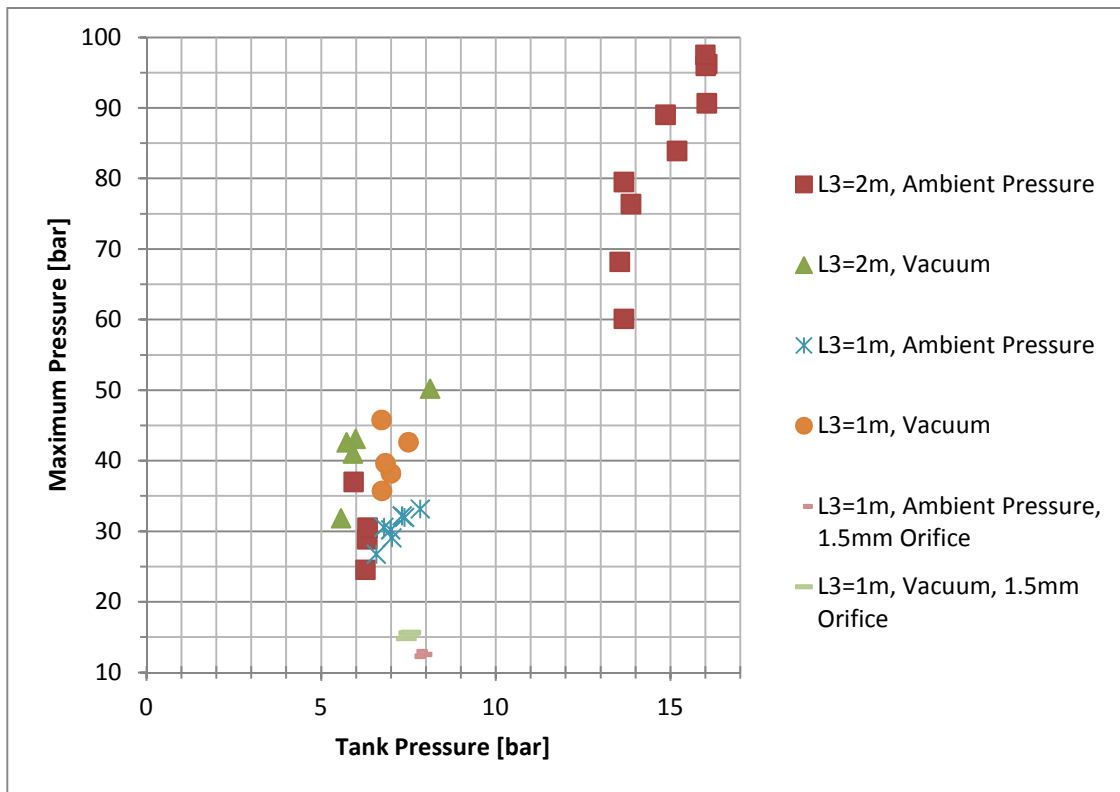


**Figure 5-3.** Test results: maximum pressure versus tank pressure graph

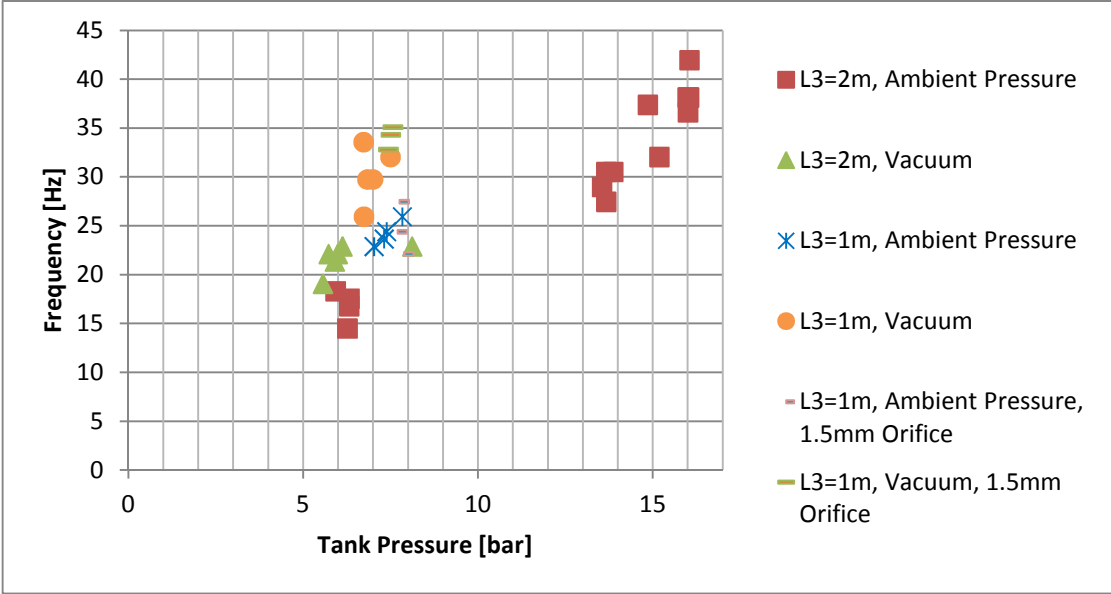


**Figure 5-4.** Test results: frequency versus tank pressure graph

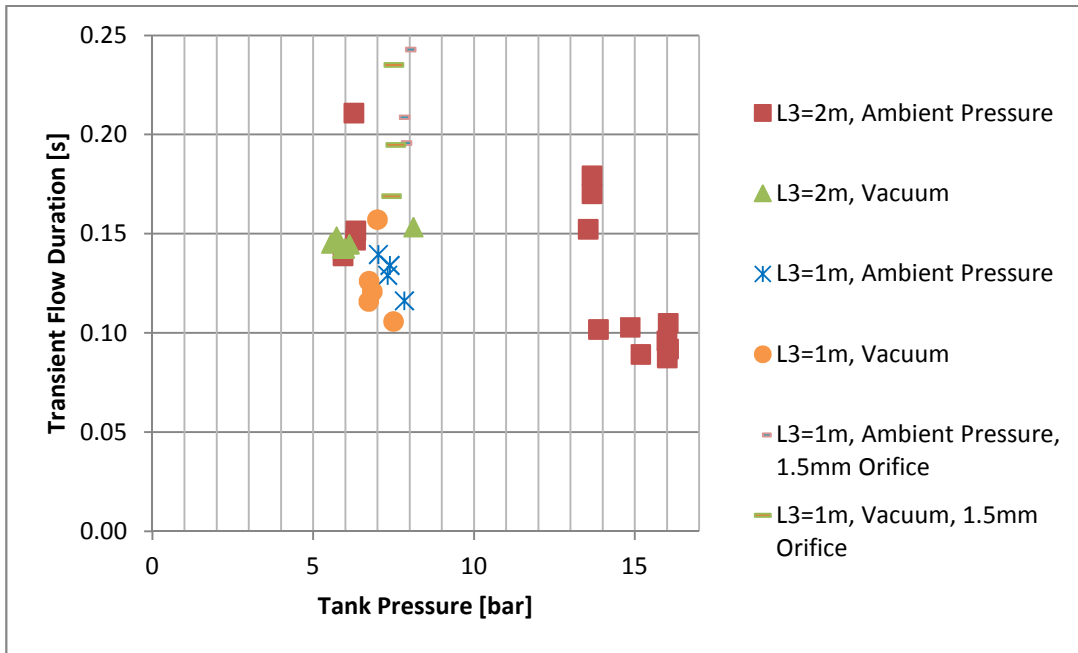


**Figure 5-5.** Test results: transient flow duration versus tank pressure graph

In below section, the trends of pressure change of exit solenoid valve are presented and discussed in detail for each test case.

### 5.1.1 Case A: Test With L3=2 m, Downstream Line Condition= Ambient Pressure

Tests from 1 to 13 and 20 are performed with L3 length of 2 m and downstream line condition of ambient pressure. Results of Test 1 are presented in Figure 5-6 as example. The damped harmonic motion around the tank pressure can be seen from the figure. The interesting behavior of the pressure of this test is seen in the second peak. There are two peaks in the second main peak and this behavior is seen in all tests of this group in either the first main peak or the second one. It is evaluated that this behavior is caused of the interaction between the air trapped in the pipe and the water.

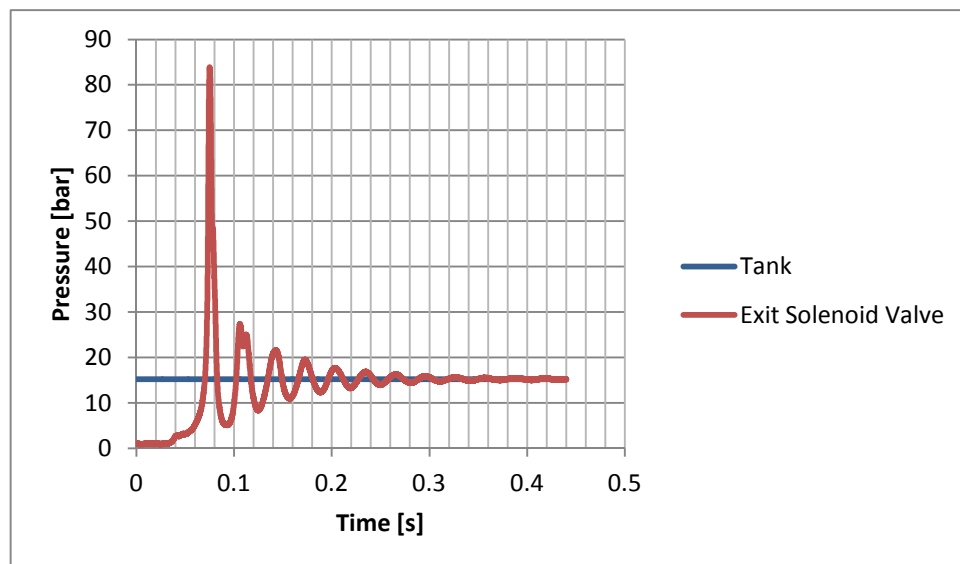


**Figure 5-6.** Pressure versus time graph for test No 1

### 5.1.2 Case B: Test With L3=2 m, Downstream Line Condition= Vacuum

Tests from 14 to 19 are performed with L3 length of 2 m and downstream line condition of vacuum (0.15-0.20 bar). Results of Test 18 are presented in Figure 5-7 as example. The damped harmonic motion around the tank pressure can be seen from the figure. The horn (two peaks in one main peak) seen in the first or second peak in tests with ambient pressure are not seen in this group of tests. It is assessed that the reason of this difference is the decreased amount of air in L3.

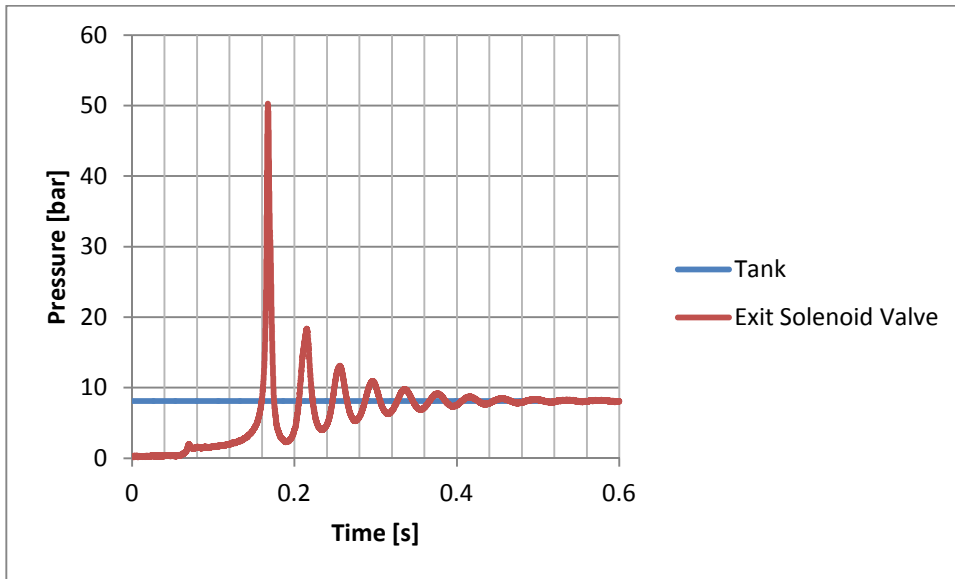
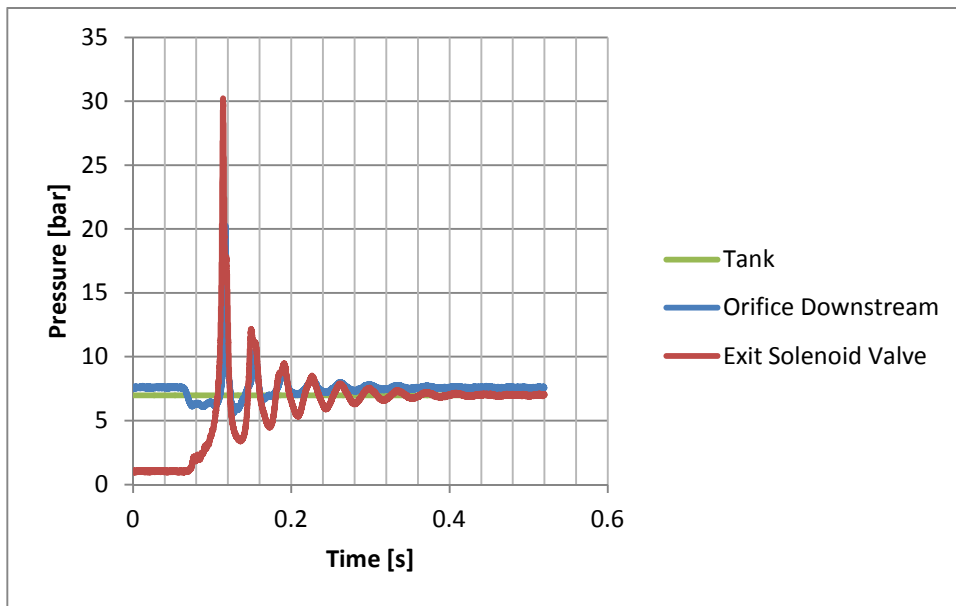


Figure 5-7. Pressure versus time graph for test No 18

### **5.1.3 Case C: Test With L3=1 m, Downstream Line Condition= Ambient Pressure**

Tests from 21 to 24 and 27 to 29 are performed with L3 length of 1 m and downstream line condition of ambient pressure. Results of Test 29 are presented in Figure 5-8 as example. Starting from this group of tests, the pressure data from the pressure transducer in the just downstream of the orifice are collected and presented. From the Figure, it is evaluated that as the latch valve is opened, water in the line from tank to latch valve starts to fill the line L3. Before the arrival of wave front to the exit solenoid valve, as the water column advances, the air in L3 starts to squeeze. When the pressure of trapped air in L3 and water in the upstream of latch valve are equalized, the pressure of these parts starts to increase together. Following that, the water wave front hits to the exit solenoid valve and the pressure peak occurs. The pressure rise speed depends on the latch valve opening model. The pressure rise at the orifice downstream pressure transducer is about  $L/a$  later than the pressure rise at the thruster valve.



**Figure 5-8.** Pressure versus time graph for test No 29

#### **5.1.4 Case D: Test With $L_3=1$ m, Downstream Line Condition= Vacuum**

Tests 25, 26 and 30, 31, 32 are performed with  $L_3$  length of 1 m and downstream line condition of vacuum. Results of Test 30 are presented in Figure 5-9 as example. Analyzing the Figure, it is evaluated that as the latch valve is opened, the water in the upstream of latch valve starts to flow into  $L_3$ . However before the increase in pressure of  $L_3$  line, the pressure of upstream of latch valve decreases. It is assessed that the reason of this behavior is that the information of squeeze in the air particles close to the latch valve is transmitted to the air particles close to the exit solenoid valve lately since the air is a compressible fluid. The small pressure peak before the main pressure peak is a result of squeezed air in  $L_3$ . After that small pressure peak, the pressure in exit solenoid valve starts to increase regularly. Following that the water wave front hits to the exit solenoid valve and the main pressure peak occurs.

It shall be noted that the small pressure peak mentioned above is also observed in the study of Ref [18] where experiments are done with the vacuum condition in the downstream of latch valve.

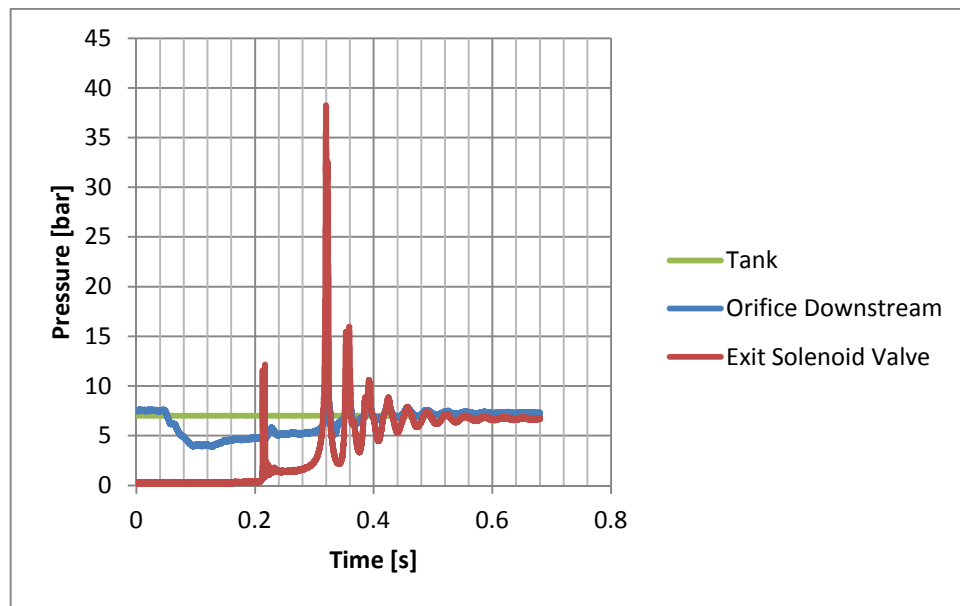


**Figure 5-9.** Pressure versus time graph for test No 30

### **5.1.5 Case E: Test With L3=1 m, Downstream Line Condition= Ambient Pressure, 1.5 mm Orifice**

Tests 33, 34, 35 are performed with L3 length of 1 m and downstream line condition of ambient pressure and 1.5 mm orifice. Results of Test 33 are presented in Figure 5-10 as example.

From the Figure, it is evaluated that as the latch valve is opened, water starts to flow into L3. Before the pressure increase in L3, the pressure drops in the upstream of

latch valve. The reason of this behavior is that before the information of squeeze in the air particles close to the latch valve is transmitted to the air particles close to the exit solenoid valve (since the air is a compressible fluid), large pressure drop occurs in the upstream of latch valve due to the orifice. After the pressures in the upstream and downstream of latch valve are equalized, the pressure of the total line starts to increase continuously. Following that, the water wave front hits to the exit solenoid valve and the main pressure peak occurs.

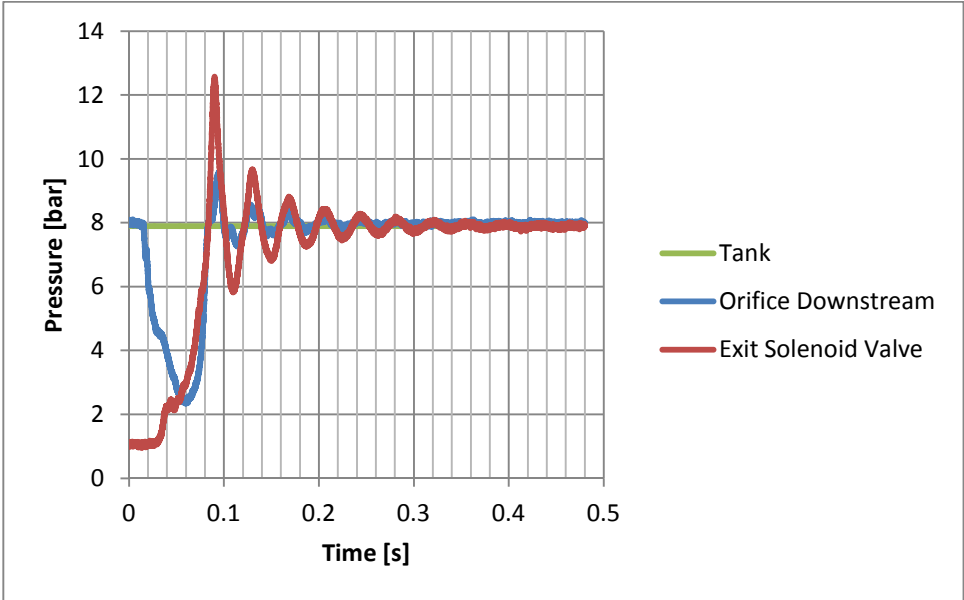


**Figure 5-10.** Pressure versus time graph for test No 33

### **5.1.6 Case F: Test With L3=1 m, Downstream Line Condition= Vacuum, 1.5 mm Orifice**

Tests 36, 37, 38 are performed with L3 length of 1 m and downstream line condition of vacuum and 1.5 mm orifice. Results of Test 37 are presented in Figure 5-11 as example.

From the Figure, it is evaluated that similar to the case with downstream line condition of ambient pressure and 1.5 mm of orifice, the pressure in the downstream of orifice decreases before the increase in pressure of exit solenoid valve with the same reason explained above. However, in this case, as can be seen from the Figure, the pressure in the downstream of the orifice drops below the vapor pressure. It can be explained such that as the water flows into L3, the tank cannot provide enough water to the pipeline and separation of water columns occurs. As a result, the pressure drops below vapor pressure and cavitation occurs. As the water flows into L3, the air in vacuum conditions is squeezed and the pressure in L3 starts to increase slowly. When the tank is able to supply enough water to the pipeline, collapse of water columns occur and the pressure in the upstream of the line increases and a pressure peak is seen in the pressure transducer in the downstream of orifice. Following that, the water wave front hits to the exit solenoid valve and water hammer occurs.

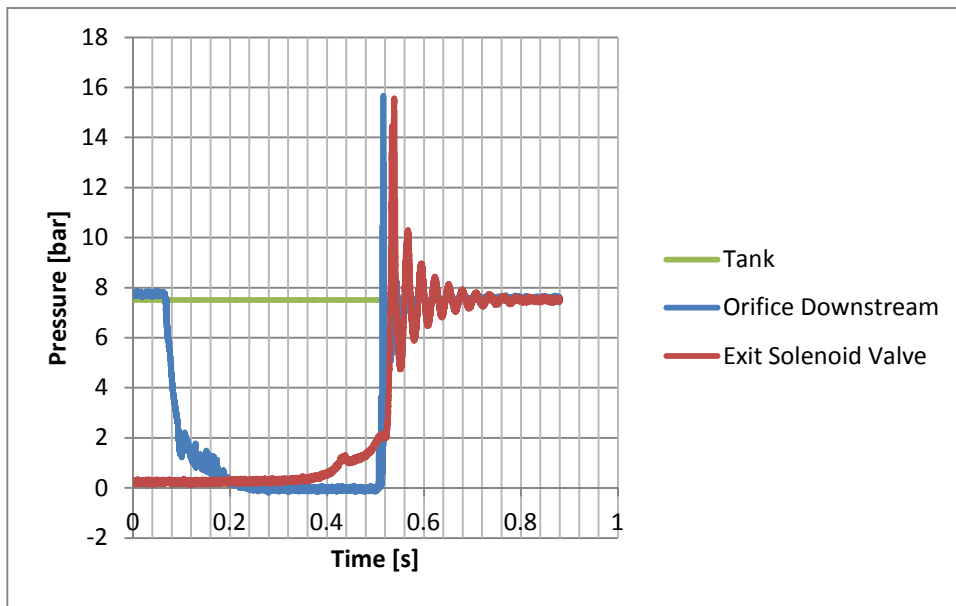


**Figure 5-11.** Pressure versus time graph for test No 37

## CHAPTER 6

### RESULTS AND DISCUSSION

In this chapter, the test and analysis results are compared and discussed in detail. During the comparison, the differences of results are presented in percentages. These differences are calculated as below:

$$\text{Difference \%} = \frac{\text{Test Value} - \text{Analysis Value}}{\text{Test Value}} \times 100$$

#### **6.1 Case A: Test and Analysis with L3=2 m, Downstream Line Condition= Ambient Pressure**

- Tests from 1 to 13 and 20 are the tests with L3 length of 2 m and downstream line condition of ambient pressure.
- Analyses 40, 42, 44, and 48 to 51 are the analyses with L3 length of 2 m and downstream line condition of ambient pressure.

Maximum Pressure change with respect to the tank pressure change is presented in Figure 6-1. In the range of 5-7 bar tank pressure, maximum pressure of tests are higher than the maximum pressure of analyses with maximum 54.2% rate (Test 20 versus Analysis 42). In the 13-16 bar tank pressure range, the analysis results are higher than the test results with minimum 0.2% rate (Test 10 and Analysis 51).

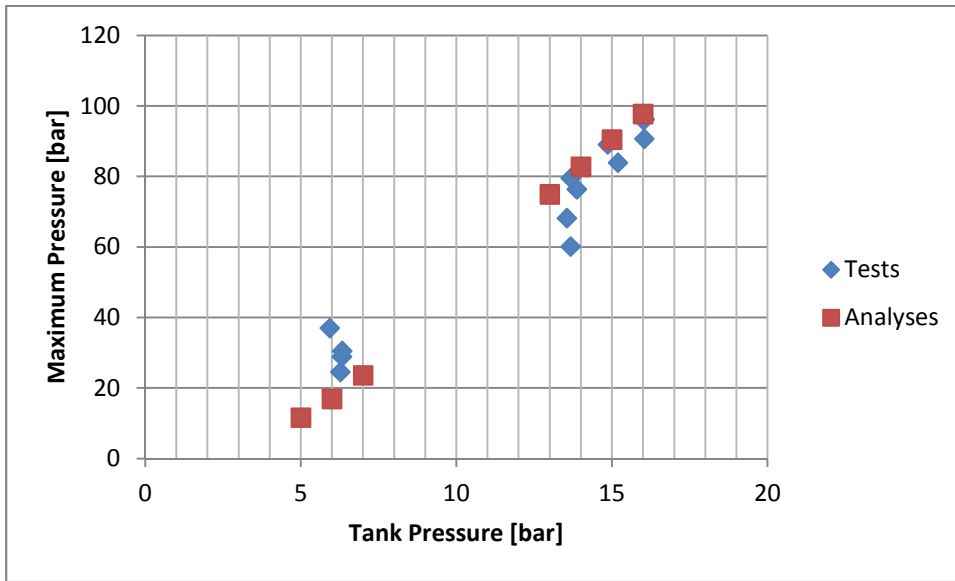


**Figure 6-1.** Maximum pressure versus tank pressure graph for L3=2 m and ambient pressure downstream line condition

Frequency change with respect to the tank pressure change is presented in Figure 6-2. In the range of 5-7 bar, the frequency of tests are maximum 63.3% higher than the frequency of analyses (Test 20 and Analysis 42). In the 13-16 bar range, the frequencies of tests are maximum 56.4% higher than the frequencies of analyses (Test 7 and Analysis 51).

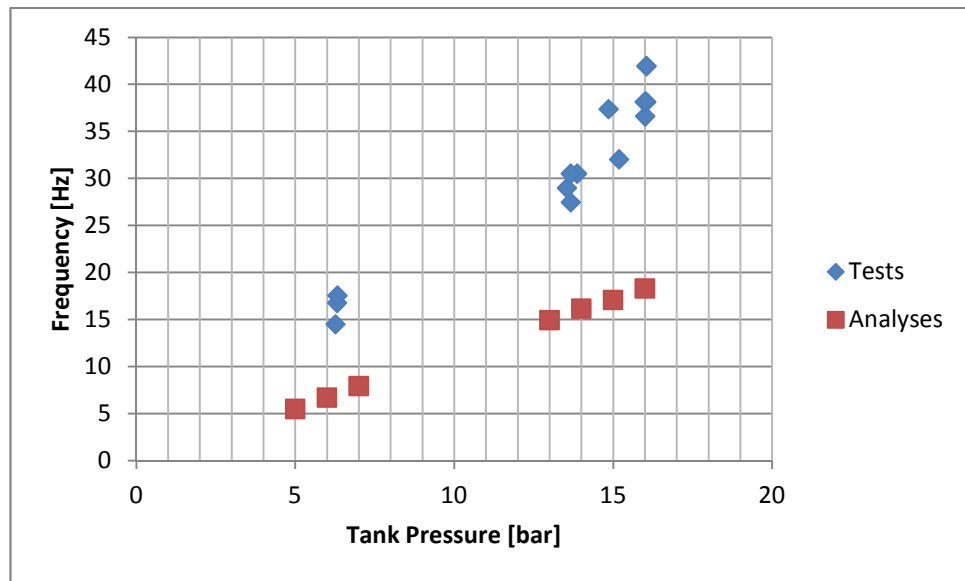


**Figure 6-2.** Frequency versus tank pressure graph for L3=2 m and ambient pressure downstream line condition

Transient Flow Duration change with respect to the tank pressure change is presented in Figure 6-3. In the 5-7 bar range, the transient flow duration of analyses are minimum 190% higher than the transient flow duration of tests (Test 11 and Analysis 42). In the 13-17 bar range, the transient flow duration of analyses are minimum 66% higher than the transient flow duration of tests (Test 4 and Analysis 49).

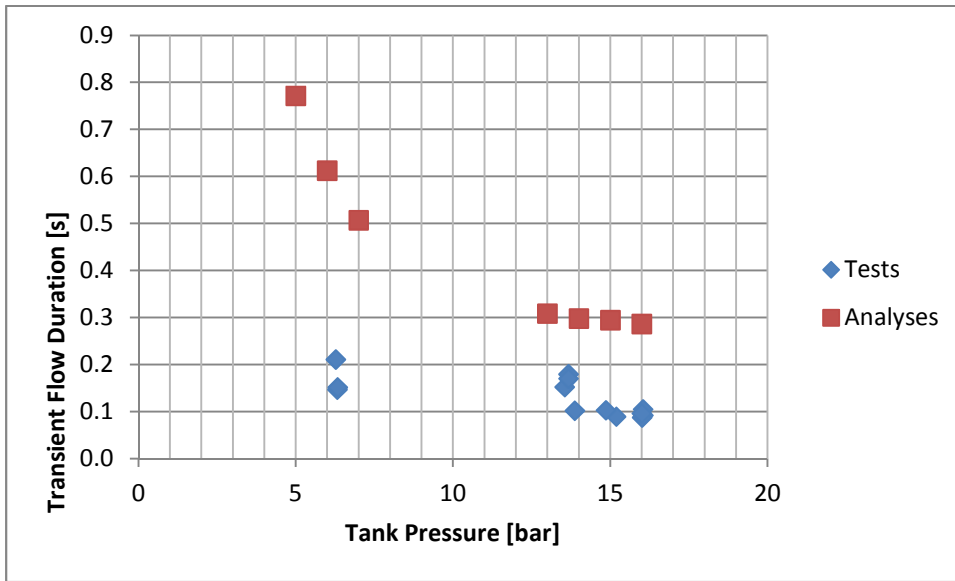


**Figure 6-3.** Transient flow duration versus tank pressure graph for L3=2 m and ambient pressure downstream line condition

In this group, the pressure versus time change of Analysis 50 and Test 1 are presented in Figure 6-4 as example. The inputs and results of these analyses/tests are given in Table 6-1 for the ease of tracking. The difference in maximum pressure and the frequency can be seen easily from the figure.

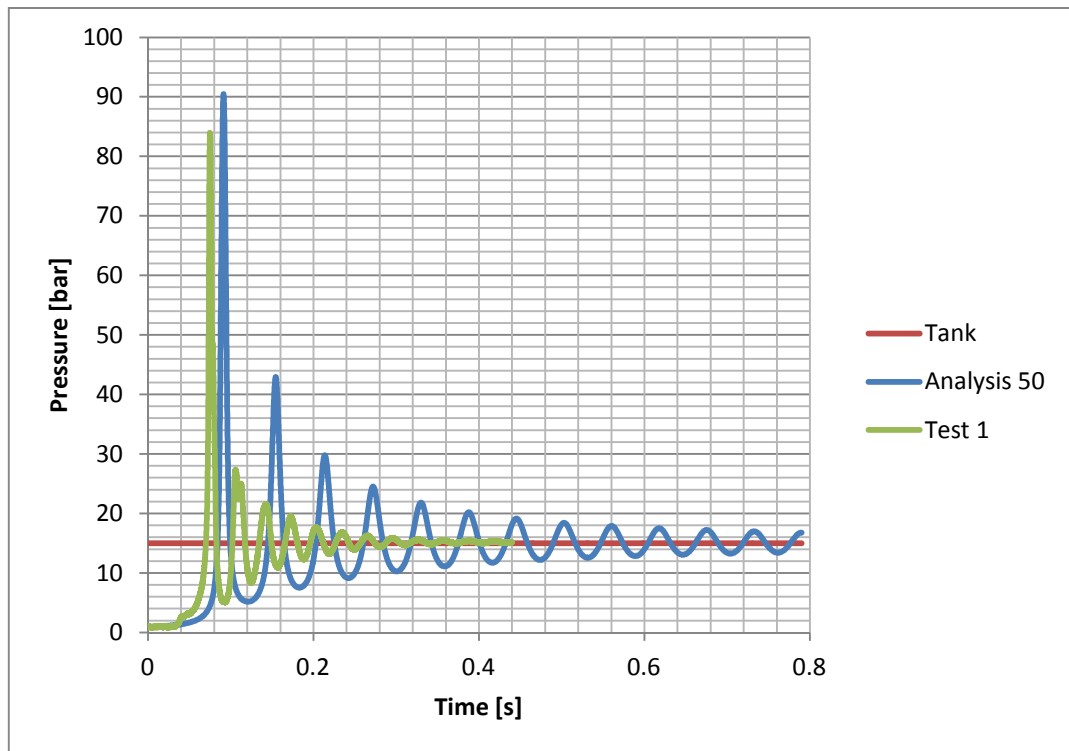


**Figure 6-4.** Comparison of Analysis 50 and Test 1

**Table 6-1.** Comparison of Analysis 50 and Test 1 inputs and results

Name	Tank Pressure [bar]	Downstream Line Pressure [bar]	Maximum Pressure [bar]	Frequency [Hz]	Time Constant [s]	Transient Flow Duration [s]
Analysis 50	15.00	0.94	90.44	17.09	0.0589	0.2944
Test 1	15.19	0.92	83.92	32.04	0.0179	0.0893

## 6.2 Case B: Test and Analysis with L3=2 m, Downstream Line Condition= Vacuum

- Tests from 14 to 19 are the tests with L3 length of 2 m and downstream line condition of vacuum.
- Analyses 41, 43, 45, 46 and 47 are the analyses with L3 length of 2 m and downstream line condition of vacuum.

Maximum Pressure change with respect to the tank pressure change is presented in Figure 6-5. Maximum pressures of analyses are minimum 48.5% higher than the maximum pressures of tests (Test 19 and Analysis 43).

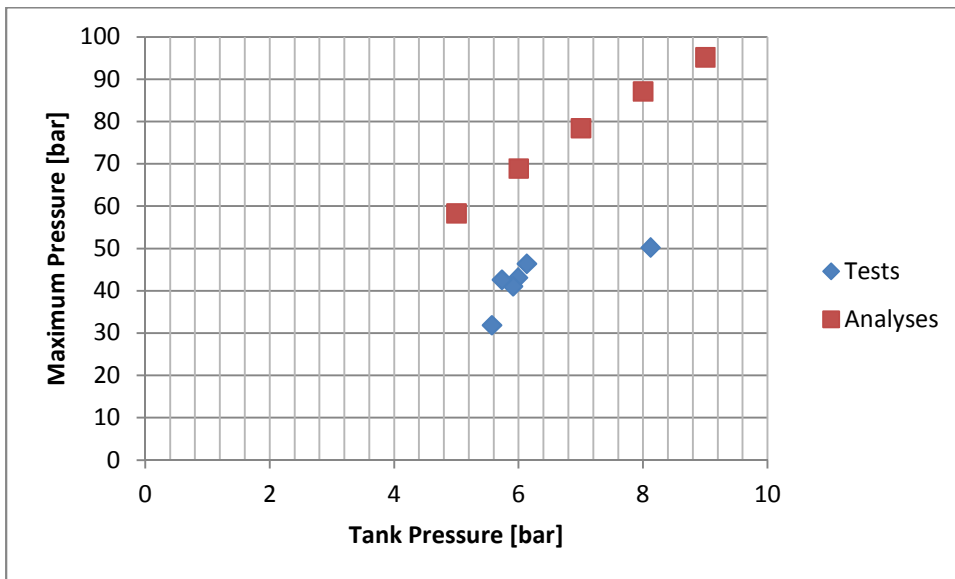


**Figure 6-5.** Maximum pressure versus tank pressure graph for L3=2 m and vacuum downstream line condition

Frequency change with respect to the tank pressure change is presented in Figure 6-6. The frequencies of tests are maximum 28% higher than the frequencies of analyses (Test 19 and Analysis 43).

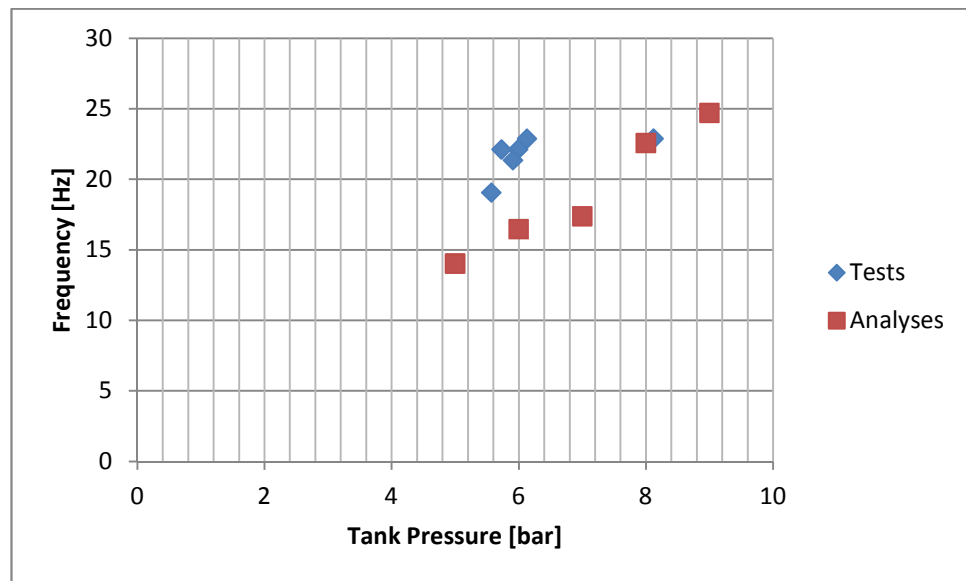


**Figure 6-6.** Frequency versus tank pressure graph for L3=2 m and vacuum downstream line condition

Transient Flow Duration change with respect to the tank pressure change is presented in Figure 6-7. Transient Flow Duration of analyses are minimum 121.2% higher than the Transient Flow Duration of tests (Test 18 and Analysis 46).

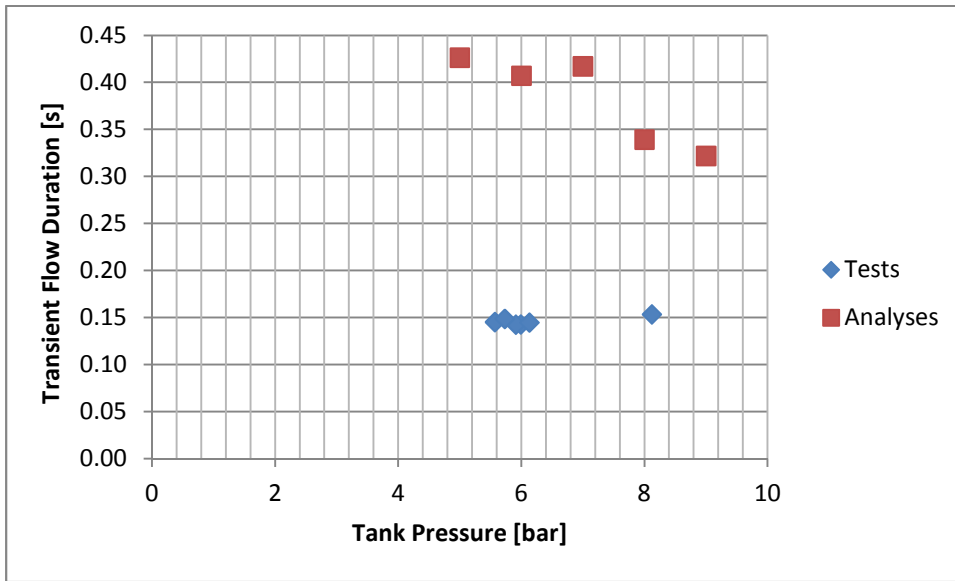


**Figure 6-7.** Transient flow duration versus tank pressure graph for L3=2 m and vacuum downstream line condition

In this group, the pressure versus time change of Analysis 46 and Test 18 are presented in Figure 6-8 as example. The inputs and results of these analyses/tests are given in Table 6-2 for the ease of tracking. The difference in maximum pressure and the frequency can be seen easily from the figure.

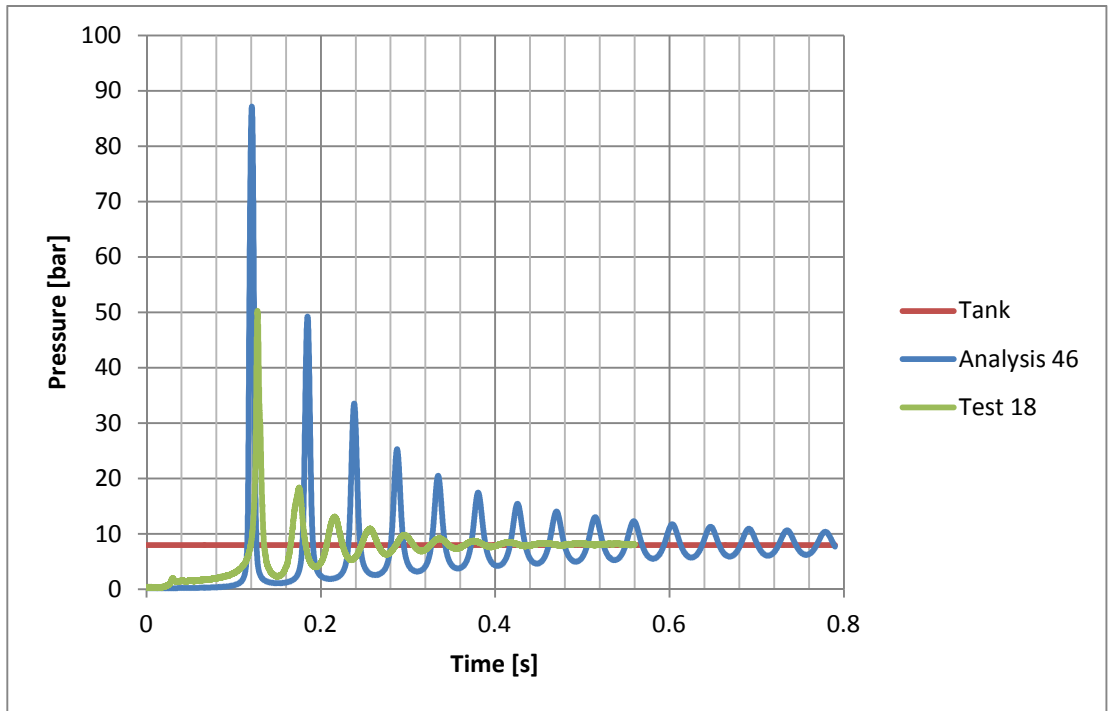


**Figure 6-8.** Comparison of Analysis 46 and Test 18

**Table 6-2.** Comparison of Analysis 46 and Test 18 inputs and results

Name	Tank Pressure [bar]	Downstream Line Pressure [bar]	Maximum Pressure [bar]	Frequency [Hz]	Time Constant [s]	Transient Flow Duration [s]
Analysis 46	8.00	0.15	87.12	22.58	0.0679	0.3393
Test 18	8.12	0.23	50.24	22.89	0.0307	0.1534

### 6.3 Case C: Test and Analysis with L3=1 m, Downstream Line Condition= Ambient Pressure

- Tests from 21 to 24 and 27 to 29 are the tests with L3 length of 1 m and downstream line condition of ambient pressure.
- Analyses from 52 to 54 are the analyses with L3 length of 1 m and downstream line condition of ambient pressure.

Maximum Pressure change with respect to the tank pressure change is presented in Figure 6-9. Maximum pressures of analyses are minimum 54% higher than the maximum pressures of tests (Test 24 and Analysis 53).

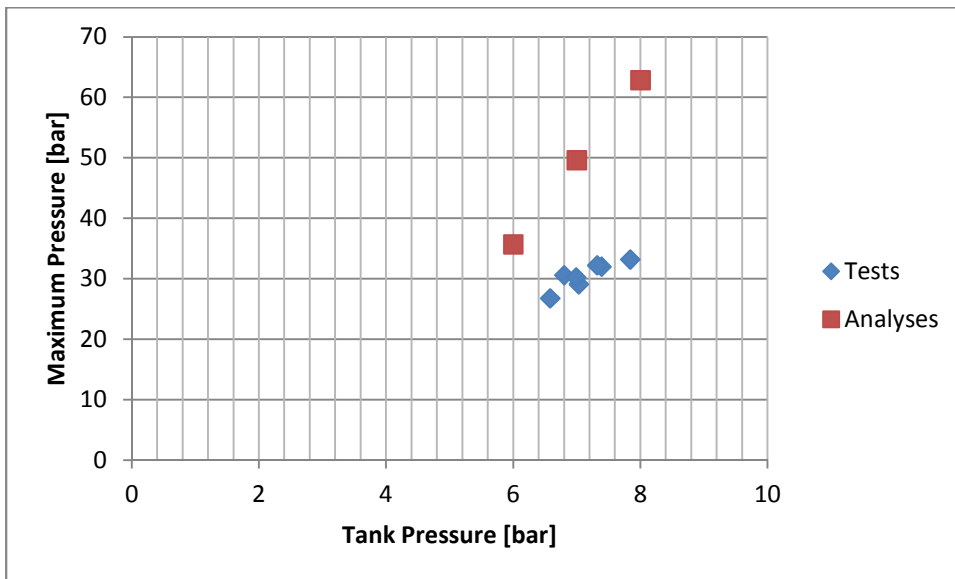


**Figure 6-9.** Maximum pressure versus tank pressure graph for L3=1 m and ambient pressure downstream line condition

Frequency change with respect to the tank pressure change is presented in Figure 6-10. Frequencies of tests are maximum 50.9% higher than the frequencies of analyses (Test 29 and Analysis 53).

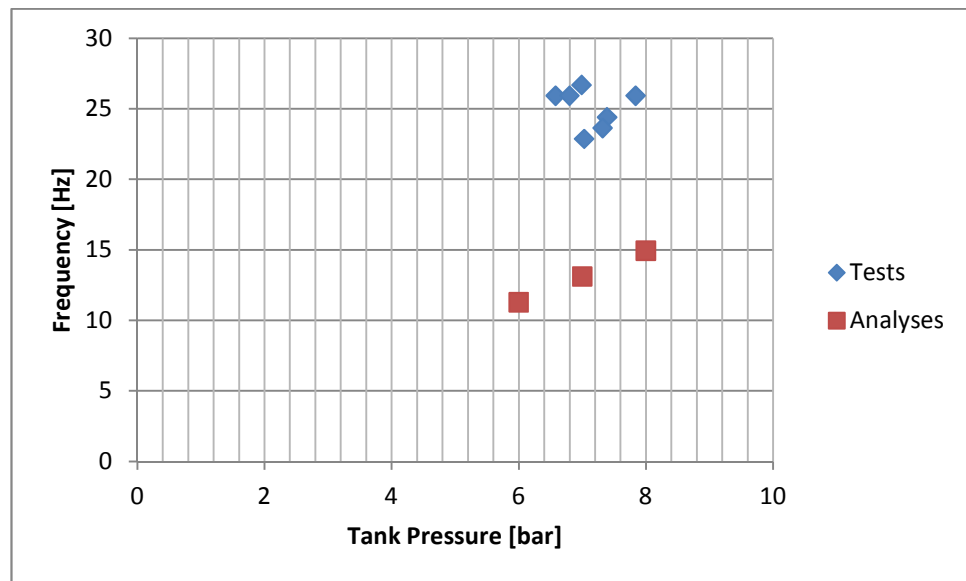


**Figure 6-10.** Frequency versus tank pressure graph for L3=1 m and ambient pressure downstream line condition

Transient flow duration change with respect to the tank pressure change is presented in Figure 6-11. The transient flow duration of analyses are minimum 81.8% higher than the transient flow duration of tests (Test 28 and Analysis 53).

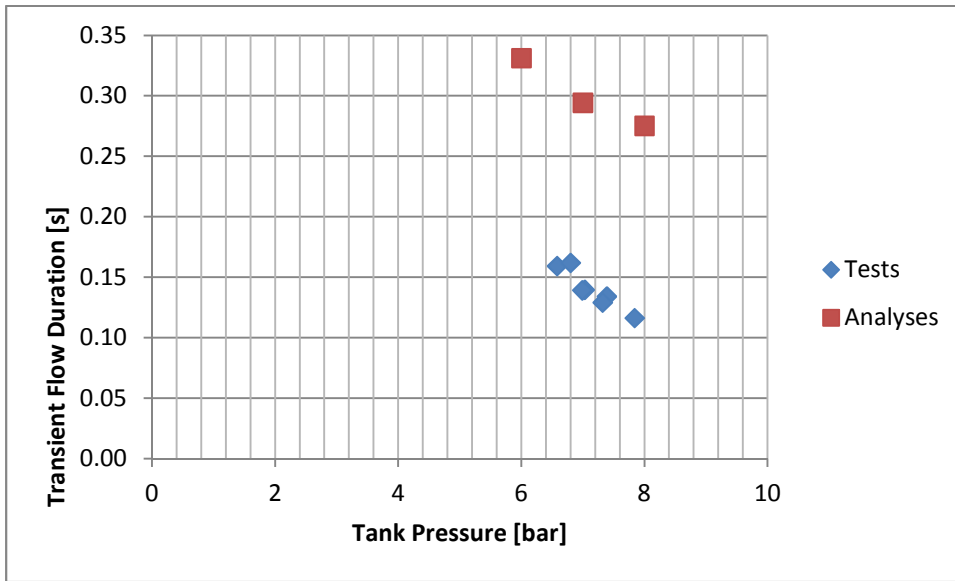


**Figure 6-11.** Transient flow duration versus tank pressure graph for L3=1 m and ambient pressure downstream line condition

In this group, the pressure versus time change of Analysis 53 and Test 29 are presented in Figure 6-12 as example. The inputs and results of these analyses/tests are given in Table 6-3 for the ease of tracking. The difference in maximum pressure and the frequency can be seen easily from the figure.

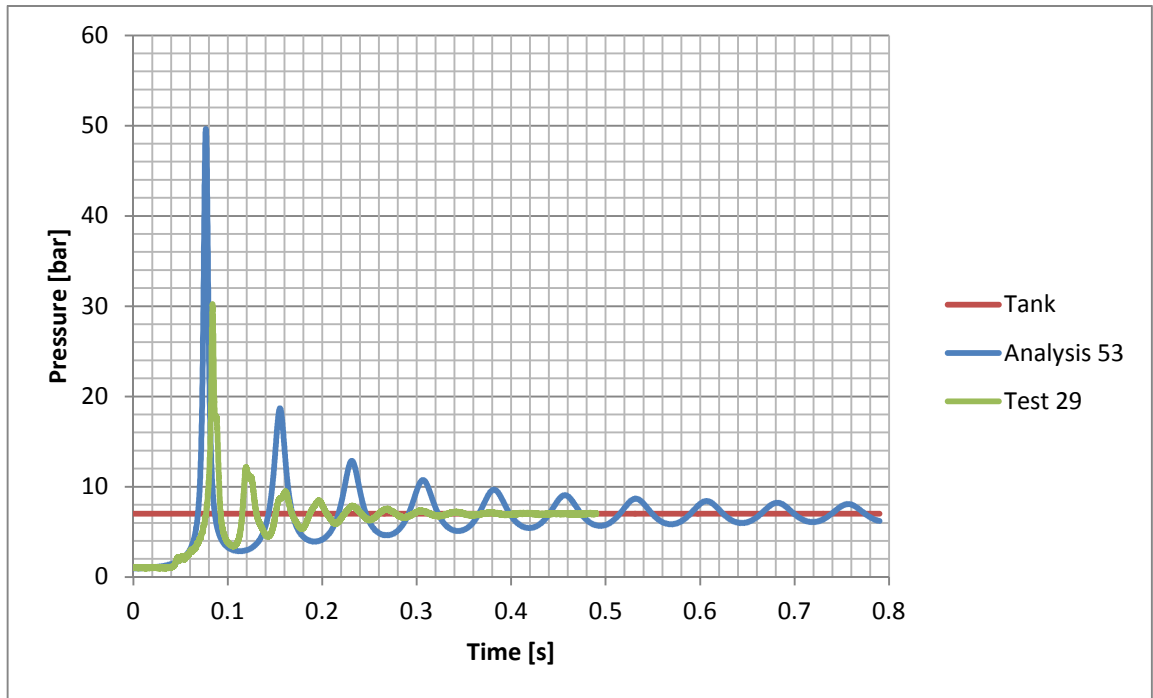


**Figure 6-12.** Comparison of Analysis 53 and Test 29

**Table 6-3.** Comparison of Analysis 53 and Test 29 inputs and results

Name	Tank Pressure [bar]	Downstream Line Pressure [bar]	Maximum Pressure [bar]	Frequency [Hz]	Time Constant [s]	Transient Flow Duration [s]
Analysis 53	7.00	0.94	49.62	13.12	0.0589	0.2943
Test 29	6.99	0.94	30.23	26.70	0.0278	0.1392

#### 6.4 Case D: Test and Analysis with L3=1 m, Downstream Line Condition= Vacuum

- Tests 25, 26 and 30, 31, 32 are the tests with L3 length of 1 m and downstream line condition of vacuum.
- Analyses from 55, 56 are the analyses with L3 length of 1 m and downstream line condition of vacuum.

Maximum Pressure change with respect to the tank pressure change is presented in Figure 6-13. Maximum pressures of analyses are minimum 127% higher than the maximum pressures of tests (Test 26 and Analysis 56).

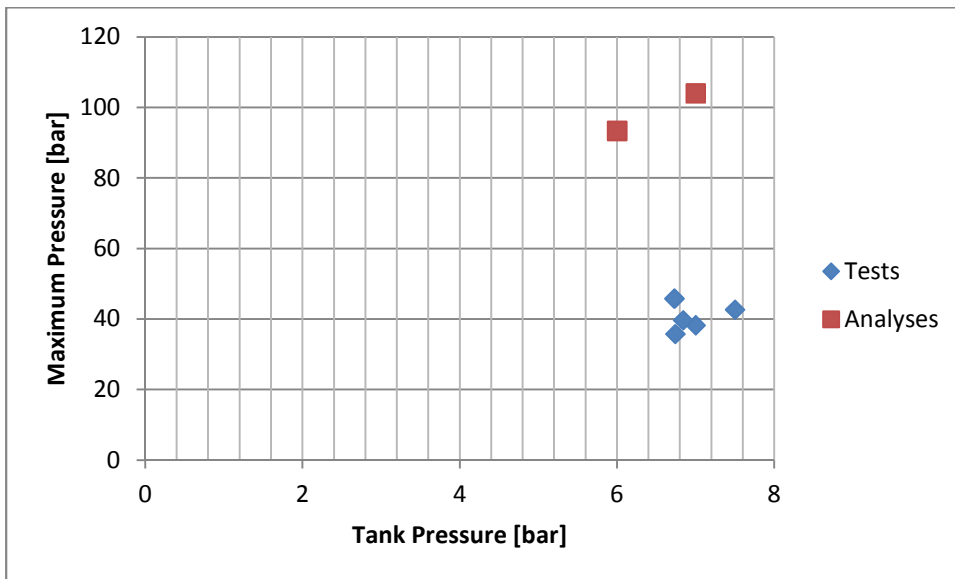


**Figure 6-13.** Maximum pressure versus tank pressure graph for L3=1 m and vacuum downstream line condition

Frequency change with respect to the tank pressure change is presented in Figure 6-14. As can be seen from the Figure, the frequencies of analyses are in the middle of frequencies of tests. At 7 bar tank pressure condition, the frequency of the analysis is 2.6% higher than the frequency of test (Test 30 and Analysis 56).

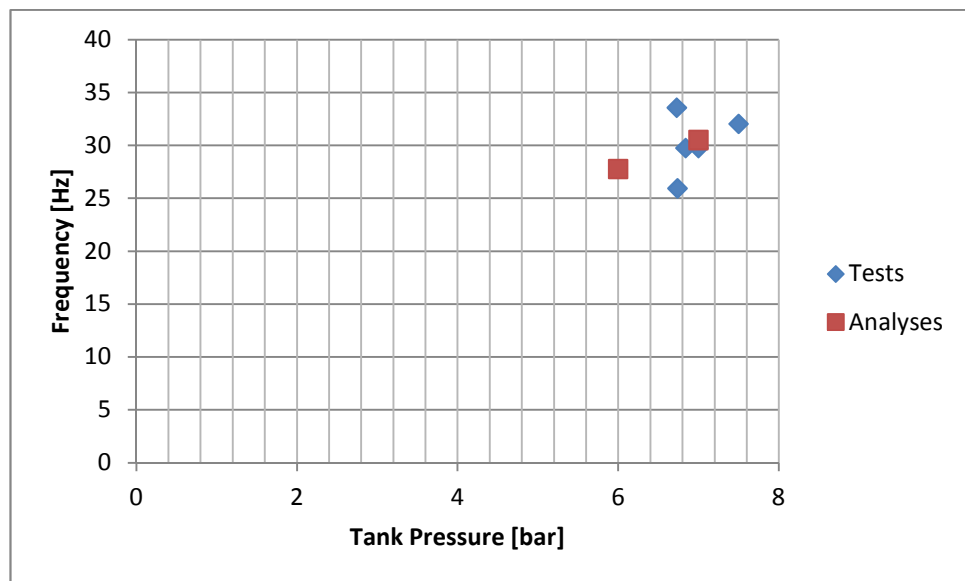


**Figure 6-14.** Frequency versus tank pressure graph for L3=1 m and vacuum downstream line condition

Transient flow duration change with respect to the tank pressure change is presented in Figure 6-15. Transient flow duration of analyses are minimum 78% higher than the transient flow duration of tests.

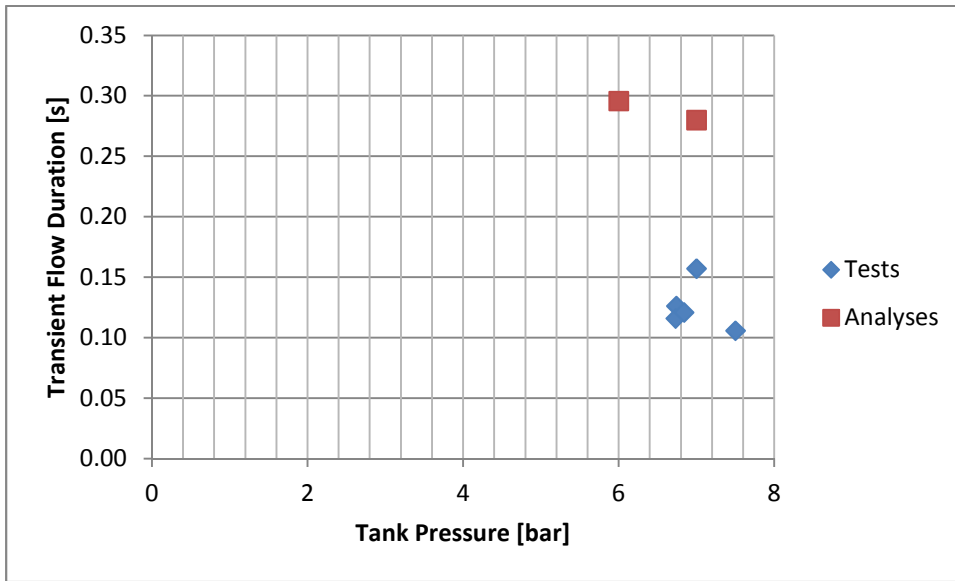


**Figure 6-15.** Transient flow duration versus tank pressure graph for L3=1 m and vacuum downstream line condition

In this group, the pressure versus time change of Analysis 56 and Test 30 are presented in Figure 6-16 as example. The inputs and results of these analyses/tests are given in Table 6-4 for the ease of tracking. The difference in maximum pressure and the frequency can be seen easily from the figure.

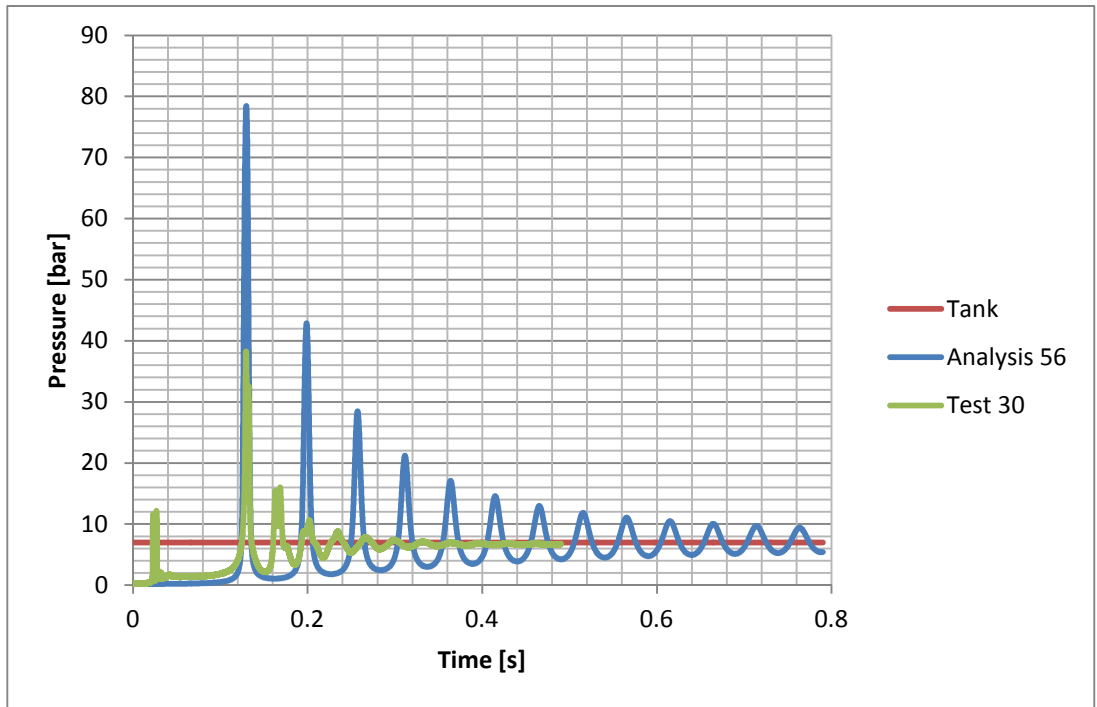


**Figure 6-16.** Comparison of Analysis 56 and Test 30

**Table 6-4.** Comparison of Analysis 56 and Test 30 inputs and results

Name	Tank Pressure [bar]	Downstream Line Pressure [bar]	Maximum Pressure [bar]	Frequency [Hz]	Time Constant [s]	Transient Flow Duration [s]
Analysis 56	7.00	0.15	104.01	30.52	0.0560	0.2800
Test 30	7.00	0.23	38.23	29.75	0.0314	0.1572

**6.5 Case E: Test and Analysis with L3=1 m, Downstream Line Condition= Ambient Pressure, 1.5 mm Orifice**

- Tests 33, 34, 35 are the tests with L3 length of 1 m, downstream line condition of ambient pressure and 1.5 mm orifice.
- Analyses from 57 and 58 are the analyses with L3 length of 1 m, downstream line condition of ambient pressure and 1.5 mm orifice.

Maximum Pressure change with respect to the tank pressure change is presented in Figure 6-17. Maximum pressures of tests are maximum 15% higher than the maximum pressures of analyses (Test 35 and Analysis 58).

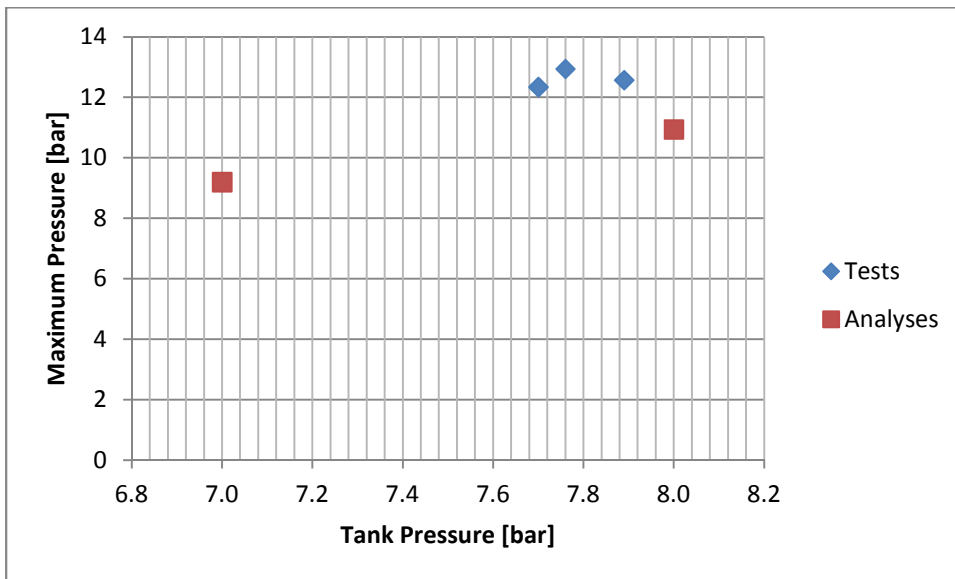


**Figure 6-17.** Maximum pressure versus tank pressure graph for L3=1 m and ambient pressure downstream line condition and 1.5 mm orifice

Frequency change with respect to the tank pressure change is presented in Figure 6-18. The frequencies of tests are maximum 45.6% higher than the frequency of analyses (Test 35 and Analysis 58).

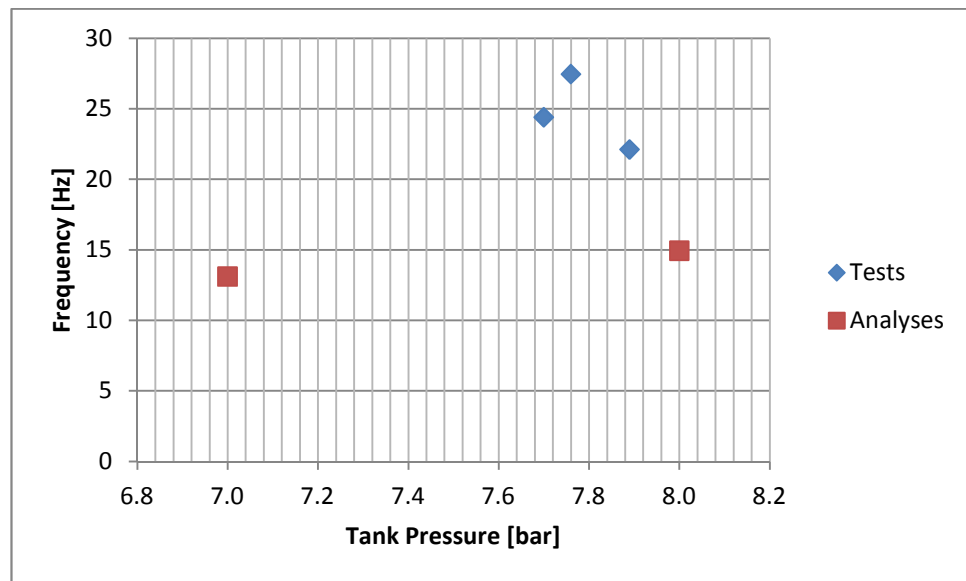


**Figure 6-18.** Frequency versus tank pressure graph for  $L_3=1$  m and ambient pressure downstream line condition and 1.5 mm orifice

Transient flow duration change with respect to the tank pressure change is presented in Figure 6-19. The transient flow duration of analyses are minimum 52% higher than the transient flow duration of tests (Test 33 and Analysis 58).

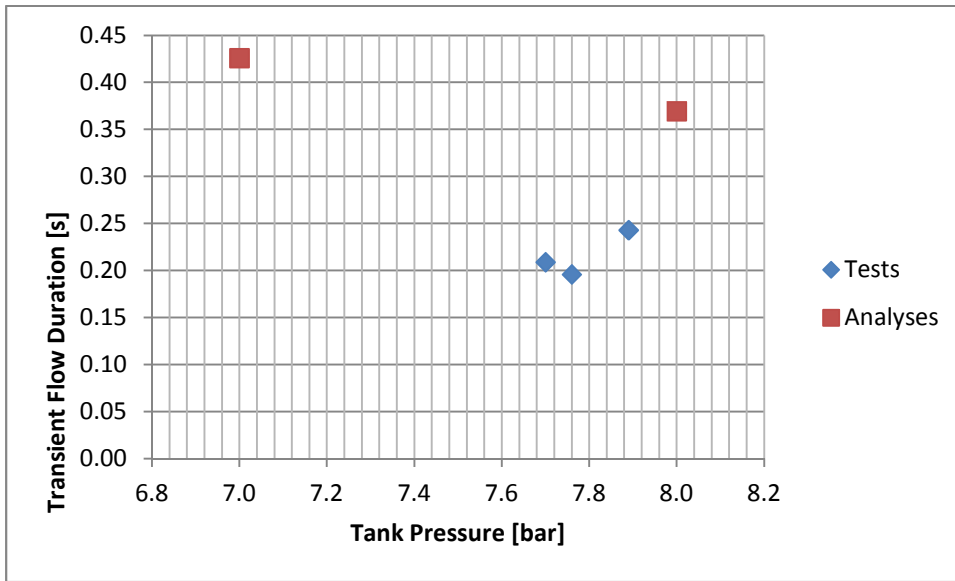


**Figure 6-19.** Transient flow duration versus tank pressure graph for L3=1 m and ambient pressure downstream line condition and 1.5 mm orifice

In this group, the pressure versus time change of Analysis 58 and Test 33 are presented in Figure 6-20 as example. The inputs and results of these analyses/tests are given in Table 6-5 for the ease of tracking. The difference in maximum pressure and the frequency can be seen easily from the figure.

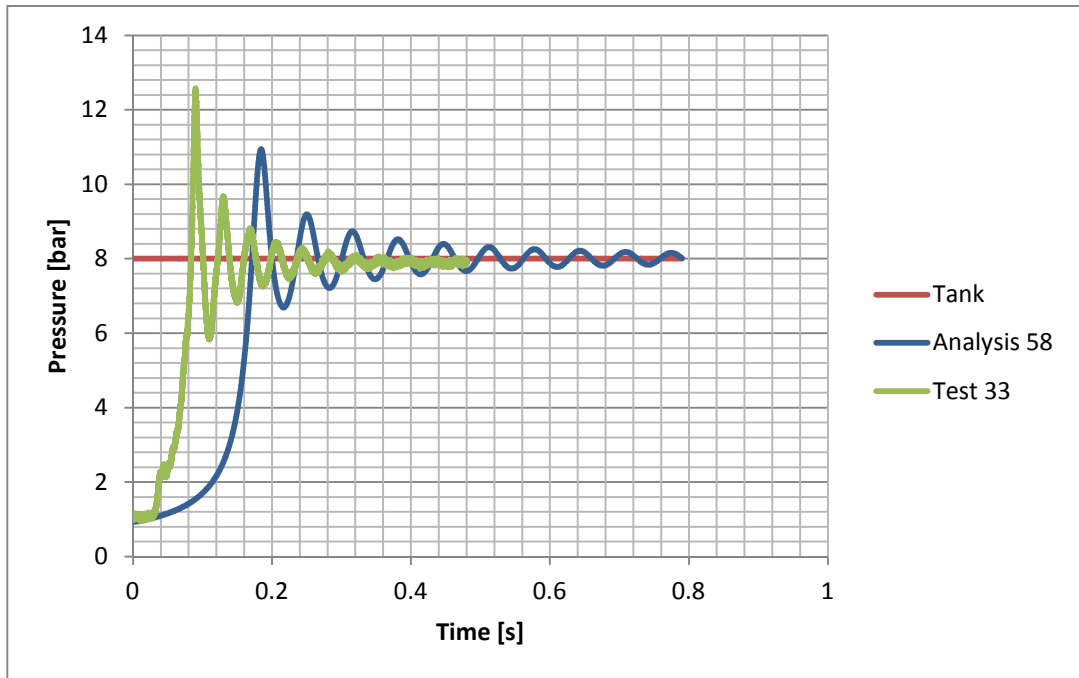


**Figure 6-20.** Comparison of Analysis 58 and Test 33

**Table 6-5.** Comparison of Analysis 58 and Test 33 inputs and results

Name	Tank Pressure [bar]	Downstream Line Pressure [bar]	Maximum Pressure [bar]	Frequency [Hz]	Time Constant [s]	Transient Flow Duration [s]
Analysis 58	8.00	0.94	10.94	14.95	0.0739	0.3694
Test 33	7.89	0.94	12.57	22.13	0.0486	0.2429

**6.6 Case F: Test and Analysis with L3=1 m, Downstream Line Condition= Vacuum, 1.5 mm Orifice**

- Tests 36, 37, 38 are the tests with L3 length of 1 m, downstream line condition of vacuum and 1.5 mm orifice.
- Analyses from 59 and 60 are the analyses with L3 length of 1 m, downstream line condition of vacuum and 1.5 mm orifice.

Maximum Pressure change with respect to the tank pressure change is presented in Figure 6-21. Maximum pressures of analyses are minimum 43% higher than the maximum pressures of tests (Test 38 and Analysis 59).

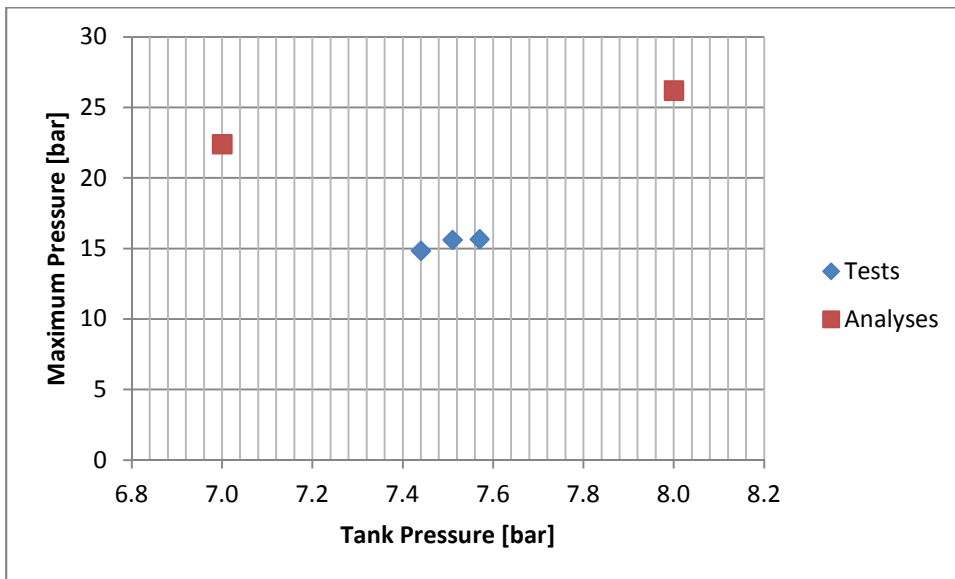


**Figure 6-21.** Maximum pressure versus tank pressure graph for L3=1 m and vacuum downstream line condition and 1.5 mm orifice

Frequency change with respect to the tank pressure change is presented in Figure 6-22. As can be seen from the figure, the frequencies of tests are in the middle of frequency of analyses.

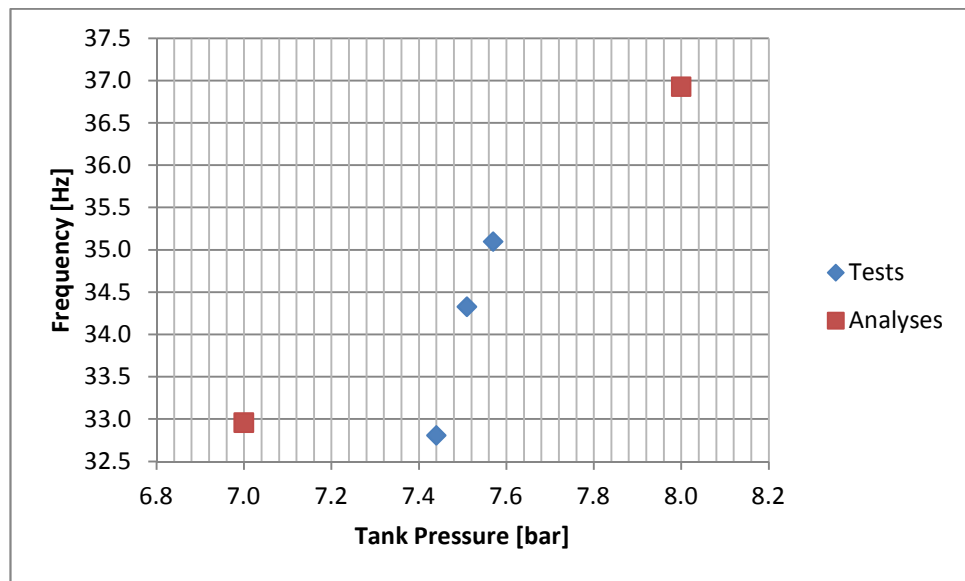


**Figure 6-22.** Frequency versus tank pressure graph for L3=1 m and vacuum downstream line condition and 1.5 mm orifice

Transient flow duration change with respect to the tank pressure change is presented in Figure 6-23. Transient flow duration of tests are maximum 31.6% higher than the transient flow duration of analyses (Test 37 and Analysis 59).

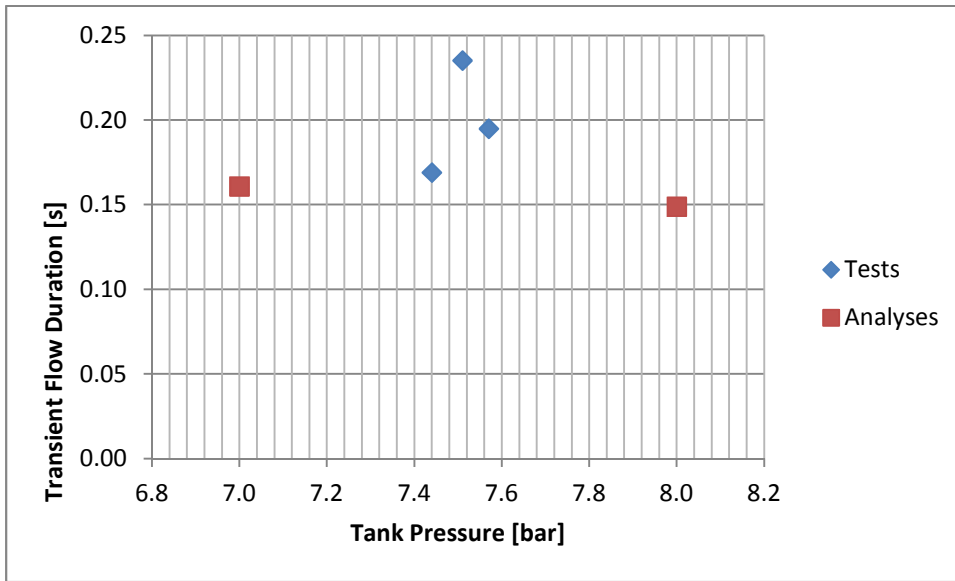


**Figure 6-23.** Transient flow duration versus tank pressure graph for L3=1 m and vacuum downstream line condition and 1.5 mm orifice

In this group, the pressure versus time change of Analysis 59 and Test 37 are presented in Figure 6-24 as example. The inputs and results of these analyses/tests are given in Table 6-6 for the ease of tracking. The difference in maximum pressure and the similarity in frequency can be seen easily from the figure.

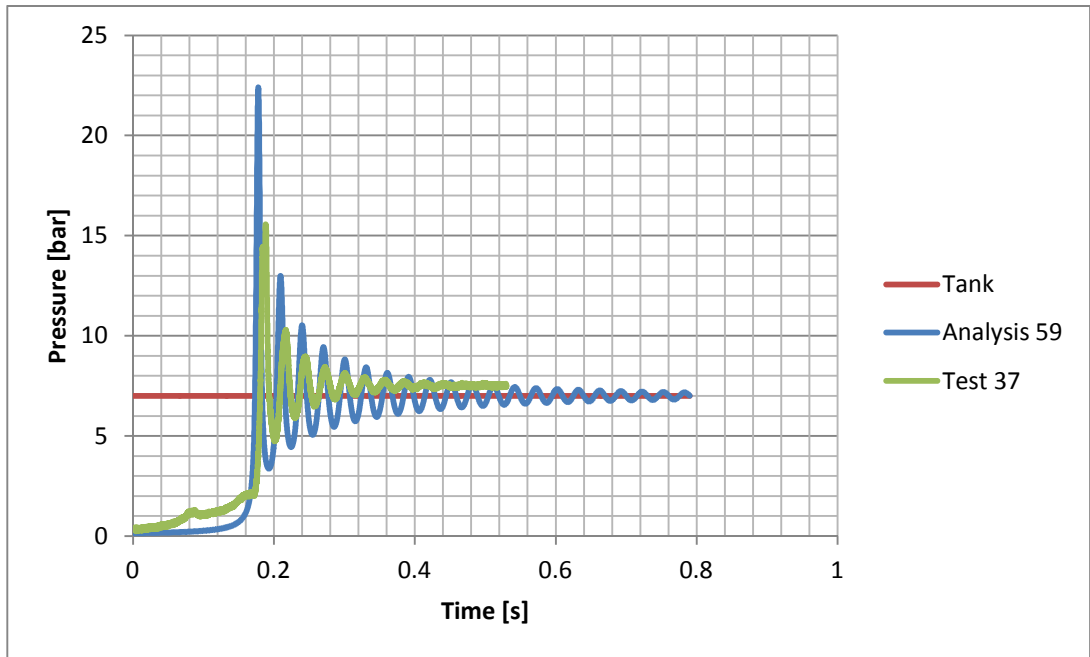


**Figure 6-24.** Comparison of Analysis 59 and Test 37

**Table 6-6.** Comparison of Analysis 59 and Test 37 inputs and results

Name	Tank Pressure [bar]	Downstream Line Pressure [bar]	Maximum Pressure [bar]	Frequency [Hz]	Time Constant [s]	Transient Flow Duration [s]
Analysis 59	7.00	0.15	22.40	32.96	0.0322	0.1608
Test 37	7.51	0.24	15.61	34.33	0.0470	0.2351

To sum up with the results of tests and analyses:

- In estimation of Maximum Pressure:
  - The success rate of Flownex changes from 54.2% less estimation to 127% higher estimation.
  - Under vacuum condition of downstream line, Flownex can make higher estimation than tests. So it is safe to use Flownex for the cases with vacuum condition in downstream line.
  - Under ambient condition of downstream line, Flownex can make either higher or less estimations than tests. So, it is evaluated that using only Flownex in maximum pressure estimation in this condition is not enough.
- In estimation of Frequency:
  - The success rate of Flownex changes from 63.3% less estimation to successful fit.
  - Under vacuum condition of downstream line, Flownex can make either less estimation or successful fit. So, it is evaluated that using only Flownex in frequency estimation in this condition is not enough.
  - Under ambient condition of downstream line, Flownex always makes less estimation. So, it is evaluated that Flownex is not successful in frequency estimation under ambient pressure downstream line condition and other software should be preferred for this condition.
- In estimation of Transient Flow Duration:
  - The success rate of Flownex changes from 190% higher estimation to 31.6% less estimation.
  - Flownex generally estimates the transient flow duration higher. So, it is evaluated that it is safe to use Flownex in transient flow rate duration.
  - From analyses, it is observed that the transient flow duration generally does not follow a certain trend. So, it is better not to use the transient flow duration as a design criterion in satellite propulsion system.

## CHAPTER 7

### CONCLUSION

In this thesis, a simplified satellite monopropellant propulsion system has been experimentally studied for the investigation of water hammer. In addition to experimental study, a numerical approach by using a commercial software was also conducted. By numerical means, wider range of test parameters was analyzed.

Some outcomes from the analyses are as follows:

- Maximum pressure, amplitude of the pressure and frequency increases as the tank pressure increases.
- Maximum pressure and frequency decreases as the downstream line pressure increases.
- The transient flow duration does not follow a certain trend as the tank pressure or downstream line pressure changes.
- Maximum pressure and frequency decreases as L1, L2 and L3 length increases.
- The transient flow duration first decreases but the increases, as the L3 length increases. However it is assessed that that trend might change in case of more analyses with more L3 data points.
- The transient flow duration increases as L1 and L2 lengths increases.
- The change in L1 and L2 lengths does not affect the maximum pressure, frequency and transient flow duration but the increase in L3 decreases the maximum pressure, frequency and transient flow duration while the total pipeline length is kept constant.
- As the orifice diameter gets smaller, the maximum pressure decreases.
- Frequency and transient flow duration do not follow a certain trend as the orifice diameter changes.

- As the pipe inner diameter increases, the maximum pressure and transient flow duration increases, frequency changes abruptly.

Some outcomes from the tests are as follows:

- In some tests, even though less tank pressure is used in the test, higher maximum pressures could be obtained for the same test condition.
- In the tests with vacuum downstream line condition, higher maximum pressures are obtained with respect to the tests with ambient pressure in L3.
- Orifice usage decreases the maximum pressure significantly.
- No significant effect of the L3 pipe length change could be observed in the tests.
- Frequency of pressure waves changes with the tank pressure, downstream line pressure and length of L3.
- Usage of orifice does not affect the frequency of pressure waves significantly.
- Different frequencies could be obtained from the tests with the same tank pressures.
- With the increasing tank pressure, the transient flow duration can both increase and decrease.
- Transient flow duration does not change significantly with the downstream line condition, e.g. ambient pressure or vacuum.
- Orifice usage increases the transient flow duration significantly.

As a conclusion within this study, the water hammer effect is observed. The water hammer peak pressure is effectively reduced by implementing an orifice in the pipeline system. As a conclusion, usage of orifice is essential in satellite propulsion systems. Moreover, change of pipeline length is not effective in maximum pressure when the length change is small. And the maximum pressure increases as the downstream line pressure decreases.

Regarding the comparison of analyses and tests, it is evaluated that the numerical approach cannot satisfy a collective success in estimation of water hammer effects. So, it is suggested to use another software or change the analysis model in Flownex. It is evaluated that, in order to understand the behavior of the propulsion system transients well, it is necessary to perform the tests and analyses for the thruster operational case where the thruster valve is opened/closed suddenly while the latch valve is kept open, as a future study. Also, in order to have full knowledge of satellite propulsion system in priming phase, the adiabatic compression should be studied. In this frame, the temperatures of the system should be measured during the priming tests.

This page is left intentionally blank.

## REFERENCES

- [1] Euroconsult, “Satellites to be Built and Launched by 2022 World Market Survey”, 2013 Brochure.
- [2] ECSS-Q-40B : Space Product Assurance – Safety Standard, European Cooperation for Space Standardization, 17 May 2002.
- [3] G.P. Sutton, O. Biblarz, *Rocket Propulsion Elements*, John Wiley & Sons, Inc., Seventh Edition, 2001.
- [4] C. Brown, *Spacecraft Propulsion*, American Institute of Aeronautics and Astronautics (AIAA) Education Series, Second Printing, 1996.
- [5] Buchheim, W. R., *Space Handbook : Astronautics and Its Applications*, Modern Library Paperbacks, 1959
- [6] Propulsion Systems , Thales Alenia Space.  
[http://www.thalesgroup.com/Portfolio/Documents/Propulsion\\_Systems/](http://www.thalesgroup.com/Portfolio/Documents/Propulsion_Systems/), 2012.
- [7] R.P. Prickett, E. Mayer, J. Hermel, “Water Hammer in a Spacecraft Propellant Feed System”, *Journal of Propulsion and Power*, Vol. 8, No. 3, May-June 1992.
- [8] C. Leca, P. Boh, S. D’Halewyn, “MON and MMH Pressure Surges For a Simplified Propellant Feed System”, *Proc. 3rd International Conference on Spacecraft Propulsion*, Cannes, 10-13 October 2000, ESA SP-465, December 2000.
- [9] L. Ounougha, F. Colozzi, “Correlation Between Simulations and Experiments on Water Hammer Effects in a Propulsion System”, *Proc. Second European Spacecraft Propulsion Conference*, 27-29 May, 1997, ESA SP-398, August 1997.
- [10] I. Gibek, Y. Maisonneuve, “Waterhammer Tests with Real Propellants”, AIAA.

- [11] C.R. Koppel, J. Moral, M. De Rosa, R.P. Vara, J. Steelant, P. Omaly, “Satellite Propulsion Modeling with EcosimPro Comparison Between Simulation and Ground Tests”, *Progress in Propulsion Physics 2* (2011) 743-764, 2011.
- [12] C.R. Koppel, J. Moral, R.P. Vara, M.D. Rosa, J. Steelant, P. Omaly, “A Platform Satellite Modelling with EcosimPro: Simulation Results”, 45th AIAA/ASME/SAE/ASEE Joint Propulsion Conference & Exhibit, 2-5 August 2009, Denver, Colorado.
- [13] R. Lecourt, J. Steelant, “Experimental Investigation of Water Hammer in Simplified Feed Lines of Satellite Propulsion Systems”, *Journal of Propulsion and Power*, Vol. 23, No. 6, November-December 2007.
- [14] A.S. Yang, “Satellite Hydrazine Propulsion System Design Trades”, *Journal of Da-Yeh University*, Vol. 10, No. 1, pp.41-50 (2001).
- [15] A.S. Yang, T.C. Kuo, “Numerical Simulation for the Satellite Hydrazine Propulsion System”, AIAA 2001-3829.
- [16] J.G. Sun, X. Q. Wang, “Pressure Transient in Liquid Lines”, ASME/JSME Pressure Vessels and Piping Conference, July 23-27, 1995, Honolulu, Hawaii.
- [17] K.L. Yaggy, “Analysis of Propellant Flow Into Evacuated and Pressurized Lines”, AIAA, 1984.
- [18] M. Lema, et al., “Multiphase Fluid Hammer in Propellant Lines”, Space Propulsion Conference, 2010.
- [19] W.H. Hsieh, C.Y. Lin, A.S. Yang, “Blowdown and Waterhammer Behaviour of Mono-propellant Feed Systems for Satellite Attitude and Reaction Control”, AIAA, 1997.
- [20] J. Molinsky, “Water Hammer Test of the Seastar Hydrazine Propulsion System”, 33rd AIAA/ ASME/SAE/ASEE Joint Propulsion Conference & Exhibit, 1997.

- [21] F. Bidner et al., Senior Design Symposium Hydrazine Hammer, Engineering Excellence Fund, Ball Aerospace & Technologies Corp..
- [22] V.D. Ronco, “Simplified Analysis of Pressure Spikes Due to Water Hammer During Priming of Spacecraft Propulsion Systems”, 6<sup>th</sup> Space Propulsion Conference, 2010.
- [23] J.H. Williams, “Water hammer Modeling for the Ares I Upper Stage Reaction Control System Cold Flow Development Test Article”, Master’s Thesis in Aerospace Engineering Faculty of Mississippi State University , 2010.
- [24] H. Stockfleth, et al., “Safe Priming and Depletion Test Performance for the VEGA Launcher Hydrazine Roll and Attitude Control System (RACS)”, 6<sup>th</sup> Space Propulsion Conference, 2010.
- [25] M. Ozer, “Solution of Transient Flow in Pipe Networks”, Master’s Thesis in Civil Engineering, Middle East Technical University, September, 1980.
- [26] E.A. Aksel, “Simulation of Unsteady Flow in Liquid Pipelines”, Master’s Thesis in Mechanical Engineering Middle East Technical University, May 1991.
- [27] E. N. Koncagül, “Transient Analysis of Liquid Pipeline Systems”, Master’s Thesis in Mechanical Engineering, Middle East Technical University, 1996.
- [28] G. Koc, “Simulation of Flow Transients in Liquid Pipeline Systems”, Master’s Thesis in Mechanical Engineering, Middle East Technical University, November 2007.
- [29] M. Calamak, “Investigation Of Waterhammer Problems In The Penstocks Of Small Hydropower Plants”, Master’s Thesis in Civil Engineering, Middle East Technical University, 2010.
- [30] E. Sakabas, “Investigation Of Waterhammer Problems In Çamlıdere Dam - İvedik Water Treatment Plant Pipeline At Various Hydraulic Conditions”, Master’s Thesis in Civil Engineering, Middle East Technical University, 2012.

- [31] A. S. Tijsseling, “Fluid-Structure Interaction in Liquid Filled Pipe Systems: A Review”, *Journal of Fluids and Structures* 10, 109-146, 1996.
- [32] A. Bergant, et al. “Water hammer with column separation: A historical review”, *Journal of Fluids and Structures* 22, 135-171, 2006.
- [33] A. Bergant, et. al. “Water hammer with column separation: A review of research in the twentieth century”, Department of mathematics and computer science, University of technology, 2004.
- [34] European Space Propulsion System Simulation, ESPSS, EcosimPro [http://www.ecosimpro.com/download/brochures/ecosimpro\\_brochure\\_library\\_esps.pdf](http://www.ecosimpro.com/download/brochures/ecosimpro_brochure_library_esps.pdf), 2013.
- [35] AFT Impulse, Waterhammer & Surge Analysis Software, <http://www.aft.com/products/impulse>, 2013.
- [36] Wanda, <http://www.deltares.nl/en/software/980173/wanda>, 2013.
- [37] Flowmaster, <http://www.flowmaster.com/>, 2013.
- [38] Flownex Simulation Environment, <http://www.flownex.com/>, 2013.
- [39] Ansys CFX, <http://www.ansys.com/Products/Simulation+Technology/Fluid+Dynamics/Fluid+Dynamics+Products/ANSYS+CFX>, 2013.
- [40] Hammer V8i, <http://www.bentley.com/en-US/Products/HAMMER/>, 2013
- [41] Easy 5, <http://www.mscsoftware.com/product/easy5>, 2013.
- [42] COMMIX-1C, <http://www.osti.gov/scitech/biblio/6287160>, 2013.
- [43] KYPipe, <http://kypipe.com/>, 2013.

- [44] Pipeline Studio,  
<http://www.technotrade.com.pk/4/Pipeline%20Studio/?catid=1&purl=PIPEFLO>,  
2013.
- [45] Larock, B. E., Jeppson, R.W., Watters, G.Z., *Hydraulics of Pipeline Systems*,  
CRC Press, 2000.
- [46] Wylie, E. B., Streeter, V. L., *Fluid Transients in Systems*, Prentice-Hall,  
Englewood Cliffs, New Jersey, 1993.
- [47] Flownex Simulation Environment, [www.flownex.com](http://www.flownex.com).
- [48] Flownex Library Theory Manual, Flownex Simulation Environment, January  
2013.
- [49] Sahib M. et al, “The Effect of Water Hammer upon Pipes at Suddenly Closed  
Valve”, Journal of Thi-Qar University, Special number, Vol. 5, March 2010.
- [50] Valencia-Bel, F., et al., “Assessment for Hydrazine Detonability During  
Priming System Activities”, Space Propulsion Conference, Cologne, Germany, May  
2014.

This page is left intentionally blank.

## APPENDIX A

### PIPELINE HYDRAULICS

The theory of fluid flow in case of water hammer effect is presented in this section utilizing the information given in Ref [45].

#### A.1. Euler Equation

Newton's second law of motion that is force applied to a control volume equals to the product of the corresponding mass and its acceleration is utilized for the derivation of Euler equation. In this frame, applying Newton's second law to a cylindrical control volume at the pipe centerline as shown in Figure A. 1, below equations are derived.

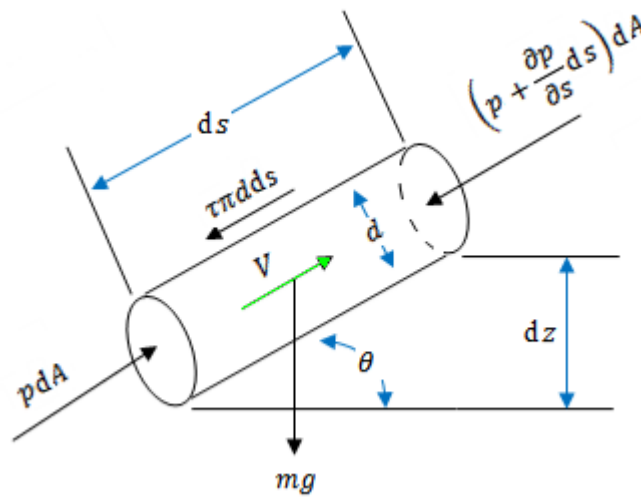


**Figure A. 1** Fluid control volume at the pipe centerline

$$\sum F = ma = m \frac{DV}{Dt}$$

$$pdA - \left( p + \frac{\partial p}{\partial s} ds \right) dA - mg \sin \theta - \tau \pi d ds = m \frac{DV}{Dt}$$

where  $p$  is the pressure,  $m$  is the mass,  $\tau$  is the shear stress at the walls of control volume,  $s$  is the distance along streamline,  $d$  is the diameter of control volume,  $V$  is the velocity of flow,  $t$  is time and  $A$  is the area of the cross section of control volume. Mass can be expressed as:

$$m = \rho \mathcal{V} = \frac{\rho \pi d^2 ds}{4} = \frac{\gamma \pi d^2 ds}{4g}$$

since  $\gamma = \rho g$

Dividing above equation with:

$$mg = \frac{\gamma \pi d^2 ds}{4} = \gamma d A ds$$

gives,

$$-\frac{1}{\gamma} \frac{\partial p}{\partial s} - \sin \theta - \frac{4\tau}{\gamma d} = \frac{1}{g} \frac{DV}{Dt}$$

Since :

$$\sin \theta = \frac{\partial z}{\partial s}$$

It is possible to obtain

$$-\frac{1}{\gamma} \frac{\partial p}{\partial s} - \frac{\partial z}{\partial s} - \frac{4\tau}{\gamma d} = \frac{1}{g} \frac{DV}{Dt}$$

Expanding the control volume diameter to the pipe diameter ( $d \rightarrow D$ ), introducing the average velocity  $V$  and utilizing  $\tau_0$  as the shear stress at the wall:

$$-\frac{1}{\gamma} \frac{\partial p}{\partial s} - \frac{\partial z}{\partial s} - \frac{4\tau_0}{\gamma D} = \frac{1}{g} \frac{DV}{Dt}$$

Utilizing Darcy-Weisbach friction factor  $f$  as:

$$\tau_0 = \frac{1}{8} f g V |V|$$

One can obtain

$$\frac{1}{g} \frac{DV}{Dt} + \frac{1}{\gamma} \frac{\partial p}{\partial s} + \frac{\partial z}{\partial s} + \frac{f}{D} \frac{V|V|}{2g} = 0 \quad (\text{A-1})$$

## A.2. Pressure Head Change

For  $0 < t < L/\alpha$ , the unsteady flow is as shown in Figure A. 2.

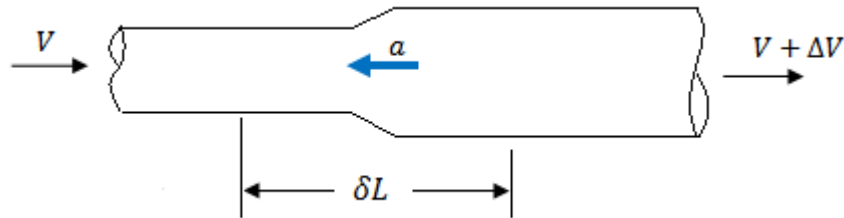


**Figure A. 2.** Unsteady Flow

$\alpha$  is the wave speed relative to an observer at rest with respect to the pipe and  $\Delta V$  is the negative velocity change.

Since the unsteady flow exists, the linear momentum equation for steady flow is not applicable. Because of that, a translating coordinate system possessing speed same

as the wave speed moving to the left is utilized here, as shown in Figure A. 3. In this way, the unsteady flow seems like the steady flow.

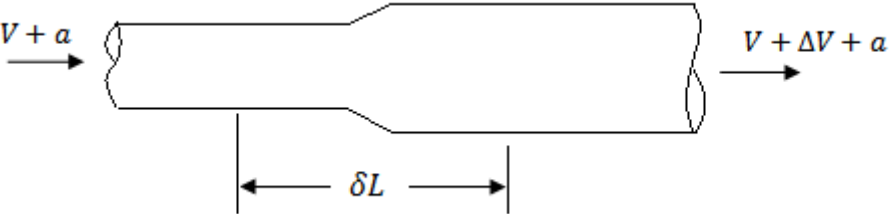


**Figure A. 3.** Steady Flow

One dimensional steady flow control volume for momentum analysis is shown in Figure A. 4

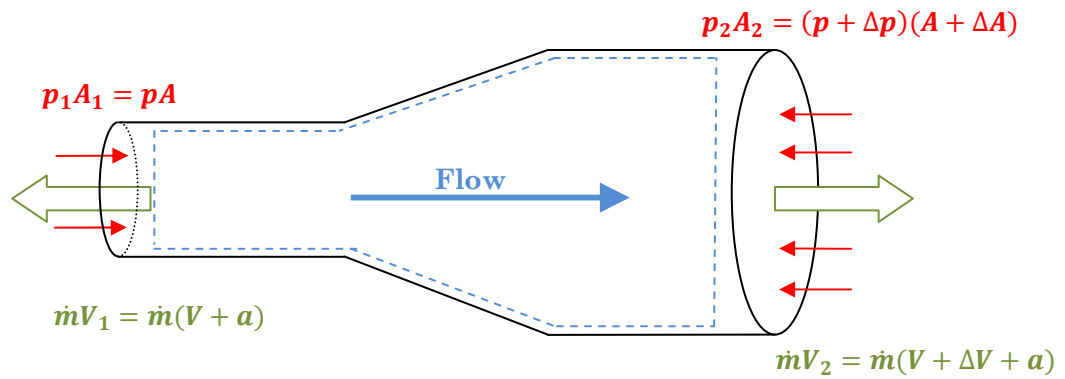


**Figure A. 4.** Steady Flow Control Volume for Momentum Analysis

$$\sum F_{ext} = \frac{D(mV)}{Dt}$$

$$pA - (p + \Delta p)(A + \Delta A) = \dot{m}(V + \Delta V + a) - \dot{m}(V + a)$$

$$-p\Delta A - \Delta pA - \Delta p\Delta A = \rho Q\Delta V$$

Neglecting  $p\Delta A$  and  $\Delta p\Delta A$ :

$$-\Delta pA = \rho Q\Delta V \tag{A- 2}$$

$$\Delta H = \frac{\Delta p}{\rho g} = \frac{\Delta p}{\gamma} \tag{A- 3}$$

$$\text{using } Q = (V + a)A \tag{A- 4}$$

and substituting equations (A- 3) and (A- 4) into (A- 2):

$$-\Delta H \rho g A = \rho(V + a)A\Delta V$$

$$\Delta H = -\frac{\Delta V}{g}(V + a) = -\frac{a}{g}\Delta V\left(1 + \frac{V}{a}\right)$$

when  $\frac{V}{a} < 0.01$ , the above expression can be expressed as

$$\Delta H = -\frac{a}{g}\Delta V \tag{A- 5}$$

Equation (A- 5) is valid for steady, 1-D and incompressible flow. As shown here, a decrease in the velocity causes an increase in the head. Utilizing equation (A- 3), equation (A- 5) becomes:

$$\Delta P = -\rho a \Delta V \tag{A- 6}$$

### A.3. Mass Accumulation

Considering the same control volume with the one used in previous chapter at time  $t$  when the pressure wave has just arrived to the control volume and at time  $t + \delta t$  when the pressure wave has just passed the control volume, the mass accumulation is calculated as presented below.

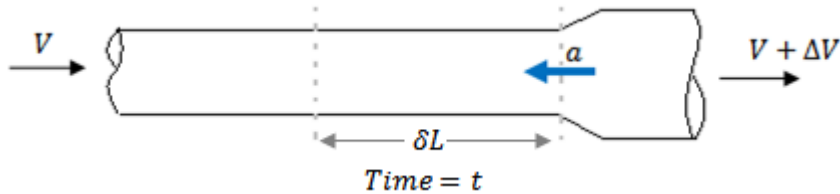


**Figure A. 5.** Flow Control Volume when the wave has just arrived to the Control Volume

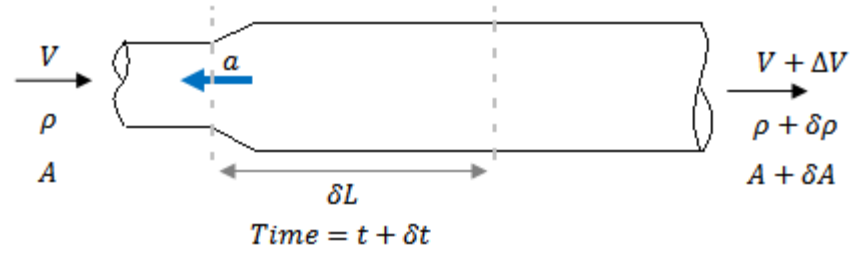


**Figure A. 6.** Flow Control Volume when the wave has just passed the Control Volume

$$\dot{m}_{acc} = \dot{m}_t - \dot{m}_{t+\delta t}$$

$$\dot{m}_{acc} = \rho AV - (\rho + \Delta\rho)(A + \Delta A)(V + \Delta V)$$

Neglecting terms with  $\Delta\rho$  and  $\Delta A$ :

$$\dot{m}_{acc} = -\rho A \Delta V$$

$$m_{acc} = \delta m = -\rho A \Delta V \delta t$$

$$\delta t = \frac{\delta L}{a}$$

$$\delta m = -\rho A \Delta V \frac{\delta L}{a} \tag{A- 7}$$

#### A.4. Change in Pipe Volume due to Elasticity

As the pressure in the pipe increases, the pipe stretches providing more space to store the accumulated net inflow of liquid. Depending on the pipe constraints, the pipe may stretch both circumferentially and longitudinally.

For the strain,  $\varepsilon_1$  in one direction, if the material is free to strain without creating stress in that direction, strain by an amount  $\varepsilon_2$  exists also in the perpendicular direction according to the formula  $\varepsilon_2 = -\mu\varepsilon_1$ , where  $\mu$  is the Poisson's ratio.

For the thin walled, homogenous and isotropic pipes:

$$\sigma_1 = \frac{\varepsilon_1 + \mu\varepsilon_2}{1 - \mu^2} E \quad \text{or} \quad \varepsilon_1 = \frac{\sigma_1 - \mu\sigma_2}{E}$$

$$\sigma_2 = \frac{\varepsilon_2 + \mu\varepsilon_1}{1 - \mu^2} E \quad \text{or} \quad \varepsilon_2 = \frac{\sigma_2 - \mu\sigma_1}{E}$$

where,  $\sigma_1$  and  $\varepsilon_1$  are stress and strain in the direction along the pipe axis,  $\sigma_2$  and  $\varepsilon_2$  are stress and strain in the circumferential direction and

$$E = \frac{\sigma}{\varepsilon} \quad \text{is the modulus of elasticity of the pipe material.}$$

In case of water hammer in the flow, it is accepted that a stress and strain is already resident in the pipe caused by the steady state flow. Hence, the equations are written in incremental form, as given in Ref [45].

$$\Delta\sigma_1 = \frac{\Delta\varepsilon_1 + \mu\Delta\varepsilon_2}{1 - \mu^2} E \quad \text{or} \quad \Delta\varepsilon_1 = \frac{\Delta\sigma_1 - \mu\Delta\sigma_2}{E} \quad (\text{A- 8})$$

$$\Delta\sigma_2 = \frac{\Delta\varepsilon_2 + \mu\Delta\varepsilon_1}{1 - \mu^2} E \quad \text{or} \quad \Delta\varepsilon_2 = \frac{\Delta\sigma_2 - \mu\Delta\sigma_1}{E}$$

Change in volume caused by circumferential stretching is:

$$\delta V_c = \pi D \frac{\delta D}{2} \delta L$$

where

$$\pi\delta D = \pi D \Delta\varepsilon_2$$

Combining the above equations as

$$\delta V_c = \frac{1}{2} \pi D^2 \delta L \Delta \varepsilon_2 \quad (\text{A- 9})$$

Change in volume caused by longitudinal stretching is given as

$$\delta V_l = \frac{\pi}{4} D^2 \delta L \Delta \varepsilon_1 \quad (\text{A- 10})$$

Combining equations (A- 9) and (A- 10) total volume change due to pipe stretching is:

$$\delta V = \frac{\pi}{4} D^2 \delta L (\Delta \varepsilon_1 + 2\Delta \varepsilon_2) \quad (\text{A- 11})$$

Change in circumferential stress in the pipe wall under static conditions:

$$\Delta \sigma_2 = \frac{\Delta p D}{2e} \quad (\text{A- 12})$$

where,  $e$  is the pipe wall thickness. Substituting equation (A- 12) into equation (A- 8):

$$\frac{\Delta p D}{2e} = \frac{\Delta \varepsilon_2 + \mu \Delta \varepsilon_1}{1 - \mu^2} E \quad (\text{A- 13})$$

The relation between the circumferential stress and pressure is valid for all types of restraints. On contrary, the relation between the longitudinal stress and strain varies with the restraint type.

For longitudinal stress and strain, three cases exists:

- Case (a): Pipe anchorage only at the upstream end
- Case (b): Full pipe restraint from axial movement
- Case (c): Longitudinal expansion joints along the pipeline

For Case (a):  $\Delta \sigma_1 = \frac{\Delta p D}{4e}$

For Case (b):  $\Delta\varepsilon_1 = 0$  and  $\Delta\sigma_1 = \mu\Delta\sigma_2$

For Case (c):  $\Delta\sigma_1 = 0$  and  $\Delta\varepsilon_1$  : No interest

Practically, the actual pipe restraint situation probably will not conform precisely to any of these cases but it stays somewhere in this range of possibilities.

### A.5. Wave Speed for Case (b) Restraint

For Case (b):  $\Delta\varepsilon_1 = 0$  Hence, there is no axial strain.

$$\Delta\sigma_1 = \mu\Delta\sigma_2 = \mu \frac{\Delta\varepsilon_2}{1 - \mu^2} E$$

From equation (A- 13):

$$\frac{\Delta p D}{2e} = \frac{\Delta\varepsilon_2}{1 - \mu^2} E$$

$$\Delta\varepsilon_2 = \frac{\Delta p D}{2eE} (1 - \mu^2)$$

Utilizing equation (A- 11):

$$\delta V = \frac{\pi}{4} D^2 \delta L \frac{\Delta p D (1 - \mu^2)}{e E} \quad (\text{A- 14})$$

$$m_{accumulation} = \delta m = m_{t+\delta t} - m_t = \rho_{final} \delta V_{final} - \rho_{initial} \delta V_{initial}$$

$$\delta m = (\rho + \delta\rho)(A\delta L + \delta V) - \rho A\delta L = \rho\delta V + \delta\rho A\delta L + \delta\rho\delta V$$

Neglecting  $\delta\rho\delta V$  term and using equation (A- 7);

$$\rho\delta V + \delta\rho A\delta L = -\rho A\Delta V \frac{\delta L}{a} \quad (\text{A- 15})$$

Substituting equation (A- 14) into equation (A- 15):

$$\rho \frac{\pi}{4} D^2 \delta L \frac{\Delta p D (1 - \mu^2)}{e} \frac{1}{E} + \delta \rho A \delta L = -\rho A \Delta V \frac{\delta L}{a}$$

Simplifying above equation  $A = \frac{\pi D^2}{4}$

where,

$$\rho \frac{\Delta p D (1 - \mu^2)}{e} \frac{1}{E} + \delta \rho = -\rho \frac{\Delta V}{a} \quad (\text{A- 16})$$

Note that, for a given mass of material,  $m = \rho V = \text{constant}$ . Hence,

$$\frac{dm}{dt} = \frac{d(\rho V)}{dt} = 0$$

$$V \delta \rho + \rho \delta V = 0$$

Hence,

$$\delta \rho = -\rho \frac{\delta V}{V} \quad (\text{A- 17})$$

From equation (2-1):  $\frac{\delta V}{V} = -\frac{\Delta p}{K}$

Then, equation (A- 17) becomes:

$$\delta \rho = -\rho \left( -\frac{\Delta p}{K} \right) = \rho \frac{\Delta p}{K}$$

Putting  $\delta \rho$  into equation (A- 16):

$$\rho \frac{\Delta p D (1 - \mu^2)}{e} \frac{1}{E} + \rho \frac{\Delta p}{K} = -\rho \frac{\Delta V}{a}$$

Simplifying above equation:

$$\Delta p \left[ \frac{1}{K} + \frac{D(1-\mu^2)}{eE} \right] = -\frac{\Delta V}{a} \quad (\text{A- 18})$$

From equation (A- 3):  $\Delta H = \frac{\Delta p}{\rho g} = \frac{\Delta p}{\gamma}$

From equation (A- 5):  $\Delta H = -\frac{a}{g}\Delta V$

Using above equations:

$$\frac{\Delta p}{\rho g} = -\frac{a}{g}\Delta V$$

$$\Delta p = -a\rho\Delta V \quad (\text{A- 19})$$

Putting equation (A- 19) into equation (A- 18):

$$-a\rho\Delta V \left[ \frac{1}{K} + \frac{D(1-\mu^2)}{eE} \right] = -\frac{\Delta V}{a}$$

Simplifying above equation:

$$a^2\rho \left[ \frac{1}{K} + \frac{D(1-\mu^2)}{eE} \right] = 1$$

$$a = \sqrt{\frac{\frac{1}{\rho}}{\frac{1}{K} + \frac{D(1-\mu^2)}{eE}}}$$

$$a = \frac{\sqrt{\frac{K}{\rho}}}{\sqrt{1 + \frac{KD}{Ee}(1-\mu^2)}} \quad (\text{A- 20})$$

Wylie and Streeter (Ref [46]) show that the equation for wave speed can be

conveniently expressed in the general form:

$$a = \frac{\sqrt{\frac{K}{\rho}}}{\sqrt{1 + \frac{KD}{Ee}(C)}} \quad (\text{A-21})$$

Where, For Case (a) restraint:  $C = \frac{5}{4} - \mu$

For Case (b) restraint:  $C = 1 - \mu^2$

For Case (c) restraint:  $C = 1.0$

### A.6. Conservation of Mass

Applying conservation of mass to a control volume coinciding with the interior of the pipe with length  $ds$ :

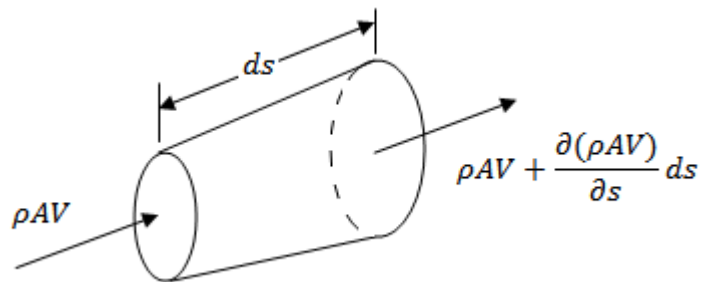


**Figure A. 7.** Control Volume used for Applying Mass Conservation

$$\rho AV - \left[ \rho AV + \frac{\partial(\rho AV)}{\partial s} ds \right] = \frac{\partial(\rho Ads)}{\partial t}$$

$$\frac{-\partial(\rho AV)}{\partial s} ds = \frac{\partial(\rho Ads)}{\partial t}$$

It is accepted that the sides of the control volume are attached to the side walls of the pipe, hence the control volume elongates as the pipe stretches longitudinally. An exception is made for Case (c) such that the length of the control volume is accepted as constant even though the pipe elongates.

$$-\left[ \rho A \frac{\partial V}{\partial s} ds + \rho V \frac{\partial A}{\partial s} ds + AV \frac{\partial \rho}{\partial s} ds \right] = \rho A \frac{\partial(ds)}{\partial t} + \rho ds \frac{\partial A}{\partial t} + Ads \frac{\partial \rho}{\partial t}$$

Dividing each side by  $\rho ads$ :

$$\frac{1}{\rho} \left( \frac{\partial \rho}{\partial t} + V \frac{\partial \rho}{\partial s} \right) + \frac{1}{A} \left( \frac{\partial A}{\partial t} + V \frac{\partial A}{\partial s} \right) + \frac{1}{ds} \frac{\partial(ds)}{\partial t} + \frac{\partial V}{\partial s} = 0$$

Recognizing that:  $\frac{\partial \rho}{\partial t} + V \frac{\partial \rho}{\partial s} = \frac{d\rho}{dt}$  and  $\frac{\partial A}{\partial t} + V \frac{\partial A}{\partial s} = \frac{dA}{dt}$

$$\frac{1}{\rho} \frac{d\rho}{dt} + \frac{1}{A} \frac{dA}{dt} + \frac{\partial V}{\partial s} + \frac{1}{ds} \frac{\partial(ds)}{\partial t} = 0 \quad (\text{A- 22})$$

From equation (2-1):  $K = -\frac{dp}{dV/V}$

From equation (A- 17):  $\frac{dV}{V} = -\frac{d\rho}{\rho}$

Synthesizing above equations:

$$K = -\frac{dp}{dV/V} = \frac{dp}{d\rho/\rho} \quad \text{Then,} \quad \frac{d\rho}{\rho} = \frac{dp}{K}$$

$$\frac{1}{\rho} \frac{d\rho}{dt} = \frac{1}{K} \frac{dp}{dt} \quad (\text{A- 23})$$

From equation (A- 9):  $\delta V_c = \frac{1}{2} \pi D^2 \delta L \Delta \varepsilon_2$

For  $dA = \frac{dV}{dL}$  And for Case (b), where  $\Delta \varepsilon_1 = 0$

$$dA = \frac{dV_c}{dL} = \frac{1}{2} \pi D^2 d\varepsilon_2$$

From equation (A- 8):  $d\varepsilon_2 = \frac{d\sigma_2 - \mu d\sigma_1}{E}$  and  $A = \frac{\pi D^2}{4}$

$$dA = \frac{dV_c}{dL} = \frac{1}{2} \pi D^2 d\varepsilon_2 = \frac{1}{2} \pi \frac{D^2}{E} (d\sigma_2 - \mu d\sigma_1) = \frac{2A}{E} (d\sigma_2 - \mu d\sigma_1)$$

$$\frac{dA}{A} = \frac{2}{E} (d\sigma_2 - \mu d\sigma_1) \quad (\text{A- 24})$$

From equation (A- 12):  $\Delta \sigma_2 = \frac{\Delta p D}{2e}$

From equation (A- 8) and for Case (b) where,  $\Delta \varepsilon_1 = 0$  ,  $d\sigma_1 = \mu d\sigma_2$

$$d\sigma_2 - \mu d\sigma_1 = d\sigma_2 - \mu^2 d\sigma_2 = d\sigma_2 (1 - \mu^2) = \frac{dp D}{2e} (1 - \mu^2) \quad (\text{A- 25})$$

Combining equations (A- 24) and (A- 25):

$$\frac{1}{A} \frac{dA}{dt} = \frac{2}{E} \frac{D}{2e} (1 - \mu^2) \frac{dp}{dt}$$

Simplifying above equation:

$$\frac{1}{A} \frac{dA}{dt} = (1 - \mu^2) \frac{D}{eE} \frac{dp}{dt} \quad (\text{A- 26})$$

For longitudinal expansion:

$$d(ds) = d\varepsilon_1 ds$$

Since  $d\varepsilon_1 = 0$  for Case (b):

$$d(ds) = 0$$

$$\frac{1}{ds} \frac{\partial(ds)}{\partial t} = 0 \quad (\text{A- 27})$$

Inserting equations (A- 23), (A- 26) and (A- 27) into equation (A- 22):

$$\frac{dp}{dt} \left[ \frac{1}{K} + (1 - \mu^2) \frac{D}{eE} \right] + \frac{\partial V}{\partial s} = 0 \quad (\text{A- 28})$$

From equation (A- 20):  $\frac{1}{K} + (1 - \mu^2) \frac{D}{eE} = \frac{1}{a^2 \rho}$

$$\frac{1}{\rho} \frac{dp}{dt} = a^2 \frac{\partial V}{\partial s} \quad (\text{A- 29})$$

## APPENDIX B

### FFT Calculation in MATLAB

```
function[max_freq]=FFT_THESIS(Dosya)

Time=xlsread(Dosya,'A:A');
Pressure_Thruster_Valve=xlsread(Dosya,'B:B');

m=length(Time);      % Window length
DeltaTime=0.0001;    % Sampling time[Second]
fs=1/DeltaTime;      % Sampling frequency [Hz]

n=8192*4;
f = fs/2*linspace(0,1,n/2+1);

FFT_Thruster_Valve=fft(detrend(Pressure_Thruster_Valve),n)/m; % DFT

% Plot single-sided amplitude spectrum.
h=figure;
x=f(1:(n/2+1));
y=2*abs(FFT_Thruster_Valve(1:n/2+1));
[max_val,index] = max(y);
stem(x,y); hold on;
plot(x(index),max_val,'ks','markerfacecolor',[0 0 0]);
text(x(index)+0.3,max_val+0.1,['Max Freq: ', num2str(x(index))])
max_freq=x(index);
xlabel('Frequency (Hz)')
ylabel('Power')
grid on
xlim([0 150]);

end
```